

**New tools for maggot debridement therapy research:  
From the establishment of qRT-PCR to the characterization of  
*Lucilia sericata* Urate Oxidase**



**INAUGURAL-DISSERTATION**

zur Erlangung des akademischen Grades

Dr. rer. nat.

der Naturwissenschaftlichen Fachbereiche

der Justus-Liebig-Universität Gießen

vorgelegt von

**M. Sc. Andre Baumann**

aus Herne

Gießen, im Februar 2017

1. Gutachter: **Professor Dr. Andreas Vilcinskas**  
Institut für Insektenbiotechnologie  
Fachbereich Agrarwissenschaften, Ökotoxikologie und  
Umweltmanagement  
Justus-Liebig-Universität Gießen

2. Gutachter: **Professor Dr.-Ing. Peter Czermak**  
THM Fachbereich LSE-IBPT  
Fachbereich Biologie und Chemie  
Justus-Liebig-Universität Gießen

Die wahren Optimisten sind nicht überzeugt, dass alles gut gehen wird, aber sie sind überzeugt, dass nicht alles schief gehen kann.

Johann Christoph Friedrich von Schiller (1759 - 1805)

## Table of contents

Table of contents .....	IV
Summary.....	1
<b>1. Introduction.....</b>	<b>2</b>
<b>1.1. <i>Lucilia sericata</i> .....</b>	<b>3</b>
1.1.1. Taxonomy .....	3
1.1.2. Life-cycle .....	4
1.1.3. Anatomy.....	5
<b>1.2. Chronic wounds.....</b>	<b>7</b>
<b>1.3. Maggot debridement therapy (MDT).....</b>	<b>8</b>
<b>1.4. qRT-PCR and reference genes.....</b>	<b>13</b>
<b>1.5. Urate Oxidases, allantoin and purine catabolism.....</b>	<b>15</b>
<b>2. Aim of the project .....</b>	<b>18</b>
<b>3. Methods.....</b>	<b>19</b>
<b>3.1. <i>Lucilia sericata</i> .....</b>	<b>19</b>
3.1.1. Maggot rearing.....	19
3.1.2. Immune challenge and zone of inhibition assays.....	19
3.1.3. Tissue dissection .....	19
<b>3.2. RNA based <i>L. sericata</i> studies.....</b>	<b>20</b>
3.2.1. RNA isolation.....	20
3.2.2. RNA purification by sodium acetate precipitation.....	20
3.2.3. RNA quality control by agarose gel electrophoresis.....	20
3.2.4. cDNA synthesis.....	21
3.2.5. Candidate gene sequence assembly.....	21
3.2.6. Primer design and evaluation for qRT-PCR .....	22
3.2.7. Quantitative RT-PCR.....	22
3.2.8. Normfinder and GeNorm analysis .....	23
3.2.9. Gene expressions analysis.....	24
3.2.10. RNA in situ hybridization (ISH).....	25
<b>3.3. Production and characterization of recombinant Urate Oxidase (UO<sub>r</sub>) .....</b>	<b>26</b>
3.3.1. UO <sub>r</sub> sequence synthesis.....	26
3.3.2. Production of UO <sub>r</sub> in <i>E. coli</i> .....	27

---

3.3.3.	IMAC purification of UO <sub>r</sub> .....	27
3.3.4.	SDS-PAGE.....	27
3.3.5.	UO <sub>r</sub> refolding by dialysis.....	27
3.3.6.	Determination of UO <sub>r</sub> pH optimum.....	28
3.3.7.	Determination of UO <sub>r</sub> temperature optimum, competitive inhibition, metal ion dependence and stability.....	29
<b>3.4.</b>	<b>Localization of native UO in larval tissue.....</b>	<b>29</b>
3.4.1.	Production of polyclonal anti-UO antibodies.....	29
3.4.2.	Western blot.....	29
3.4.3.	Whole mount fluorescence immunohistochemistry.....	30
<b>4.</b>	<b>Results.....</b>	<b>31</b>
<b>4.1.</b>	<b><i>L. sericata</i> reference gene assessment.....</b>	<b>31</b>
4.1.1.	Candidate genes selection.....	31
4.1.2.	Tissue specific RNA quality.....	31
4.1.3.	Quantitative RT-PCR.....	32
4.1.4.	Zone of inhibition assays and initial analysis of attacin-2 expression.....	33
4.1.5.	Validation of candidate reference genes using Normfinder.....	34
4.1.6.	Validation of candidate reference genes using GeNorm.....	35
4.1.7.	Gene expression analysis after <i>P. aeruginosa</i> immune challenge.....	37
<b>4.2.</b>	<b>Characterization of <i>L. sericata</i> Urate Oxidase.....</b>	<b>39</b>
4.2.1.	<i>UO</i> is expressed by Malpighian tube cells.....	39
4.2.2.	Recombinant production and refolding of <i>L. sericata</i> UO.....	41
4.2.3.	UO <sub>r</sub> pH and temperature optimum.....	42
4.2.4.	UO <sub>r</sub> competitive inhibition, metal ion dependence and stability.....	43
4.2.5.	Native UO is exclusively present in Malpighian tubes.....	44
<b>5.</b>	<b>Discussion.....</b>	<b>46</b>
<b>5.1.</b>	<b><i>L. sericata</i> reference gene assessment.....</b>	<b>46</b>
<b>5.2.</b>	<b>UO and purine catabolism.....</b>	<b>49</b>
<b>5.3.</b>	<b>UO<sub>r</sub> and application potential.....</b>	<b>51</b>
<b>5.4.</b>	<b>Outlook.....</b>	<b>53</b>
<b>6.</b>	<b>References.....</b>	<b>55</b>
	<b>Abbreviations.....</b>	<b>65</b>
	<b>List of figures.....</b>	<b>67</b>

---

<b>List of tables</b> .....	<b>68</b>
<b>Supplement A: Materials</b> .....	<b>69</b>
<b>A.1 Chemicals and reagents</b> .....	<b>69</b>
<b>A.2 Consumables</b> .....	<b>72</b>
<b>A.3 Devices</b> .....	<b>73</b>
<b>A.4 Standards and kits</b> .....	<b>73</b>
<b>A.5 Buffer and solutions</b> .....	<b>74</b>
<b>Supplement B: Support information</b> .....	<b>75</b>
<b>B.1 Melt curves of all applied qRT-PCR primer pairs</b> .....	<b>75</b>
<b>B.2 Normfinder intra and intergroup variations</b> .....	<b>79</b>
<b>Licenses and copyright</b> .....	<b>80</b>
<b>Zusammenfassung</b> .....	<b>81</b>
<b>Danksagung</b> .....	<b>83</b>
<b>Erklärung</b> .....	<b>84</b>

## Summary

Maggot debridement therapy (MDT) is an U.S. Food and Drug Administration (FDA) as well as European Medicines Agency (EMA) approved treatment for various chronic and recalcitrant wounds. MDT was successfully applied in numerous case studies (Sherman 2002; Sherman 2003) and shown to have beneficial effects on wound debridement, disinfection and hastened healing processes (Sherman 2014). Larval secretions and excretions (E/S) represent a complex mixture of enzymes, AMPs and small molecules and as such serves as a rich source of new therapeutics (Sherman 2014). Unfortunately, the complexity of this mixture makes it very hard to decipher the exact roles and benefits of individual components in the wound healing process and requires more detailed studies (Davydov 2011).

This thesis is based on two parts. The first part, published in PLOS ONE (Baumann et al. 2015), focused on the establishment of a qRT-PCR approach by investigating tissue specific expression stability of 10 candidate reference genes in immune challenge experiments. Quantitative RT-PCR serves as a golden standard in the field of gene expression (Bustin et al. 2009; Nolan et al. 2006) and its establishment in *L. sericata* serves as an important tool for identification and validation of genes involved in maggot therapy. My study shows that the combination of three reference genes *RPLP0*, *EF1 $\alpha$*  and *RPS3* provides reliable normalization of *L. sericata* expression data among all tested samples, thus allowing for the first time the precise normalization of gene expression in larval tissues involved in production of E/S. The methods of tissue sample preparation and gene expression analysis established during this thesis also contributed to Beckert et al. (2015) and Beckert et al. (2016). Reference genes were applied in Pöppel et al. (2016) and Franta et al. (2016).

Second part of this thesis, submitted to Insect Biochemistry and Molecular Biology (Baumann et al. 2016), focuses on recombinant production and characterization of *L. sericata* Urate Oxidase (UO) an enzyme that exclusively creates allantoin, which contributes to the wound healing process (Araujo et al. 2010; DiSalvo 2002). I was the first to produce and characterize an insect UO. Recombinant UO was produced using *E. coli* expression system, purified via IMAC (denaturing chromatography), refolded and tested for its pH optimum (in the alkaline), temperature optimum (20-25 °C), competitive inhibition (typical for UO), cofactors (cofactor independent) and stability (short shelf life). Furthermore, I monitored the presence of *L. sericata* UO on mRNA as well as protein level in various *L. sericata* tissues and showed that both *UO* gene as well as native UO localize predominately inside Malpighian tube cells sharing strictly cytosolic localization. Based on these data it can be assumed that allantoin is produced by UO to remove uric acid from the insect hemolymph by the Malpighian tubes and is excreted via the hindgut as nitrogenous waste product. Those findings support the hypothesis that not only actively secreted molecules, but also excretion products contribute to the beneficial effects of MDT.

## 1. Introduction

Insects are the biggest and the most diverse animal class on earth representing more than 70 % of all known species (Figure 1; (Chapman 2009)). With more than 1 million species described (Groombridge and Jenkins 2002) and 5-6 million estimated in total (Raven and Yeates 2007) only a small fraction of insects variety is recognized so far. Insects are the most successful terrestrial colonizers on Earth and can be found everywhere around the globe surviving under harshest conditions. The Antarctic midge *Belgica antarctica* can withstand the extreme cold in Antarctica and is the largest land animal living there the whole year (Lee et al. 2006).

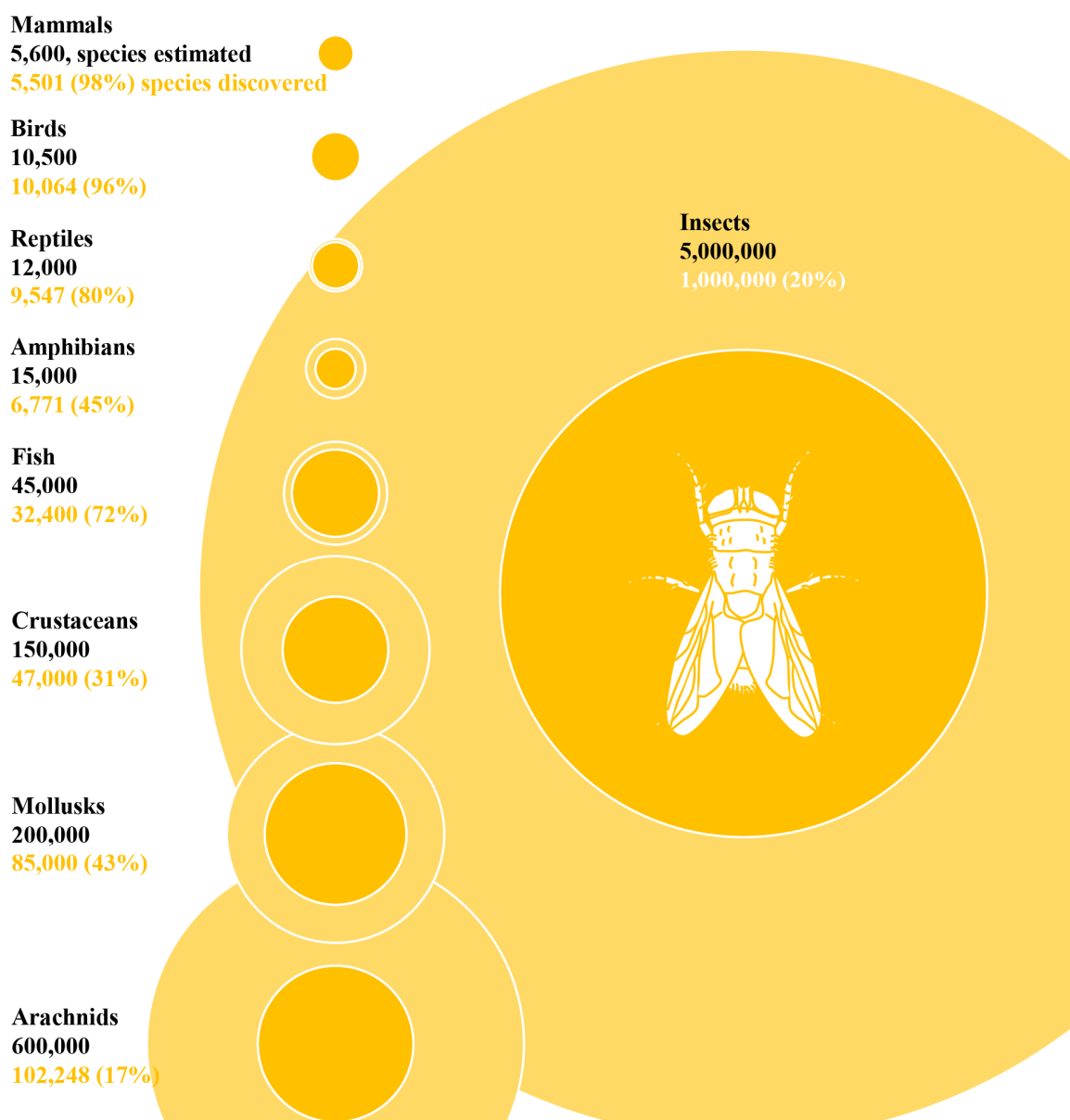


Figure 1: Animal species infographics according to Chapman (2009).

The Sahara Desert ant *Cataglyphis bicolor* can permanently withstand temperatures above 50 °C, which makes it the only land animal capable of surviving such an extreme heat (Sherwood 1996). In addition to extreme conditions such as temperature or high salinity levels, there are insects like the larvae of *Eristalis tenax* (Jacobs and Renner 2007) that live and feed in places with high bacterial load like cesspools or sewages. Taken together, remarkable resilience and biodiversity make insects the rich source of molecules with medical and/or biotechnological potential.

Insects' enormous adaptability and ability to overcome severe conditions was recognized by different human cultures centuries ago. Various insect species as well as their secretions, venoms but also their products (e.g. honey) became a part of the traditional medicines and are recently reevaluated as a rich source of therapeutic molecules for modern western medicine (Cherniack 2010) with *L. sericata* maggots and honey bees as the vanguard of this field. Many clinical trials proved the beneficial effects and healing potential of insect compounds (McIntosh and Thomson 2006; Steenvoorde et al. 2007). Among others honey is used for treatment of burns (Subrahmanyam 1991) or ant venoms for treatment of *rheumatoid arthritis* (Altman et al. 1984). Furthermore as a direct live animal application *L. sericata* maggots are used as an alternative treatment for chronic and recalcitrant wounds that is nowadays known as maggot debridement therapy (MDT) (Sherman 2014). In addition, the investigation of insect scavengers such as blowflies (e.g. *L. sericata*) is exploited in forensic entomology to estimate the time of the death on a crime scene. There the postmortem interval of a corpse is determined by calculating the age of immature insect stages feeding on a corpse as well as by analyzing the exact species present. By this the postmortem intervals of a dead body can be estimated ranging from day one up to several weeks (Amendt et al. 2004). The detailed understanding of insect anatomy, life-cycle and way of life is the crucial to unlock the full potential of various insect like *L. sericata* for bio-applications e.g. in medicine or forensic entomology.

## **1.1. *Lucilia sericata***

### **1.1.1. Taxonomy**

The green bottle fly *Lucilia sericata* (Meigen, 1826) represents the exclusive species in MDT. It belongs to the class *Insecta* and the order *Diptera* (Figure 2A). The term originates from the Greek *di* = two and *ptera* = wings) (Honomichl 2010). Order *Diptera* consist of more than 100 000 described species and its members are typified by only a single set of functional wings (forewings), while the second pair of wings (hindwings) evolved into halteres a knob-shaped sensory organs, which monitor body rotation during the flight (Wendler 2010). The family *Calliphoridae* commonly known as blowflies consist of about 1100 species and includes many important parasitic species, but also pollinators that are attracted by plants resembling the odors of rotten meat (Willemstein 1987).

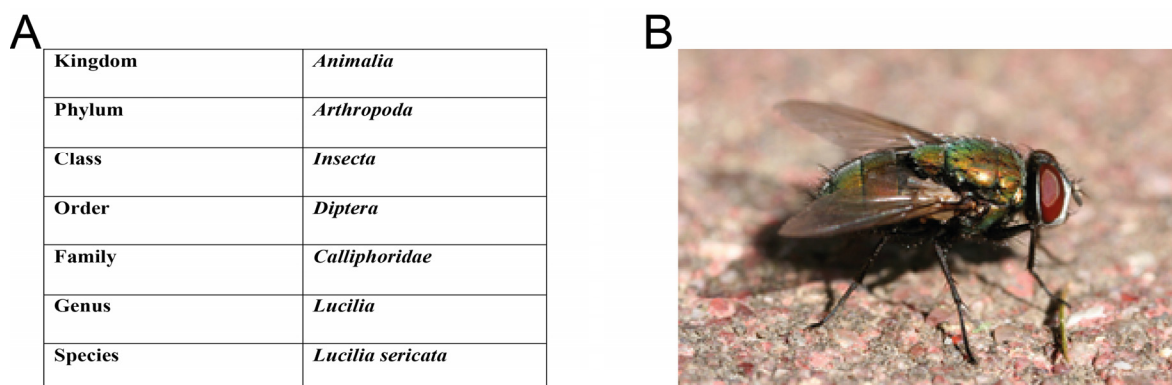


Figure 2: *Lucilia sericata* A: *L. sericata* taxonomy. B: Adult *L. sericata* (green blowfly) (“[Green\\_bottle\\_fly3.jpg](#)“ [Calibas](#) is licensed under [CC-BY-SA 4.0](#)).

Flies from the genus *Lucilia* commonly share the metallic blue or green-golden color (Figure 2B) which develops once the cuticle of the freshly emerged adult stretches, dries and hardens. All members of this genus feed on animal tissues or feces, but differ in their prevalence for necrotic tissue as well as in the antimicrobial properties of their secretions (Grassberger et al. 2013). To distinguish between *L. sericata* and other closely related species of the genus *Lucilia*, the precise investigation of various morphological parameters like femur color, numbers of paravertical setulae or width of the frontal stripe (Williams and Villet 2014). Those small details are important while choosing the right insect for the treatment or coming to the correct conclusion at the crime scene. An alternative to the morphological identification are genetic analysis of molecular markers that can also identify *Lucilia* hybrids (Stevens and Wall 1996).

### 1.1.2. Life-cycle

The *L. sericata* life-cycle consists of 4-stages including egg, larva, pupa and adult (Eggert et al. 2010). Adult *L. sericata* females lay up to 200 eggs on dead and/or decaying tissues, open wounds or feces. The female places eggs by unfolding her ovipositor and laying (“blowing”) the eggs onto the food source, which led to the name blowfly. One female can produce up to 3000 eggs during her lifetime (Fleischmann et al. 2004). 1<sup>st</sup> Instar larvae hatch after 8-24 h depending on the external temperature. 2<sup>nd</sup> and 3<sup>rd</sup> instar larvae molt and shed their undersized cuticle within the next 4-7 days, but this is highly dependent on several exogenous factors like temperature, food quality or quantity of the larvae. Fed 3<sup>rd</sup> instar larvae crawl away from the food source and search for a dark and humid place to enter the pupal stage (Grassberger et al. 2013). During pupation, which lasts 10-20 days the larvae transform (metamorphoses) and emerge as an adult fly (Figure 3). The life span of the adult is around 1–2 months. *L. sericata* has a seasonal activity peaking during the warmer period of the year from May to October, which can lead to up to eight generations of flies (Fleischmann et al. 2004).

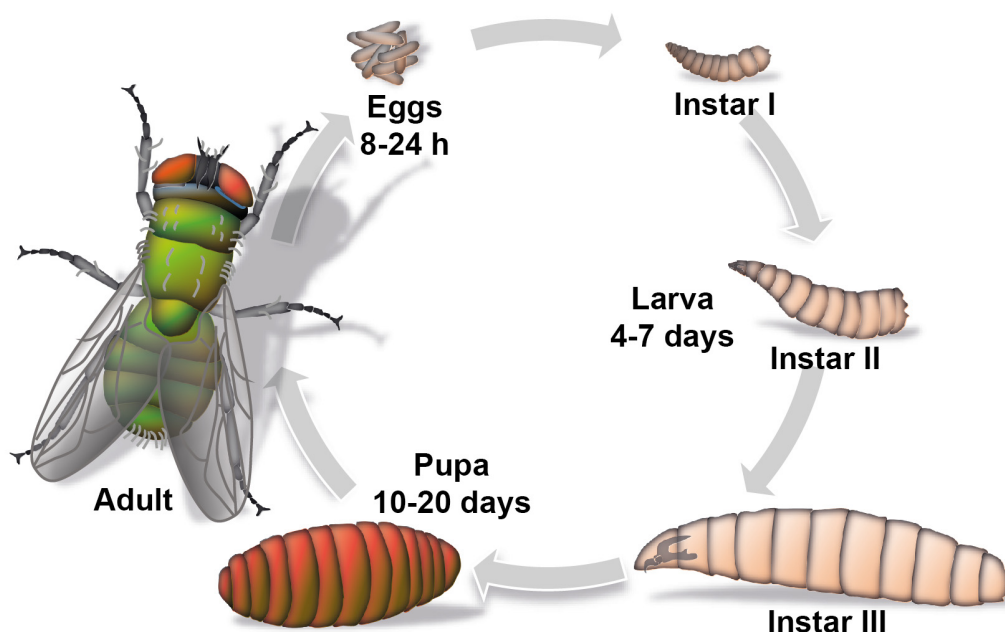


Figure 3: The life-cycle of *L. sericata*. Designed by and courtesy of Dr. Henrike Schmidtberg.

### 1.1.3. Anatomy

In maggot therapy only the 1<sup>st</sup> instar larvae are applied to the wound bed. The larval body is simple and exhibits few organs (salivary glands, crop, gut, Malpighian tubes, fat body, nerve ganglion and trachea). It is optimized for the uptake of large amounts of food. In five minutes a larva can ingest an amount of food reaching almost the half of its body weight and due to this larva can increase its weight 100 times in the first 72 h after hatching (Grassberger et al. 2013). The larvae have a pair of mouth hooks, which facilitate larval movement and in addition tears the tissue apart thus easing digestive enzymes to sink in (Figure 4) (Fleischmann et al. 2004). Larvae perform extracorporeal digestion. They secrete various digestive enzymes into the wound to liquefy/predigest the tissue, which is subsequently ingested. Many of these digestive enzymes which are predominantly produced in the salivary glands are a promising target for further investigations. The very flexible crop serves as a short-term food storage e.g. to provide food during migration of pupation. The enzymatically liquefied tissue is sucked in and concentrated up to 5 times in the proventriculus before it reaches the midgut (Grassberger et al. 2013).

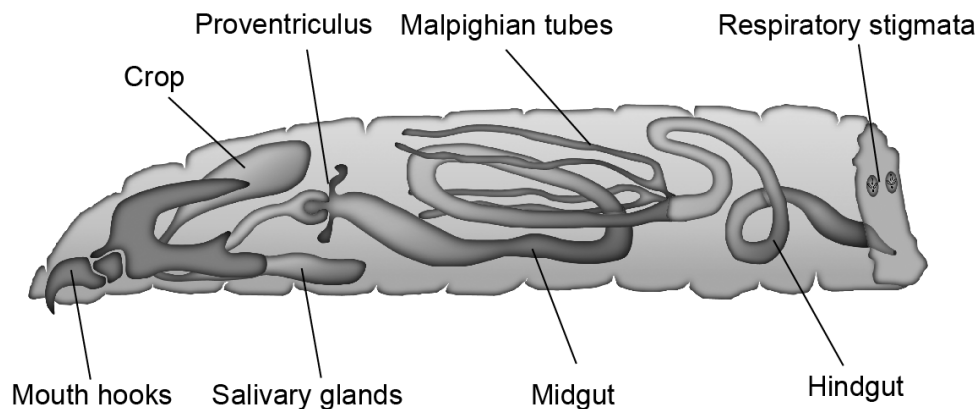


Figure 4: Maggot anatomy. Designed by and courtesy of Dr. Henrike Schmidtberg.

The food is further processed in the midgut by digestive enzymes, bacteria are here eliminated and nutrients are absorbed by the gut walls, therefrom they pass over into the hemolymph. The intersection between the thick midgut and the thinner hindgut is easily distinguishable by the Malpighian tubes connection. These single cell layer tubes serve as drainage pipes and filter excretion products from the hemolymph while keeping the osmotic pressure (Peters 2010). Excretion products are further processed and emptied into the hindgut where they mix with partially digested food coming from the midgut. In the hindgut further breakdown of excretion products and nutrition uptake takes place before the final end products are excreted over the anus while keeping liquid and ion balance. The fat body has no direct involvement in digestion. Fat body cells encase most organs and are surrounded by hemolymph. They carry out multiple metabolic functions like energy storage in the form of glycogen, lipid storage and they are also the major tissue for internal immune defense that facilitates the rapid production of the AMPs arsenal (Peters 2010). The nerve ganglion located in the head part is the central nerve cluster of the maggot (Milde 2010). The trachea system of air-filled tubes spans the whole larvae and provides oxygen directly to the tissues. The air exchanges through the two respiratory stigmata located on the back part of the maggot above the anus (Wasserthal 2010). *L. sericata* Larvae are remarkable microsurgeons that liquefy and remove wound material without damaging the healthy tissue. This surgical ability together with combination of both external and internal bacteria elimination make *L. sericata* larvae a valuable tool for treatment of chronic wounds. Thus a deeper understanding of maggot anatomy and behavior can strongly enhance their biotechnological application (Fleischmann et al. 2004).

## 1.2. Chronic wounds

Maggots that feed on necrotic and decaying tissue have been shown to be beneficial in the treatment of chronic human wounds. Wound healing is a crucial, life-maintaining process, which can be divided into 4 overlapping phases: (I) hemostasis, (II) inflammation, (III) proliferation and (IV) maturation. In this highly complex process many cells and mediators interact in a well-orchestrated manner that is still not completely understood. Immediately after injury (I) hemostasis is triggered to stop blood loss. The (II) inflammation phase (day 0-6) is initiated to clear the wound from all the foreign material including bacteria and necrotic tissue. Once the wound is cleaned (III) the proliferative phase (day 4-14) is initiated to close the wound and finally (IV) the maturation phase (starting day 8, but can take up to a year) leads to tissue remodeling (Broughton et al. 2006).

A chronic wound is defined as a wound that does not reach the final maturation phase within 12 weeks. In such wounds the transition between the healing phases is impaired and most of them are stuck in the inflammatory phase. They are characterized by the presence of necrotic and infected tissue, which was not removed adequately and show only weak immune response due to the disconnection from the blood stream (Eming et al. 2007). Such an environment, rich in nutrition and lacking any immune defense, offers ideal growth conditions for many microorganisms including pathogenic strains (Dow et al. 1999). Pressure ulcers (~20 % of all hospital patients across Europe (Vanderwee et al. 2007)) and diabetic foot ulcers with a lifetime risk of 15 % (60 million diabetics across Europe) (Jeffcoate and Harding 2003) are prominent among chronic and recalcitrant wounds. In chronic wounds with a high bacterial population the use of systemic antibiotics is challenging, because the wound is often disconnected from the bloodstream (Hernandez 2006). Topical antibiotics often show no effect, because the bacteria are protected by biofilm or feature a resistance (e.g. Methicillin-resistant *Staphylococcus aureus* (MRSA)) (Attinger and Wolcott 2012; Howell-Jones et al. 2005). In such severe cases surgery is inevitable. For diabetic foot ulcers standard treatment often involves extensive surgery as well, which leads in 15 % of all cases to the amputation of a toe, foot or leg. Surgical removal of the necrotic tissue results in enlargement of the wound bed as well as in hard bleeding and direct damage of healthy tissue (Thomas 2006). Post surgery the wound is covered by a dressing (e.g. hydrogel), which normally does not increase the healing rate, but should offer ideal conditions for healing. Those post surgical wounds are highly susceptible to bacterial infections and thus need to be kept sterile and under careful supervision (Yao et al. 2013). In an aging population treatment of chronic wounds requires costly intensive care reaching to 2-4 % of total EU health care expenses (Posnett et al. 2009; Sen et al. 2009), but also causes severe emotional and psychological stress to patients and as such create a demand for new alternatives.

A promising alternative treatment for many chronic wounds that reemerged over the last 20 years is maggot debridement therapy (MDT). MDT can be defined as an artificially induced myiasis, which is carefully controlled. Fly larvae, applied to the wound bed, debride more precisely than any surgeon (only the necrotic tissue) resulting in no increase of the wound bed and almost no bleeding. Moreover, larvae alone or in combination with antibiotics (Sherman 2009) were also shown to degrade bacterial biofilms and eliminate a wide range of pathogens including multi-resistant strains like MRSA (Bexfield et al. 2008). MDT exhibit not only remarkable direct effects on wound healing but is also important from the economic point of view. It has been shown to hastened healing properties, thus reducing the hospital time and associated costs amounting up to 80 % of conventional chronic wound treatment (Church 1996).

### **1.3. Maggot debridement therapy (MDT)**

Fly maggots have been known to positively influence the wound healing for centuries. First reports can be found from Australian Aborigines (Dunbar 1944) and Mayas (Weil et al. 1933). Various military surgeons observed that maggots populate wounds and written reports date back to the 16<sup>th</sup> century when Ambroise Paré noted the remarkably quick recovery of maggot-infested patients. Paré was not attributing this to the maggots or even comprehended those were fly larvae (Goldstein 1931). Baron Dominique-Jean Larrey a surgeon in Napoleon's army recognized the maggot's prevalence for necrotic tissue and the accelerated healing properties, but did not actively apply them (Larrey 1829). The first direct application came during the American Civil War, when Confederate surgeon John Forney Zacharias lacking supply of conventional dressing material used maggots as an alternative (Chernin 1986). US podiatrist, William S. Bear made his observations on maggots during the First World War and utilized his experience later as a professor at the John Hopkins University in the treatment of chronic osteomyelitis (Whitaker et al. 2007). He is the founding father of modern MDT by introducing maggot-dressings and the use of sterile larvae in treatments. Ultimately he convinced the skeptic scientific community and in the 1930s maggots were used in over 300 hospitals across the US and Europe. The hospitals that did not rear their own sterile maggots could buy commercial produced ones distributed as "Surgical Maggots-Lederle". The discovery and marketing of penicillin in 1940<sup>th</sup> together with improved surgical knowledge in wound care after the Second World War shifted the focus from maggot therapy towards the use of antibiotics. The popularity of mostly penicillin resulted in the rapid decline of MDT, which was considered as an old fashion method (Fleischmann et al. 2004). The renaissance of MDT came at the end of the 20<sup>th</sup> century, intractable wounds still represent a challenge for modern medicine. The antimicrobial and debridement properties of maggots let maggot therapy re-emerge as an alternative therapeutic approach (Figure 5) (Grassberger et al. 2013; Sherman et al. 2000).

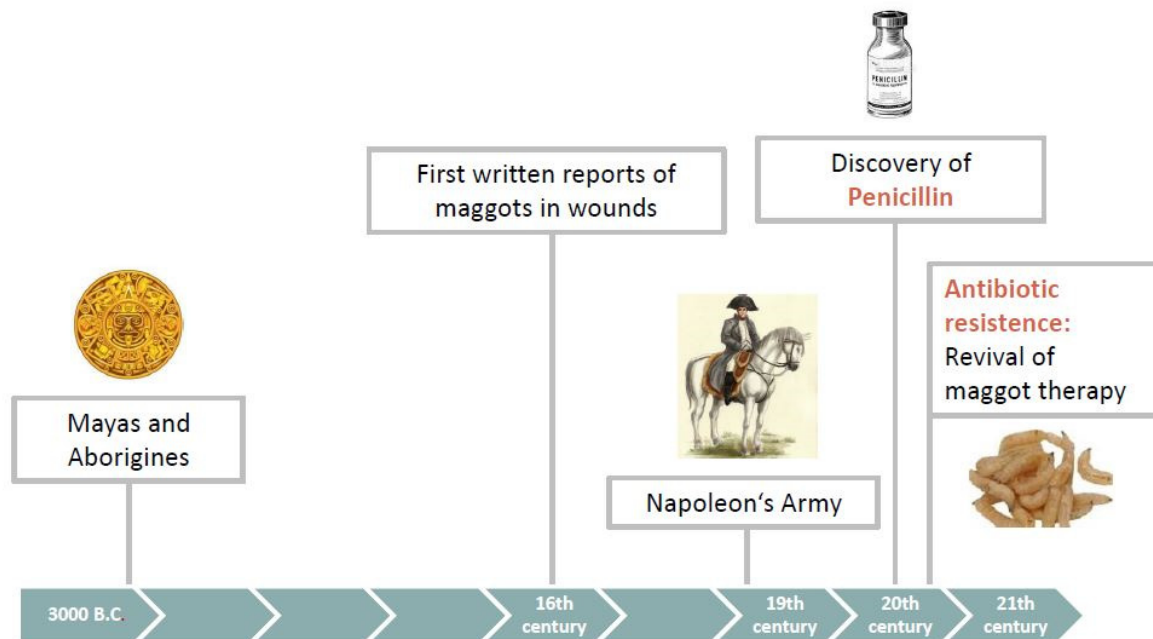


Figure 5: History of maggot therapy. According to Fleischmann et al. (2004), designed by and courtesy of Dr. Anne Pöppel.

Modern maggot debridement therapy (MDT) is based on Bears method and underpinned by clinical studies starting in the 1990s (Sherman et al. 1995) that significantly improved our knowledge about the benefits of MDT. Its superb debridement together with decreased risk of post-surgery infections (Sherman 2002; Sherman 2003; Sherman et al. 2001) led to its approval by the U.S. Food and Drug Administration (FDA; case number K033391) as a medical device in 2004. Nowadays MDT is a popular alternative treatment for chronic and recalcitrant wounds. The prime FDA approved species for MDT are maggots of the green bottle fly *Lucilia sericata*. They are the first live animal treatment approved by the FDA. In Europe the European Medicines Agency (EMA, case number EMEA-000714-PIP01-09) approved *L. sericata* maggots in 2010 only for leg ulcers in the Biobag format. In Germany *L. sericata* maggots are a prescription drug since 2014 (<http://www.kbv.de/html/11710.php>). During MDT maggots have 3 modes of action. They contribute to wound debridement (I), disinfection (II) and hastened healing process (III). Those are mediated by secretions and excretions (E/S) consisting of various compounds including enzymes, antimicrobial peptides (AMPs) and small molecules as well as by physical properties of the maggot itself (Figure 6) (Sherman 2014). In this complex multi-stage process many components work synergistically together. In consequence it is still challenging to understand many key mediators on a molecular level.

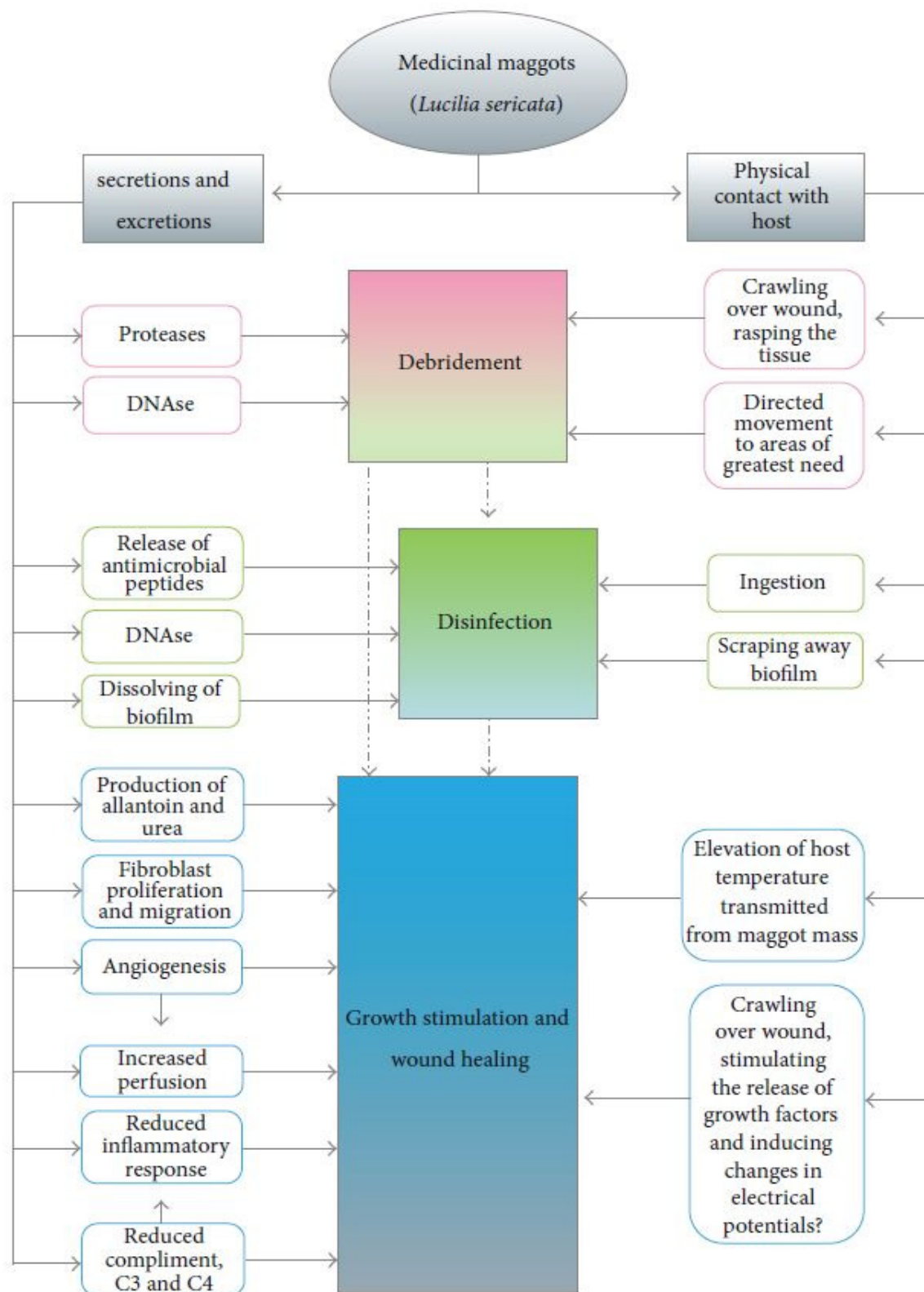


Figure 6: [Overview of proven and postulated mechanisms by which medical maggots promote wound healing](#) from Sherman (2014) published by Hindawi, licensed under [CC BY 4.0](#).

Removal of necrotic tissue and foreign material known as debridement (I) is crucial to promote the healing process of any chronic wound (McCallon et al. 2014). MDT represents a safe and efficient therapy which substantially contribute to wound bed debridement (Gottrup and Jorgensen 2011). Maggot E/S contain various enzymes including proteases (Chambers et al. 2003; Valachova et al. 2014) and nucleases (Brown et al. 2012), which debride the wound bed by liquefying the necrotic tissue (extracorporeal digestion) for subsequent larval ingestion. Three classes of proteolytic enzymes (serine-, aspartic- and metalloproteases) have been identified using class specific substrates and inhibitors in E/S (Chambers et al. 2003). The serine proteases (trypsin-like and chymotrypsin-like) showed predominant activity with a pH optimum of 8-9. Aspartic proteases showed an optimum around pH 5 and metalloproteases around pH 9. Recently, proteases belonging to five different clans (cysteine, aspartic, threonine, serine and metalloprotease) have been shown to be differentially expressed in various larval tissues (Franta et al. 2016). While moving in the wound bed the mouth hooks and spicules on the larval body rasps the tissue and facilitate the entry of proteolytic enzymes. Although maggot E/S represent a rich source of therapeutic proteases, until recently, only two (both serine proteases) have been produced recombinantly and evaluated for their medical potential. The chymotrypsin produced by Telford et al. (2010) was shown to degrade proteins from slough of venous leg ulcers. The Jonah-like chymotrypsin produced by Pöppel et al. (2016) was shown to reduce clotting time of human plasma as well as to cleave extracellular matrix proteins (fibronectin, laminin, collagen IV). Recently a serine protease sequence has been patented under the name debrilase for its ability to support wound debridement (Patent publication number US20120093788 A1).

Disinfection (II) represents another well-described effect of MDT. Larvae contribute to wound cleansing by secretion of a diverse spectrum of AMPs (Altincicek and Vilcinskas 2009; Cerovsky and Bem 2014; Pöppel et al. 2014; Pöppel et al. 2015) and small molecules (Bexfield et al. 2008; Huberman et al. 2007a; Huberman et al. 2007b) as well as by the direct ingestion of microbes and their elimination within the larval gut (Mumcuoglu et al. 2001). It has been shown that *L. sericata* encodes 47 AMP genes, which represent the highest amount of AMPs among *Diptera* (Pöppel et al. 2015). More than 20 of which have been synthesized or produced recombinantly and displayed activities against a broad spectrum of microbes (Barnes et al. 2010; Pöppel et al. 2014). The antimicrobial activity of maggot secretions has a dose-dependent relationship according to the number and nature of bacteria the larvae encounter (Barnes et al. 2010; Cazander et al. 2009a) and shows activity against antibiotic resistant pathogens e.g. Methicillin-resistant *Staphylococcus aureus* (MRSA) (Bexfield et al. 2008; Bowling et al. 2007). The secretions of sterile larvae do not possess antimicrobial activity whereas larvae confronted with *Staphylococcus aureus* or *Pseudomonas aeruginosa* (the most prominent Gram-positive and Gram-negative bacteria in chronic wounds, respectively) (Davies et al. 2004; Fazli et al. 2009; Mihai et al. 2014)

produce distinct antimicrobial secretions that are not mutually antagonistic (Kawabata et al. 2010). Both *S. aureus* as well as *P. aeruginosa* are well known to form biofilms, which protect them against various external cues and considerably hamper the treatment (McCarthy et al. 2015; Tolker-Nielsen 2014). Maggot proteases have been shown to be upregulated upon immune challenge (Altincicek and Vilcinskas 2009) and responsible for the inhibition or degradation of bacterial biofilm (Brown et al. 2012; Cazander et al. 2009b; Harris et al. 2013; van der Plas et al. 2008).

Wound healing and tissue remodeling (III) is an extremely complex process involving many different factors (Broughton et al. 2006). Although it is hard to quantify the direct positive effect of MDT on wound healing and tissue remodeling, there are several studies dealing with these benefits (Cazander et al. 2013). Various serine proteases have been shown to play multiple roles. They for example do not only show procoagulant properties, but cleave extra cellular matrix components (Kahl et al. 2015; Pöppel et al. 2016), thus enabling increased fibroblast migration to the wound bed to accelerate the healing process (Horobin et al. 2005; Horobin et al. 2006). The amino acid derivatives 3-guanidinopropionic acid, L-valinol and L-histidine have been shown to be secreted and stimulate angiogenesis (Bexfield et al. 2010). Also the suppression of pro-inflammatory responses (van der Plas et al. 2007; van der Plas et al. 2009) and an increased rate of tissue granulation (Sherman 2002) have been observed for MDT. Low molecular compounds, such as allantoin, urea or ammonium bicarbonate are present in E/S and involved in maintaining the alkalinity of the wound (Fleischmann et al. 2004). Moreover, allantoin and urea are presumed to have healing properties since 1930s (Robinson 1935), which led to their utilization in many cosmetic products. Recently, allantoin was shown to accelerate the establishment of normal skin in rats using an experimental open wound model (Araujo et al. 2010).

To deliver the sterile larvae for the treatment of chronic wounds fly eggs are disinfected by rinsing with sodium hypochlorite and subsequently reared on sterile culture medium. In Germany BioMonde (<http://biomonde.com/us/>) is the main distributor of medical maggots. They offer both common application forms. In the free-range format (Figure 7A) larvae are applied directly to the wound bed and kept in place by a sophisticated cage-like dressing. This is especially useful for hard to access areas (e.g. body cavities) but could be also associated with increased level of pain, especially in patients that showed wound pain even before treatment. In the second format maggots are enclosed in a Biobag, which usually consist of polyvinylalcohol mesh (Figure 7B) (Fleischmann et al. 2004). This semipermeable membrane keeps the maggot in the right place and allows E/S to reach the wound and liquefy necrotic tissue. Predigested tissue can also pass the membrane back and is ingested by larvae. This eliminates the discomfort and pain of patients caused by maggots crawling in the wound bed and the risk of maggots escaping the wound, but comes at the cost of a slower debridement (Thomas et al. 2002). In both formats

the maggots are kept on the wound for 2-4 days with  $\sim 8$  maggots per  $\text{cm}^2$ . After each treatment cycle the healing progress is evaluated and fresh 1<sup>st</sup> instar maggots are applied until the wound has entered the healing phase. A secondary occlusive dressing is always needed to soak up excessive liquid to prevent the maggots from drowning. This dressing has to allow oxygen to pass so the maggots do not suffocate. The dressing has to be checked and changed regularly (Grassberger et al. 2013).

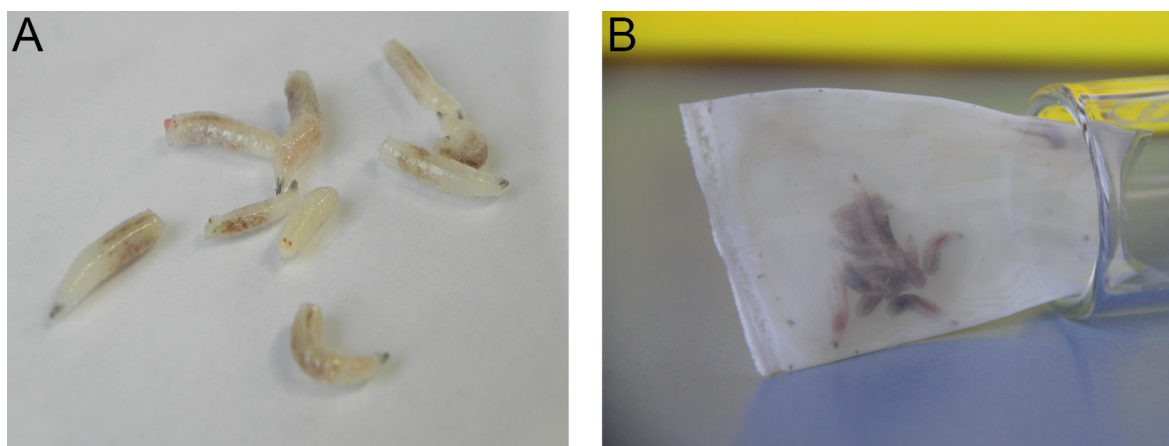


Figure 7: MDT treatment of chronic wounds. (A) Free-Range larvae, (B) larvae in Biobag.

With more than 80,000 patients treated over the last 20 years (Mumcuoglu et al. 2012), MDT holds an immense potential. However, it is still a niche treatment, because the use of living therapeutic animals is not well received neither by patients nor medical personal. In addition, short shelf life and the need for careful control to avoid the spread of disease (e.g. by mature flies) in hospitals remain a challenge. Presently, several groups worldwide have started to characterize and isolate beneficial substances from maggots (Fleischmann et al. 2004; Pöppel et al. 2016; Valachova et al. 2014). The aim of these efforts is to produce defined molecules with therapeutic value either synthetically or in recombinant form. This would provide the base for the development of maggot-derived treatments without applying live maggots, expected to be associated with significantly reduce side-effects and improved acceptance by the patients. Furthermore, defined maggot-derived compounds could be evaluated for other indications besides wound care.

#### 1.4. qRT-PCR and reference genes

Quantitative reverse transcription polymerase chain reaction (qRT-PCR) is a well established and powerful tool for mRNA detection and quantification. It exploits the proportional relationship of input target amount to amplified target in the exponential PCR amplification phase. The amount of amplified

target is detected by a fluorescent readout at the end of each PCR cycle. The first time this signal reaches a set threshold is the so called quantification cycle (Cq). This results in a method that is fast, cheap, highly sensitive and good reproducible over a wide dynamic range (Bustin 2002). In consequence many parameters have to be carefully controlled to assure the high sensitivity in order to use it as a reliable quantification method. Among these are amplification of unspecific products in PCR, mRNA integrity, efficiency of cDNA synthesis, differences in overall transcriptional activity and other random variations caused by various biological and experiment factors (Bustin et al. 2009; Nolan et al. 2006). Ultimately the absolute quantification is only possible by comparison to a standard curve of known target concentrations.

If those standards are not available relative comparison between samples can give useful and relevant answers to many biological questions (Nijhof et al. 2009), but a simple comparison of target gene Cq values is not able to give any kind of reliable results. Therefore, a comparison to a known reference is required (Bustin et al. 2009; Vandesompele et al. 2002). This is usually another gene (reference gene) in the same sample. Those reference genes are supposed to be stably expressed and because they share the sample history with the target gene they eliminate many systemic errors. This strategy is known as the  $\Delta\Delta Cq$  method displayed in equation (1). Relative change ratio is calculated under consideration of primer pair efficiency (E) and  $\Delta Cq$  of target and reference gene in sample A and B (Pfaffl et al. 2002).

$$\text{ratio} = \frac{(E_{\text{target}})^{\Delta Cq_{\text{target}} (\text{sample A} - \text{sample B})}}{(E_{\text{ref}})^{\Delta Cq_{\text{ref}} (\text{sample A} - \text{sample B})}} \quad (1)$$

An ideal reference is a gene that is stable and equal expressed over all samples under every experimental treatment. Such a gene probably does not exist and the comparison to a single gene has been proven to be insufficient so comparison to two or more genes is mandatory (Bustin et al. 2009; Gutierrez et al. 2008). To validate the stable expression of potential reference genes different algorithms like Normfinder and GeNorm have been developed that compare different candidates among each other to identify the best gene or a set of genes (Andersen et al. 2004; Vandesompele et al. 2002). This has to be done not only for every organism, because gene expression differs significantly, it is also necessary for different experiment setups like immune challenges or sampling from various tissues. Although reference genes are critical to obtain any reliable results they are often overlooked. This is one of the reasons why the strict MIQE guidelines (Minimum Information for Publication of Quantitative Real-Time PCR Experiments) were introduced (Bustin et al. 2009).

## 1.5. Urate Oxidases, allantoin and purine catabolism

Urate Oxidase (UO; EC 1.7.3.3) is a key enzyme in purine catabolism that degrades the lowly soluble uric acid to allantoin (Figure 8). Allantoin was already observed in maggot treated wounds nearly 100 years ago and attributed to healing properties (Robinson 1935). Lack of molecular methods and biochemical approaches made it impossible to identify the enzyme responsible for allantoin production and the underlying mechanism in wound healing could not be deciphered. Nowadays allantoin is assumed to cause a local and temporal multiplication of leukocytes during wound healing which hastens the healing process (DiSalvo 2002). The name Allantoin comes from allantois, an embryonic excretory organ of most mammals, where allantoin accumulates during development. Due to its presumed healing properties allantoin is a part of many cosmetically products.

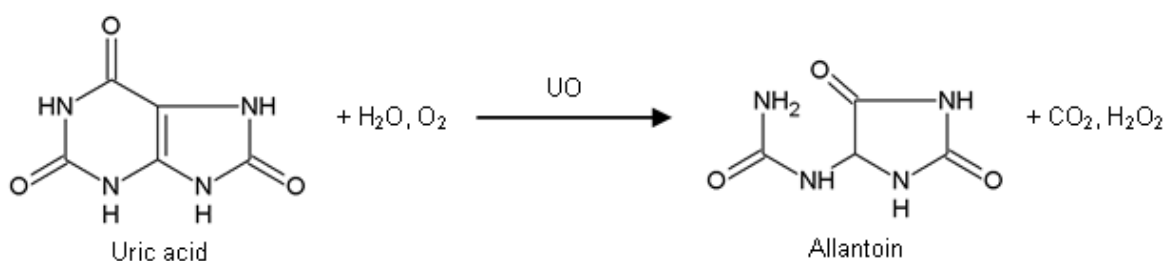


Figure 8: UO reaction mechanism.

The reaction of UOs was well studied during the last 20 years and revealed that the enzyme catalyzes the oxidation of uric acid to 5-hydroxyisourate and hydrogen peroxide. 5-hydroxyisourate spontaneously decomposes to 2-oxo-4-hydroxy-4-carboxy-5-ureidoimidazoline and subsequently to allantoin and carbon dioxide (Fetzner and Steiner 2010). UO is not depend on either a cofactor or a transition metal ion, which is uncommon for an oxidase (Gabison et al. 2006). UOs are ubiquitously present in bacteria, archaea and eukaryotes (Alvarez-Lario and Macarron-Vicente 2011). In vertebrates, the enzyme is present in the liver and frequently also in the kidney. It is located in peroxisomes and forms paracrystalline arrays, which are detectable by electron microscopy (Hayashi et al. 2000). Crystal structure of UO is so far only available for bacterial and fungal UOs, because they build soluble homotetrameric proteins. These form a dimer-dimer structure resulting in a tunneling-fold (T-fold) known for many homotetrameric proteins (Colloc'h et al. 1997; Juan et al. 2008).

Allantoin, the end product of the UO reaction, is not the end product of purine catabolism in most organisms. This ubiquitous catabolic pathway end only in mammals (except humans and higher primates) with allantoin. In fish and amphibians nitrogenous waste products are degraded down to urea and in marine invertebrates to ammonia. In purine catabolism, allantoin gets further degraded by

Allantoinase to allantoinic acid and by Allantoicase and Urease down to urea and ultimately ammonia as the most reduced nitrogen form (Alvarez-Lario and Macarron-Vicente 2011; Fujiwara and Noguchi 1995) (Figure 9). In insects Urease activity is unusual, because they lack the excess of water to counteract the toxic effects of high ammonia amounts (Wright 1995). Allantoicase activity is rare and cannot be

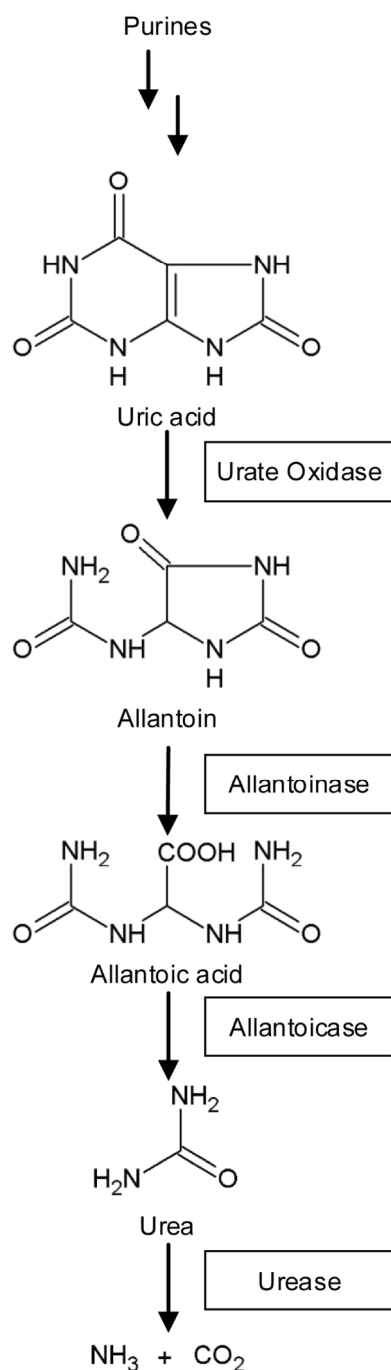


Figure 9: General purine catabolism pathway overview.

simply attributed to urea detection, because urea can also be produced by other pathways (Scaraffia et al. 2008). Urea is also observed in maggot treated wounds and like allantoin attributed to healing properties (Sherman 2014). Allantoinases activity was assumed to be present only in a few insect species (Bursell 1967; Kuzhivelil and Mohamed 1998) by the detection of allantoinic acid.

Due to multiple loss of function mutations during evolution UO is an inactive enzyme in humans and higher primates (Keebaugh and Thomas 2010). The purine catabolism in humans ends by lowly soluble uric acid with direct impact on human health (Alvarez-Lario and Macarron-Vicente 2010). At physiological pH a uric acid concentration of  $\geq 6.8$  mg/dL ( $400 \mu\text{M}$ ) in body fluids is described as hyperuricemia. Which is ten times less soluble compared to allantoin. The evolutionary advantage of high uric acid concentrations for early primates is still unclear. One prominent theory attributes it to the high antioxidant capacity of uric acid, which is responsible for the neutralization of  $> 50\%$  of free radicals in human blood (Alvarez-Lario and Macarron-Vicente 2011).

Precipitation of uric acid leads to gout, kidney stones, tumor lysis syndrome (TLS) and other medical complications (Alvarez-Lario and Macarron-Vicente 2011; Del Toro et al. 2005; Kim et al. 2016). In TLS high levels of uric acid occur by simultaneous lysis of tumor cells during chemotherapy. Those precipitate in the kidney, lead to acute renal failure and ultimately the death of patients (Davidson et al. 2004). To prevent those severe side effects the reduction of plasma uric acid levels weeks before chemotherapy is often necessary. Rasburicase is an FDA approved UO for prevention of TLS in chemotherapy (Mayne et

al. 2008). It originates from the fungus *Aspergillus flavus* and is recombinantly produced in the yeast *Saccharomyces cerevisiae* to reduce immunogenicity. Nevertheless it is not suitable for gout or kidney stones which would require long term UO application (Bomalaski et al. 2002; Goldman et al. 2001). To avoid long term uric acid precipitations allopurinol is currently the standard treatment. It is a competitive inhibitor of xanthine oxidase and thus inhibits the production of uric acid (Burns and Wortmann 2011). Long term application of allopurinol leads to accustoming in some patients. Due to its low solubility, similar to that of uric acid, this effect is not compensated by an increase in allopurinol dosage and uric acid is not reduced to the desired level anymore. Those cases are known as treatment failure gout and create an urgent need for an alternative solution UO can offer (Edwards 2008).

## 2. Aim of the project

Maggot debridement therapy (MDT) has been shown to promote wound debridement, disinfection and hastened healing processes, hence molecules present in larval E/S represent a rich source of new therapeutics (Sherman 2014). In this complex mixture of enzymes, AMPs and small molecules it is hard to decipher the roles and benefits of individual components in the wound healing process (Davydov 2011). The falling cost of next generation sequencing promote the sequencing of genome and transcriptome datasets even from non-model organisms. Those can be used as a first step to screen for medically and industrially relevant protein sequences. In a second step qRT-PCR can validate these candidates, but only if appropriate reference genes are available for the normalization of expression data (Gutierrez et al. 2008; Pfaffl et al. 2002; Vandesompele et al. 2002). This approach is ideal for the identification of *L. sericata* genes with important roles in wound healing. Thus such genes are likely to show different expression profiles in specific tissues or are modulated in the presence of wound pathogens. Once the candidate genes are identified the next challenge is to provide them in sufficient amount and purity for detailed analysis. One of the possibilities is heterologous production of recombinant proteins. In the last years the first *L. sericata* enzymes, two serine protease that support debridement and degrade extracellular matrix components (Pöppel et al. 2016; Telford et al. 2010) and three lysozymes contributing to disinfection (Valachova et al. 2014), were produced recombinantly. These enzymes were tested for their application potential and broadened our understanding of MDT mediated wound healing.

The observation that allantoin is present in maggot treated wounds was already made in 1935 (Robinson 1935). Since this time, allantoin is a part of many cosmetics products (DiSalvo 2002) and recently its accelerated establishment of normal skin was quantified in rats using an experimental open wound model (Araujo et al. 2010). The aim of this thesis was to validate reference gene candidates to enable tissue specific gene expression analysis via qRT-PCR and further to produce, characterize and understand the role of the allantoin producing enzyme(s) of *L. sericata* and its role in MDT.

Based on this state of knowledge the following topics were set as the main objectives of this thesis:

Validation of reliable *L. sericata* reference genes for candidate profiling

- For tissue specific profiling focused on secretory tissues
- For differential expression after immune challenge with Gram-negative bacteria

Identification and characterization of candidate enzyme(s) for allantoin production

- Localization in maggot tissues and role in wound healing
- Recombinant production and assessment of enzymatic properties

### 3. Methods

All standard molecular biology methods and biochemical approaches were performed based on Gentechnische Methoden 5<sup>th</sup> edition (Jansohn and Rothhämel 2012) or Molecular Cloning: A Laboratory Manual Methoden 4<sup>th</sup> edition (Green and MacCallum 2012) if not stated otherwise. For a short overview see Baumann et al. (2015) and Baumann et al. (2016) (submitted to Insect Biochemistry and Molecular Biology). For detailed information on all chemicals and material used in this study see supplement A.

#### 3.1. *Lucilia sericata*

##### 3.1.1. Maggot rearing

*L. sericata* larvae were obtained from BioMonde GmbH and transferred to Bioreactor 50 vented culture tubes (TubeSpin) using entomological forceps made of spring steel. First instar larvae were reared on Columbia Agar with Sheep Blood PLUS (Thermo Scientific Oxoid) for 72 hours (h) at 28 °C in the dark. The 3<sup>rd</sup> instar larvae were cleaned using sterile water before immune challenge or dissection.

##### 3.1.2. Immune challenge and zone of inhibition assays

Larvae were placed in Petri dishes on ice to reduce motility and facilitate injection of larvae with *Pseudomonas aeruginosa*. The dorsal posterior was pricked with a sterile 0.5 x 16 mm needle (wounded) or with a needle dipped in *P. aeruginosa* (DSM 50071) suspension (OD<sub>600</sub> = 60) in PBS (immune-challenged). Treated larvae were supplied with fresh blood agar and incubated for additional 24 h at 28 °C in the dark followed by the dissection of individual tissues. For the zone of inhibition assays, 7 ml of 1 % LB agar per plate was cooled to 42 °C, supplemented with 7 µl of fresh *E. coli* D31 (Monner et al. 1971) culture (OD<sub>600</sub> = 0.5) and poured into a Petri dish, before 3-mm wells were stamped into the agar using a sterile hole puncher. After 24 h equal volumes (3 µl) of hemolymph from naïve, wounded and immune-challenged larvae were collected and immediately applied to the agar wells. The plates were incubated at 37 °C for 24 h and 3 µl of 100 mg/ml ampicillin were used as a positive control.

##### 3.1.3. Tissue dissection

Larvae were cooled on ice and dissected using fine tip tweezers (Type 5, Dumont) by ripping the dorso-anterior cuticle in sterile 0.1 % DEPC treated PBS under a binocular microscope. The midgut, hindgut, salivary glands, crop, fat body, Malpighian tubes and nerve ganglion were harvested following Freeman and Bracegirdle (1971). Tissues were dissected in RA1 buffer (Macherey-Nagel) for RNA isolation (see 3.2.1) or in 1 x Laemmli-buffer for protein isolation (see 3.4.2).

## **3.2. RNA based *L. sericata* studies**

### **3.2.1. RNA isolation**

Total RNA from naïve and immune-challenged larvae as well as tissues, was extracted using the NucleoSpin RNA kit (Macherey-Nagel) according to manufacturer's recommendations. Those included a 15-min DNase I on-column digest and RNA was ultimately eluted in 60 µl (larvae) or 40 µl (tissues) RNase free H<sub>2</sub>O, respectively. Three pools of midgut (n = 5), hindgut (n = 10), salivary glands, crop, fat body, Malpighian tubes and nerve ganglion, (each n = 25) were collected in RA1 buffer, before RNA isolation. Total RNA from naïve and immune-challenged larvae (n = 5) was subsequently pooled in equimolar RNA amounts. Concentration and purity of RNA were determined by spectrophotometry (Take3, BioTek). Only samples with  $A_{260}/A_{280}$  and  $A_{260}/A_{230} > 1.8$  were further tested for quality by agarose gel electrophoresis. Samples that did not meet these criteria were cleaned and concentrated by sodium acetate precipitation (see 3.2.2).

### **3.2.2. RNA purification by sodium acetate precipitation**

To clean and concentrate isolated RNA, which was not already suitable for cDNA synthesis sodium acetate precipitation based on Walker and Lorsch (2013) was applied. RNA was supplemented with 3 M RNase free sodium acetate (pH 5.2, Thermo Fisher Scientific) to a final concentration of 0.3 M. 3 volumes of ice cold p. a. ethanol (100 %) were added, mixed and RNA precipitated at -20 °C overnight. Samples were centrifuged (18000 g, 30 min, 4 °C), washed (2 x) with 500 µl ice cold ethanol (80 %) and centrifuged (18000 g, 10 min, 4 °C). After the second wash the solution was removed and the pellet allowed to air dry. The pellet was resuspended in RNase free H<sub>2</sub>O and resulting RNA concentration and purity were determined spectrophotometrically (Take3, BioTek) like in 3.2.1.

### **3.2.3. RNA quality control by agarose gel electrophoresis**

Since photometric analysis are unable to indicate RNA degradations the RNA quality was determined by agarose gel electrophoresis. 1 µg total RNA was supplemented with 5 x RNA loading buffer (8 M urea, 0.5 mM EDTA, 0.1 % Bromphenol blue, 0.1 % Xylene cyanol) and filled with ddH<sub>2</sub>O to 10 µl. Samples were not heated to avoid degradation and transferred to a 1.2 % agarose gel with fresh TAE buffer. RNA was size separated for 45 min at 100V and samples were post stained with SYBR Safe (0.005 % in TAE) for 10 min. Followed by visualization using a Versadoc Imaging System (Bio-Rad). Only samples with at least one sharp band representing 18S rRNA were used for cDNA synthesis.

### 3.2.4. cDNA synthesis

Complementary DNA (cDNA) was synthesized using 1.5 µg of total RNA, oligo(dT)<sub>18</sub> primers and the First Strand cDNA Synthesis Kit (Thermo Fisher Scientific) according to manufacturer's recommendations. The resulting cDNA was diluted to a working concentration of 400 pg/µl, divided into aliquots and stored at -80 °C.

### 3.2.5. Candidate gene sequence assembly

The 10 *L. sericata* reference gene candidates were selected based on known reference genes from the closely-related species *Lucilia cuprina* (Bagnall and Kotze 2010) and other arthropods (Beckert et al. 2015; Nijhof et al. 2009). *Urate oxidase* and further purine catabolism gene candidates (*allantoinase*, *allantoicase* and *urease*) were searched based on sequences from insects (Scaraffia et al. 2008) and other organism (Fujiwara and Noguchi 1995). The peptide sequences of each gene (or the nucleotide sequences of *18S* and *28S rRNA*) were queried against the *L. sericata* transcriptome database (Pöppel et al. 2015) using the BLAST algorithm. BLASTn was used to find all reads matching the search results and the pool of these reads was expanded to include further paired-end read partners. The final group of reads was assembled using Trinity (Grabherr et al. 2011) and this step was repeated until the complete coding sequences were acquired. Finally, Gap5 (Bonfield and Whitwham 2010) was used to verify the finished sequences with mapped reads assembled by Bowtie (Langmead et al. 2009). Whole coding sequences of all assembled genes were submitted to GenBank (Table 1).

Table 1: Genes and qRT-PCR primers evaluated in this thesis.

Gene name	Abbreviation	Accession no.	Primer sequences (5'-3')	L (bp) <sup>a</sup>	E (%) <sup>b</sup>	R <sup>2c</sup>
<i>18S ribosomal RNA</i>	<i>18S rRNA</i>	KR133393*	Fwd 5' AGCAGTTTGGGGCATTAG 3' Rev 5' GCTGGCATCGTTTATGGTTAG 3'	171	94	0.996
<i>28S ribosomal RNA</i>	<i>28S rRNA</i>	KR133394*	Fwd 5' CCAAAGAGTCGTGTGCTTG 3' Rev 5' ATTCAGGTTTCATCGGGCTTA 3'	180	91	0.997
<i>40S ribosomal protein S3</i>	<i>RPS3</i>	KR133395*	Fwd 5' TCAAGGTGTTTTGGGTATCAAGG 3' Rev 5' GCGGGCATTTTGTATTCTGTTTC 3'	156	90	0.999
<i>60S acidic ribosomal protein P0</i>	<i>RPLP0</i>	KR133397*	Fwd 5' GGTGCTGATAATGTTGGTTC 3' Rev 5' ACCCATAAGGACGACACC 3'	78	101	0.995
<i>actin</i>	<i>actin</i>	KR133398*	Fwd 5' TGCCGATCGTATGCAAAA 3' Rev 5' ACGGAGTATTTGCGTTCTGG 3'	90	100	0.998
<i>allantoinase</i>	<i>Alla</i>	KX840072*	Fwd 5'ATCGGAGGCGGTATATGACTTTG 3' Rev 5' TTGTGGCGGTTAAAAATCCTTC 3'	116	95	0.991
<i>attacin-2</i>	<i>atta2</i>	KR920003*	Fwd 5' GCACCTTAGCCTACAATAACAATGG 3' Rev 5' ACTGATGCTCTTGGTCAAAGTATCG 3'	92	103	0.999
<i>Beta-1-tubulin</i>	<i>β-tubulin</i>	KR133399*	Fwd 5' AAACCTAACCCACCCACATACGG 3'	173	90	0.999

Gene name	Abbreviation	Accession no.	Primer sequences (5'-3')	L (bp) <sup>a</sup>	E (%) <sup>b</sup>	R <sup>2c</sup>
			Rev 5' AGAGGAGCAAACCAGGCAT 3'			
<i>cAMP-dependent protein kinase</i>	<i>PKA</i>	KR133400*	Fwd 5' CAACACAAGCCGACAAAAGAC 3'	145	106	0.995
			Rev 5' GATAGCGTAGGGAACCAAGAA 3'			
<i>defensin-1</i>	<i>def1</i>	KT149727*	Fwd 5' CGGAGTTACATGGTCGTTACAAGAG 3'	164	109	0.993
			Rev 5' CGGTGTCCAATCAACAAACAGTG 3'			
<i>Elongation factor 1-alpha 1</i>	<i>EF1α</i>	KR133396*	Fwd 5' TGTCGGTGTCAACAAGATGG 3'	137	93	0.998
			Rev 5' GAGATGGGAACGAAGGCAAC 3'			
<i>Glutathione S-transferases 1-1</i>	<i>GST1</i>	KR133402*	Fwd 5' GCCAGTGTGACGACCTTCG 3'	120	92	0.999
			Rev 5' GCAACCTTCCCAGTTTTCATC 3'			
<i>Glyceraldehyde-3-phosphate dehydrogenase 1</i>	<i>GAPDH</i>	KR133401*	Fwd 5' GAACGGCAAACACTACTGGTATG 3'	182	104	0.997
			Rev 5' CGGTGGAAACGACTTCTTCATC 3'			
<i>lucimycin</i>	<i>lfp</i>	KJ413251	Fwd 5' TCGCTTTAATCGCCGTTGTT 3'	103	96	0.999
			Rev 5' ATGATGCCAGCCTGTTGTTTC 3'			
<i>urate oxidase</i>	<i>UO</i>	KX840071*	Fwd 5' ACCCAAACAACCGTTATTAGCG 3'	150	96	0.996
			Rev 5' TCCCAAGAACAATCAACAATCG 3'			

\*Indicates GenBank submission of sequence obtained in this thesis.

<sup>a</sup>Length of amplicon. <sup>b</sup>Quantitative RT-PCR efficiency. <sup>c</sup>Coefficient of determination.

### 3.2.6. Primer design and evaluation for qRT-PCR

Gene-specific primers were designed using Oligo Explorer v1.1.2 (<http://www.softpedia.com/get/Science-CAD/Oligo-Explorer.shtml>) to yield primers 19–23 nucleotides in length with amplification products of 50–210 bp and  $T_m$  values of ~60 °C. All primers (Table 1) were ordered from Sigma-Aldrich and subsequently tested in a standard curve assay including melt curve analysis using the StepOnePlus Real-Time PCR System (Applied Biosystems). The cDNA concentrations corresponding to 50-3.2 ng of total RNA were used in 5-fold dilutions with the cycling conditions recommended by the manufacturer. Briefly, hot-start PCR with denaturation at 95 °C for 10 min was followed by 40 cycles of 95 °C for 15 s and 60 °C for 60 s, and finally the melt curve analysis with a temperature increase from 60 °C to 95 °C in 0.5 °C steps. Reaction efficiency was calculated using StepOne Software v2.3 and only primers with an efficiency of 90–110 %,  $R^2 \geq 0.99$  and a single sharp melt curve peak were used for further analysis.

### 3.2.7. Quantitative RT-PCR

Quantitative RT-PCR was carried out on a StepOnePlus system (Applied Biosystems) using optical 96-well plates (Applied Biosystems). The total reaction volume of 10 µl contained 5 µl Power SYBR Green PCR Master Mix (Applied Biosystems), 1 µl (400 pg; 10 ng in case of *allantoinase*) cDNA and 300 nM of each primer pair except for *β-tubulin* (150 nM), *EF1α* (150 nM) and *actin* (450 nM forward primer and 150 nM reverse primer). All reactions were carried out in three technical replicates under the reaction conditions stated above (see 3.2.6). Baseline correction was performed automatically by StepOne

---

Software v2.3 and the quantification cycle (Cq) was always determined at an intensity of 0.15. All cDNA samples and corresponding RNA without reverse transcription (no-RT control) were tested with the *18S rRNA* primers to estimate the remnants of genomic DNA (Bustin 2002) and only samples with a  $\Delta Cq \geq 10$  were accepted.

### 3.2.8. Normfinder and GeNorm analysis

The Normfinder and GeNorm algorithms were used to assess all *L. sericata* reference genes. Normfinder was used as an add-in for Microsoft Excel (<http://moma.dk/normfinder-software>), raw Cq values were used and log transfer was performed by the software. The model-based Normfinder approach relies on groups of sample types (tissues in this case) and should be used with 5-10 candidate reference genes. It estimates intragroup and intergroup variation of every single reference gene separately and subsequently combines them into a so-called stability value. Lower numbers equating a more stable expression. The program does not sequentially eliminate unsuitable genes so the pre-exclusion of genes with large variances is necessary to achieve reliable results (Andersen et al. 2004).

GeNorm was used as part of the R package NormqPCR with R version 3.1.1 (Perkins et al. 2012). Raw Cq values were used and log transfer was performed by the software. The GeNorm algorithm is based on the principle that the expression ratio of two ideal control genes is identical throughout all samples. In consequence any variation implies that these genes are not equally expressed whereas the bigger this difference the lower the expression stability. By calculating the standard deviation of expression ratios for every control gene with all other candidates the algorithm determines gene variation. The gene-stability measure M is the average of this pairwise variation and genes with the lowest M value are most stable. The gene with the highest M value gets excluded and another comparison cycle is calculated until only the best two genes are left. By excluding the least suited candidate in every cycle no exclusion of unsuited genes prior to analysis is needed (Vandesompele et al. 2002).

### 3.2.9. Gene expressions analysis

To evaluate the tested reference genes three *L. sericata* immune genes (*lucimycin*, *defensin-1* and *attacin-2*) were selected. Those are known to be differentially expressed, when the larval immune system was challenged (Pöppel et al. 2015). The AMPs were chosen based on their activity spectrum, with lucimycin (afp) targeting fungi (Pöppel et al. 2014), defensin-1 targeting Gram-positive (Imler and Bulet 2005) and attacin-2 targeting Gram-negative bacteria (Imler and Bulet 2005), respectively. Gene expression profiles upon immune challenge were determined by qRT-PCR using the  $\Delta\Delta Cq$  method (Pfaffl 2001) in Rest2009 (<http://www.genequantification.de/rest-2009.html>). Efficiencies greater than 100 % were set to 100 % because Rest2009 does not allow higher values. The data were normalized using three different combinations of genes from the reference gene assessment: (a) the two best reference genes for every sample (GeNorm); (b) the three overall best reference genes (GeNorm and Normfinder); and (c) the six overall best reference genes (GeNorm).

The three overall best reference genes provided by both GeNorm and Normfinder (*RPS3*, *RPLPO* and *EF1 $\alpha$* ) were used for further analysis. To determine gene expression profiles among naïve tissues relative  $\Delta\Delta Cq$  comparison like above was applied. Expression was compared to the tissue with the lowest expression, which was nerve ganglion for *urate oxidase* and fat body for *allantoinase*.

### 3.2.10. RNA in situ hybridization (ISH)

In situ hybridization assay was modified from (Valachova et al. 2014; Zimmerman et al. 2013). Malpighian tubes were dissected directly into 4 % paraformaldehyde (in PBS) and fixed overnight at 4 °C. Samples were washed (3 x 10 min) in PBS containing 0.2 % Tween 20 (PBST) and treated by Proteinase K (50 µg/ml in PBST) for 10 min at room temperature. Samples were incubated 5 min at room temperature in PBST-Glycin (2 mg/ml), washed (2 x 5 min) in PBST, refixed in 4 % paraformaldehyde (in PBS) for 1 hour at room temperature and washed again (1 x 5 min) in PBST. Next, the samples were equilibrated in 1:1 PBS:hybridization solution (HS: 50 % formamide, 5 x saline-sodium citrate, 50 µg/ml Heparin, 100 µg/ml Salmon testes DNA, 0.1 % Tween 20, all components from Sigma-Aldrich, Munich, Germany) for 5 min and in HS for 5 min at room temperature followed by incubation in HS for 1 hour at 48 °C. *UO* and *RPS3* (positive control) specific primers (Table 2) were used to synthesize gene specific probes using PCR DIG Probe synthesis kit (Roche, Mannheim, Germany) according to manufacturer's instruction. Probes (10 µl) were mixed with 90 µl of HS solution, boiled for 45 min in a water bath and incubated with samples for 24 h at 48 °C. The probes were then removed and tissues were washed in pre-warmed (48 °C) HS overnight. Next, the samples were washed (1 x 5 min) with pre-warmed (48 °C) HS, HS:PBST (1:1) and (2 x 10 min) PBST followed by blocking with 1 % BSA in PBST for 30 min at room temperature. The blocking agent was removed and samples were incubated overnight at 4 °C with the alkaline phosphatase (AP)-labelled sheep anti-digoxigenin antibody (1:1000 in PBST; Roche, Mannheim, Germany). Samples were washed (3 x 5 min) with AP buffer (100 mM Tris pH 9.5, 50 mM MgCl<sub>2</sub>, 100 mM NaCl, 0.1 % Tween-20) and stained with nitroblue tetrazolium and bromo-chloro-indolyl-phosphate solution (NBT-BCIP, Roche, Mannheim, Germany) diluted 1:50 in AP buffer. The color development of the *UO* probe was controlled under the binocular microscope, stopped by PBS washes (3 x 5 min) and the same time applied for the control probes. Unspecific staining was removed by wash (2 x 10 min) with 70 % Ethanol (in PBS), (2 x 5 min) 100 % ethanol and samples were mounted on glass slides in 90 % glycerol. HS solution and nonspecific probe (PCR DIG Probe synthesis kit) were used as negative controls. Results were analysed using a Mz16 F microscope (Leica Microsystems).

Table 2: ISH primer used in this thesis.

Gene name	Abbreviation	Accession no.	Primer sequences (5'-3')
<i>40S ribosomal protein S3</i>	<i>RPS3</i>	KR133395	Fwd 5' GGGTTGCGAAGTCGTTGTTT 3' Rev 5' GCGGGCATTCTGATTCGTTC 3'
<i>Urate oxidase</i>	<i>UO</i>	KX840071*	Fwd 5' CTCCCAACTTTTCCACATTCAA 3' Rev 5' TCCCAAGAACAATCAACAATCG 3'

### 3.3. Production and characterization of recombinant Urate Oxidase (UO<sub>r</sub>)

#### 3.3.1. UO<sub>r</sub> sequence synthesis

To produce the *L. sericata* UO recombinant (UO<sub>r</sub>) in *E. coli* a synthetic codon-optimized gene encoding the deduced amino acid sequence was synthesized by Eurofins MWG Operon (Ebersberg, Germany) and subcloned into the *E. coli* expression plasmid pASK IBA37plus (IBA) containing an N-terminal His<sub>6</sub>-Tag (Figure 10).

```

atggctagcagaggatcgcatcaccatcaccatcacatcgaagggcgctttgctcgtccc
M A S R G S H H H H H H I E G R F A R P
ttgcagcgtcctagtggaaaggggacaccgcagcaagatcggaagcccctcatcagtac
L Q R P S G K G T P Q Q D R E A P H Q Y
acgatctccgatcatgggatggcaaagacagtggttaaagtcctgcatgttaaacgcgat
T I S D H G Y G K D S V K V L H V K R D
ggcccagtacactcgatcaaagagtttgaggtaggcacccatctgaaactctactccaag
G P V H S I K E F E V G T H L K L Y S K
aaagactactttcatggcgacaatagcgatatcgtggcgactgacagccagaaaaatacc
K D Y F H G D N S D I V A T D S Q K N T
gtatatctgctcgcgaagaaatggcattgagaatccagagaaatgggcttattctt
V Y L L A K K F G I E N P E K F G L I L
gcatcgacttctgaacaaatagcgcgatgtcgaagaagtgcacattcagtggaagaa
A S H F L N K Y A H V E E V H I H V E E
tatccctggcaacggatggccaggatcaagttggtggtacaaccggcgcatgtggtgat
Y P W Q R I C Q D Q V G G T T G A C G D
gctccgaacttcagtacgttcaataatcgccagaaacacaaccatgccttcattttcacc
A P N F S T F N N R Q K H N H A F I F T
cctacggaagttcgtattgcatgtggtgttacgctcgtactgaaccgaaacagaccgta
P T E V R Y C D V V L R R T E P K Q T T
attagcgtattcgtggactcggggttctgaaaacgacgcaaagtagcttcgtgaacttt
I S G I R G L R V L K T T Q S S F V N F
gtgaacgacgaatctcgtctctgcccggatcagtatgaccgcattttctcaaccatcgtc
V N D E F R S L P D Q Y D R I F S T I V
gattgctcttgggaatactcacgcaccaataatgtcaaattctgtcaggactggaatag
D C S W E Y S R T N N V K F C Q D W N T
gtgaagaacatcatcatcaagaaatcgcggggatccgaatggtggcacttcaagcccg
V K N I I I K K F A G D P N V G T S S P
tcggtgcaacatactctgtatctgaccgagaaagaagtcttagatgccttgccagaagta
S V Q H T L Y L T E K E V L D A L P E V
tccgtgattagcatgaccatgccgaacaaactactttaaactttgacacaaaaccgttt
S V I S M T M P N K H Y F N F D T K P F
cagtcggttgtccaggtgaaaacaacgaggtgtttatcccggtcgataaacgcgatggc
Q S V V P G E N N E V F I P V D K P H G
accatttacgcacaactggcgcgcaaggatctggcctctcacttataa
T I Y A Q L A R K D L A S H L -

```

Figure 10: DNA and protein sequence of codon optimized *L. sericata* Urate Oxidase. Including N-terminal His<sub>6</sub>-Tag (black box) and Factor Xa motive (grey box).

### 3.3.2. Production of UO<sub>r</sub> in *E. coli*

Chemical competent *E. coli* BL21(DE3) cells (New England Biolabs) were transformed with the UO<sub>r</sub> expression plasmid (25 ng) in according to manufacturer's recommendations. Cells were grown in terrific broth medium (Roth) to an OD<sub>600</sub> of 0.9 before the expression was induced by 200 µg/l anhydrotetracycline and carried out for 3 h at 37 °C and 180 rpm. Followed by harvest (5000 g, 10 min, 10 °C), resuspension in lysis buffer (30 mM Tris, 100 mM NaCl, pH 7.5) and lysis using a MP110PS high pressure microfluidiser (Microfluidics, Newton, US). Lysed cells were centrifuged (75000 g, 30 min, 10 °C) and pelleted inclusion bodies were solubilized in chaotropic buffer (8 M guanidine hydrochloride, 30 mM Tris, pH 7.5) by stirring overnight at room temperature. The remaining insoluble fraction was removed by additional centrifugation (75000 g, 30 min, 10 °C) prior purification.

### 3.3.3. IMAC purification of UO<sub>r</sub>

UO<sub>r</sub> was purified by cobalt-based IMAC under denaturing conditions using a SE-04 FPLC system (ECOM) fitted with a column containing TALON resin (Clontech). The lysate was loaded onto the column and washed with buffer A (6 M urea, 30 mM Tris, 100 mM NaCl, pH 7.5). Recombinant enzyme was eluted by buffer B (6 M urea, 30 mM Tris, 100 mM NaCl, 200 mM imidazole, pH 7.5) and fractions containing UO<sub>r</sub> were collected manually by absorption at 280 nm and analyzed by SDS-PAGE.

### 3.3.4. SDS-PAGE

Size separation of proteins by denaturing SDS-PAGE was performed with a 4–15 % Mini-PROTEAN TGX Gel (Bio-Rad) in a Mini-PROTEAN Tetra System (Bio-Rad). Samples were supplemented with 3 x Laemmli-buffer containing 2 % β-mercaptoethanol (Fc) and denatured for 10 min at 95 °C. Samples and a protein size standard (PageRuler Plus, Fermentas) were loaded on the gel and separated at constant voltage (300 V) for 18 min. Gels were used for Western Blot (3.4.2) or stained with Roti-blue quick (Roth) coomassie according to manufacturer's recommendations. Protein bands were documented using a Versadoc Imaging System (Bio-Rad).

### 3.3.5. UO<sub>r</sub> refolding by dialysis

Purified UO<sub>r</sub> was diluted to a final concentration of 100 µg/ml in elution buffer B (6 M urea, 30 mM Tris, 100 mM NaCl, 200 mM imidazole, pH 7.5), supplemented with 1 % β-mercaptoethanol and reduced at 37 °C for 20 min. UO<sub>r</sub> was dialyzed against dialysis buffer (150mM NaCl, 20mM Tris, pH 7.5) for 18 h at 4 °C and centrifuged (18000 g, 4 °C, 30 min) to remove all precipitated protein. Resulting supernatant was dialyzed once more under identical conditions to decrease β-mercaptoethanol concentration, centrifuged (18000 g, 4 °C, 30 min). Final protein concentration was determined using

the BCA Protein Assay Kit (Pierce; Thermo Scientific) according to manufacturer's recommendations and enzyme was stored at 4 °C for subsequent analysis.

### 3.3.6. Determination of UO<sub>r</sub> pH optimum

A two-step colorimetric assay (Fraisse et al. 2002) was applied to determine pH optimum of UO<sub>r</sub>. Briefly, in the first reaction step 0.5 mM uric acid in 20 mM corresponding buffer (sodium citrate pH 4-5.5, sodium phosphate pH 6-8 or sodium borate 8.5-10) were used (10 min at 25°C). Resulting in allantoin and H<sub>2</sub>O<sub>2</sub> production in equimolar amount by UO. The amount of produced H<sub>2</sub>O<sub>2</sub> was monitored in the second step by addition of quantification buffer (0.5 mM 3,5-dichloro-2-hydroxybenzene sulfonic acid (DCHBS), 0.125 mM 4-amino-antipyrine (4-AAP), 12.5 U/ml horseradish peroxidase (HRP), 0.25 M sodium phosphate, pH 6). In this step a stable red quinoneimine dye is formed over a radical-substitution reaction induced by H<sub>2</sub>O<sub>2</sub> (Figure 11). The absorbance of the final product was measured at 515 nm after 10 min at 25°C on an Eon microplate spectrophotometer (BioTek Instruments).

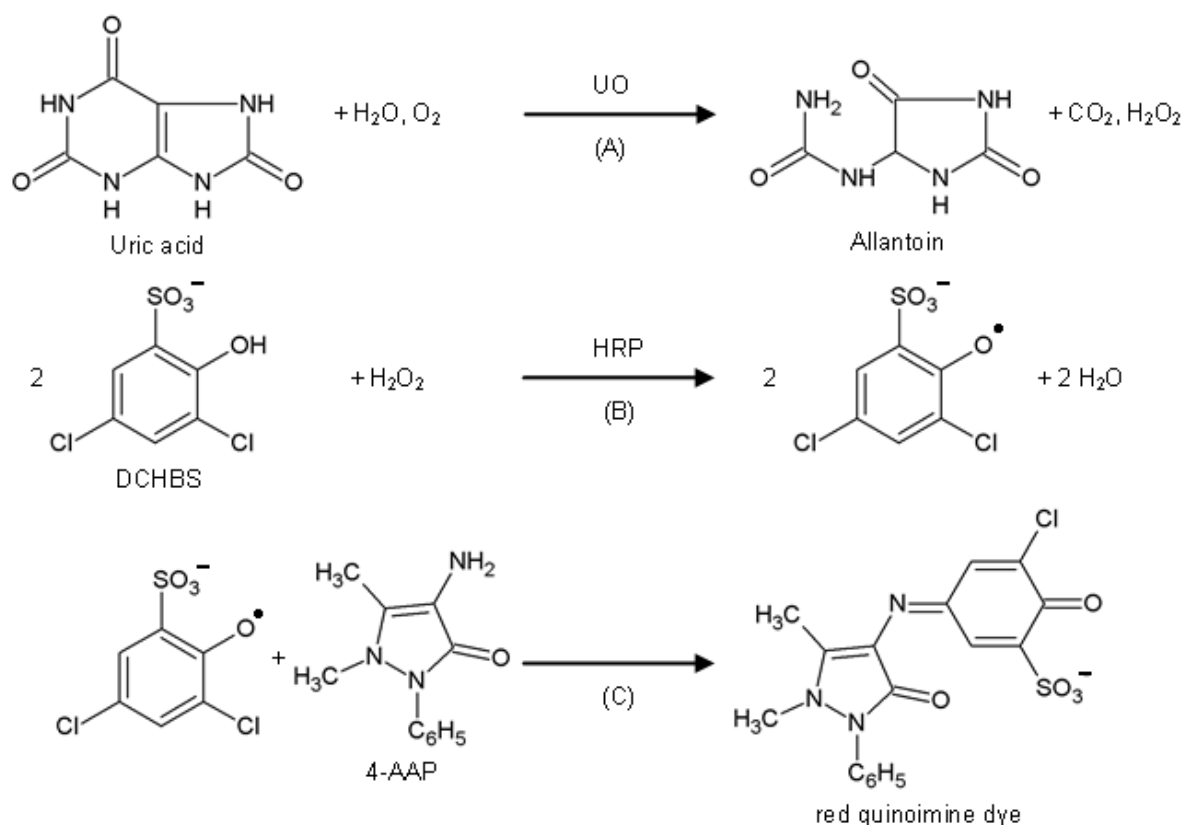


Figure 11: Two-step colorimetric UO assay. (A) Incubation of uric acid with UO results in allantoin, CO<sub>2</sub> and H<sub>2</sub>O<sub>2</sub>, (B) HRP catalysis the DCHBS oxidation in the presence of H<sub>2</sub>O<sub>2</sub>, and (C) The final red quinoneimine dye is produced by phenoxy radical reaction with 4-AAP (according to Fraisse et al. 2002).

### **3.3.7. Determination of UO<sub>r</sub> temperature optimum, competitive inhibition, metal ion dependence and stability**

In all other cases UO<sub>r</sub> activity was monitored by a continuous assay using Amplex Red Uricase Assay Kit (Fisher Scientific). 200 ng enzyme were applied and assay conditions were modified based on manufacturer's recommendations. The stable end product Resorufin was measured at 560 nm after 30 min using an Eon microplate spectrophotometer (BioTek).

Temperature optimum was determined in a range of 20-60 °C in 5 °C steps with 0.5 mM uric acid, 50 µM Amplex Red, 0.2 U/ml horseradish peroxidase and 100 mM sodium chloride in 45 mM Tris-HCl at pH 7.5. Competitive inhibition by 8-azaxanthine was tested in a range of 1-1000 µM versus 0.1 mM uric acid with 50 µM Amplex Red, 0.2 U/ml horseradish peroxidase and 100 mM sodium chloride in 45 mM Tris-HCl, pH 7.5 at 25 °C. Metal ion dependence was tested with 10 mM of corresponding ions (CaCl<sub>2</sub>, MgCl<sub>2</sub>, MnCl<sub>2</sub> ZnCl<sub>2</sub> or NiSO<sub>4</sub>) or 50 mM EDTA in 0.5 mM uric acid, 50 µM Amplex Red, 0.2 U/ml horseradish peroxidase and 100 mM sodium chloride in 45 mM Tris-HCl, pH 7.5 at 25 °C. Storage stability in assay buffer (100 mM sodium chloride, 45 mM Tris-HCl, pH 7.5) at 25 °C was determined after 0, 4, 24 and 168 h. with 0.5mM uric acid, 50 µM Amplex Red and 0.2 U/ml horseradish peroxidase at 25 °C.

## **3.4. Localization of native UO in larval tissue**

### **3.4.1. Production of polyclonal anti-UO antibodies**

Antisera containing specific UO polyclonal antibodies against refolded UO<sub>r</sub> were raised in guinea pig at Eurogentec (Seraing, Belgium). Animals were immunized on days 0, 14, 28 and 56 with 60 µg UO<sub>r</sub> and blood was collected on day 87.

### **3.4.2. Western blot**

For western blot analysis larval tissues were dissected (see 3.1.3) directly into 1 x Laemmli-buffer and homogenize with a metal pestle. Samples were incubated at 95 °C for 10 min and insoluble material was removed by centrifugation (18000 g, 5 min). The supernatant was divided into work aliquots and stored at -80 °C. Maggot secretions and excretions (E/S) from 100 maggots (3 days old) were collected in 1 ml of PBS for 1 h at 28 °C. Collected samples were supplemented with 3 x Laemmli-buffer and incubated at 95 °C for 10 min and work aliquots were stored at - 80 °C. Tissue samples as well as E/S were resolved by reducing SDS-PAGE (see 3.3.4) and stained with Roti-Blue quick (Roth) or transferred to a PVDF membrane (Merck Millipore) using the TransBlot Turbo Transfer System (Bio-Rad). Membrane was blocked for 2 h in Qiagen Blocking Reagent, washed with Tris-buffer saline (TBS) and TBS containing

0.1 % Tween 20 (TBST) (3 x 10 min) and incubated at room temperature with polyclonal UO antibodies (1:500 in blocking reagent) overnight. After washing with TBS/TBST (3 x 10 min) the membrane was incubated with secondary goat anti guinea pig F(ab')<sub>2</sub> fragment horseradish peroxidase (HRP) conjugate antibody (Dianova) (1:5000 in TBS) for 2 h at room temperature. Readout was facilitated with Lumi-Light<sup>PLUS</sup> Western Blotting Substrate (Roche) and the resulting signal was visualized using a Versadoc Imaging System (Bio-Rad).

### **3.4.3. Whole mount fluorescence immunohistochemistry**

Whole mount staining was modified based on a *Harmonia axyridis* procedure by Beckert et al. (2016). Dissected Malpighian tubes including gut parts were fixed in 4 % formaldehyde in PBS for 45 min. The samples were then washed with PBS (3 x 20 min), permeabilized with 0.5 % Triton X-100 in PBS for 1 h and blocked with blocking solution (Roti-ImmunoBlock, Roth) for 1 h. This was followed by incubation with anti-UO antibodies (1:1200 in blocking solution) overnight at 4 °C. Subsequently, samples were washed with PBS (3 x 20 min) and incubated with secondary goat anti guinea pig F(ab')<sub>2</sub> fragment Alexa488 conjugate antibody (Dianova) (1:500 in blocking solution) for 2h in the dark. Samples were washed with PBS (3 x 20 min), stained with 4, 6-Diamidino-2-phenylindole (DAPI) (1 µg/ml) in PBS for 10 min, washed with PBS (3 x 20 min) and mounted in Aqua-Poly/Mount (Polysciences) before transferred to a microscope slide. Readout was performed on a Leica Mz16 F microscope or a Leica TCS SP8 confocal microscope (Leica Microsystems).

## 4. Results

### 4.1. *L. sericata* reference gene assessment

Results presented in this section were published under Baumann et al. (2015).

#### 4.1.1. Candidate genes selection

To establish normalization of gene expression in various *L. sericata* tissues I picked 10 candidate reference genes and monitored the expression level of those before and after challenging the larvae with *P. aeruginosa*. The goal was to identify reference genes appropriate for different larval tissues, with the key criterion that gene expression is not affected by immune challenge. The tissues were selected based on their role in secretion and/or digestion (salivary glands, crop, midgut and hindgut) and supplemented by additional tissues (nerve ganglion and fat body). Candidates were chosen based on earlier studies in arthropods using orthologs of these genes (Bagnall and Kotze 2010; Nijhof et al. 2009). To minimize the risk of co-regulation, selected genes representing different functional classes of proteins. The *L. sericata* transcriptome database was explored to identify orthologs and the coding sequences of the 10 selected candidate reference genes were submitted to GenBank (Table 1).

To evaluate the tested reference genes three *L. sericata* immune genes (*lucimycin*, *defensin-1* and *attacin-2*), which are differentially expressed during immune challenge were selected (Pöppel et al. 2015).

Ultimately to identify enzyme candidates for allantoin production our *L. sericata* transcriptome was explored for UO homologs and the search was expanded for further purine catabolism enzymes to account for urea production. A single *urate oxidase* (KX840071) and a single *allantoinase gene* (KX840071) were found and both sequences were deposited to GenBank. Homologues of *L. sericata* *allantoicase* or *urease* could not be detected on mRNA level. Without a complete set of enzymes to generate urea I focused on the production and subsequent characterization of *L. sericata* UO for uric acid degradation and allantoin production.

#### 4.1.2. Tissue specific RNA quality

Spectrophotometric measurements of isolated RNA showed values of  $A_{260}/A_{280}$  and  $A_{260}/A_{230} > 1.8$  for all except one crop and three fat body samples in immune-challenged larvae. Those 4 were sodium acetate precipitated after the RNA isolation. Spectrophotometric measurements only give information regarding RNA purity, but not about overall quality and degradation. As a final quality check agarose gel electrophoresis was performed to visualize quality of 28S and 18S rRNA to give a hint about the

underlying mRNA population. All naïve and immune-challenged samples show at least one sharp band representing 18S rRNA (Figure 12) and were suitable for cDNA synthesis. The upper 28S rRNA band is visible in most samples, but never exceeds the 18S rRNA band and does not reach the ideal 2:1 ratio of a no degraded sample. Malpighian tube collection was not part of the immune-challenge experiment and only naïve samples were collected.

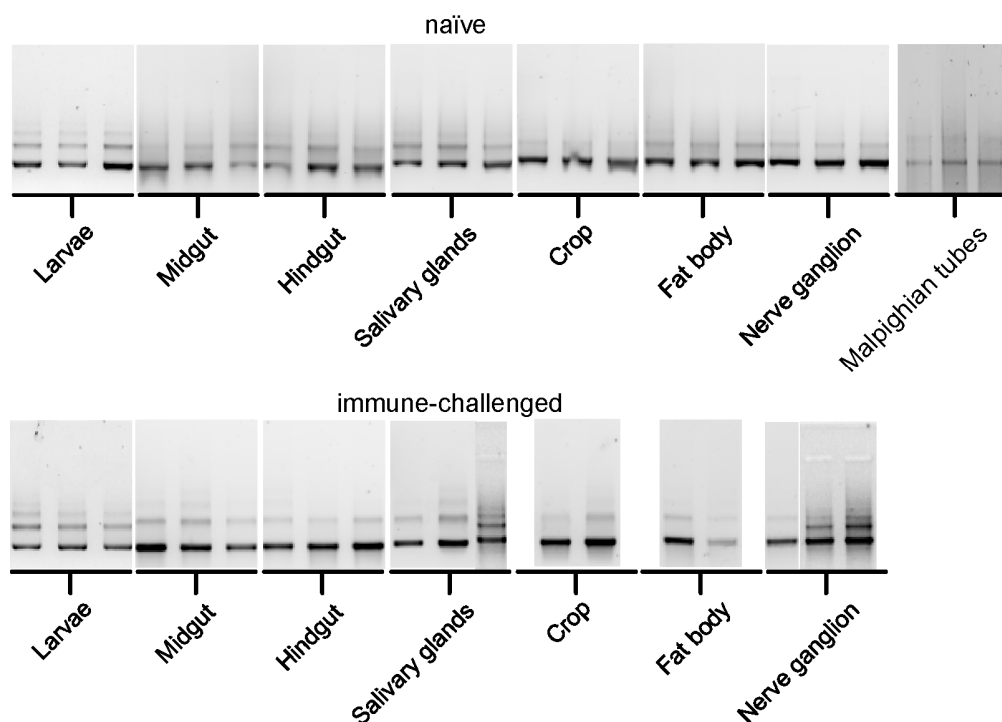


Figure 12: *L. sericata* RNA from naïve (top) and immune-challenged (bottom) larvae and tissues was analyzed using agarose gel. One crop and three fat body samples in immune-challenged larvae were sodium acetate precipitated after the RNA isolation. Thus they were limited in sample amount they are not displayed in purity used for cDNA synthesis. Malpighian tube collection was not part of the immune-challenge experiment and only naïve samples were collected.

#### 4.1.3. Quantitative RT-PCR

The efficiencies of each qRT-PCR primer pair were generally high. Based on the standard curve slopes determined using StepOne software, the efficiencies ranged from 90 % to 109 % with  $R^2$  values  $> 0.99$  for all pairs (Table 1). Linear behavior was observed over a concentration range spanning four orders of magnitude (50 ng to 3.2 pg of cDNA). The absence of primer dimers was confirmed by a melting curve analysis, which resulted in only one sharp peak for each amplicon under those experimental conditions (Figure 24 in Sup B.1). All 10 reference genes were expressed in all naïve and immune-challenged samples. Median expression values ranged from 19 Cq (18S rRNA) to 26 Cq (PKA) and standard deviations ranged from 0.75 Cq (RPS3) to 2.1 Cq (actin) as shown in Figure 13.

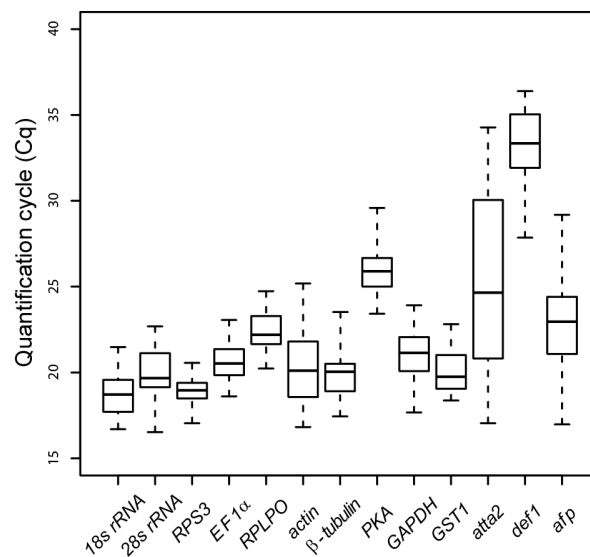


Figure 13: Distribution of quantification cycle (Cq) values for *L. sericata* candidate genes obtained by qRT-PCR. Data for all naïve and immune-challenged samples were pooled ( $n = 42$ ). Boxplots show first to third quartile of values in the box, the center line indicates the median, vertical dotted bars extend to the highest and lowest value.

#### 4.1.4. Zone of inhibition assays and initial analysis of attacin-2 expression

To monitor the changes in larval reference gene expression triggered by interaction with bacteria, I chose the opportunistic pathogen *P. aeruginosa* and direct infection by pricking the *L. sericata* larvae with a bacteria-coated needle (Mulcahy et al. 2014). *P. aeruginosa* has previously been used to induce an immune response (Pöppel et al. 2015) and is also a common pathogen found in chronic wounds. Two independent tests were used to monitor the success of the immune challenge.

The first was a zone of inhibition assay with *E. coli* strain D31 (Monner et al. 1971). Hemolymph from naïve, wounded and immune-challenged larvae were applied to the agar wells and the plates were incubated at 37 °C for 24 h. Only the hemolymph from immune-challenged larvae produced distinct inhibition zones (Figure 13A).

As a second test, I carried out an initial analysis of gene expression profiles to monitor changes at the RNA level triggered by immune challenge, using *attacin-2* mRNA as a marker because this AMP is known to be upregulated under similar conditions (Pöppel et al. 2015). The raw Cq values for *attacin-2* mRNA from two distinct populations, i.e. the naïve samples (Cq ~30) and the immune-challenged (Cq ~20), are shown in (Figure 13B). No naïve sample showed a lower value than the corresponding immune-challenged sample. These raw data supported the initial hypothesis that *L. sericata attacin-2* mRNA is induced by immune challenge with a Gram-negative bacterium, but can only be validated by normalizing against the expression levels of reliable reference gene(s).

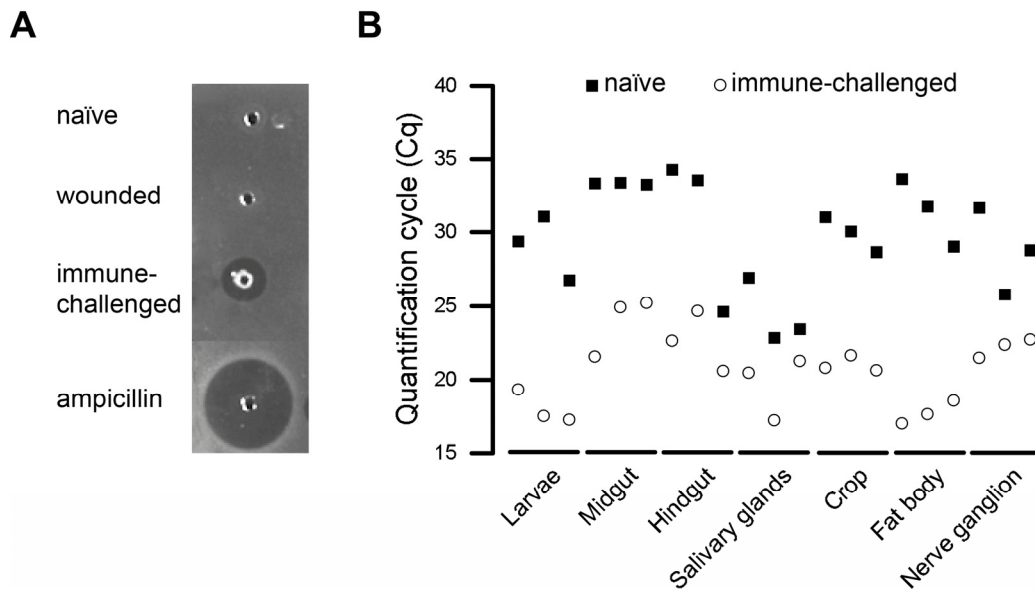


Figure 14: Validation of *P. aeruginosa* immune challenge. A: Samples of hemolymph from naïve, wounded and immune-challenged larvae were tested in the *E. coli* zone of inhibition assay, with 100 mg/ml ampicillin as a positive control. Only immune-challenged larvae generated a zone of inhibition. B: Distribution of quantification cycle (Cq) values for immune gene *attacin-2* in all naïve and immune-challenged samples. Raw values for all three biological replicates of the six tissue and the larvae samples are displayed separately.

#### 4.1.5. Validation of candidate reference genes using Normfinder

To assess reference gene expression stability a comparison among all tested genes in naïve and immune-challenged samples is performed. This comparison of  $C_q$  variation distinguishes between systematic changes among samples e.g. by pipetting errors or cDNA amount and differences in gene expression level do to tissue type or immune-challenge. For example a deviation in cDNA amount in one sample pool would lead to a global uniform change for all tested genes while expression changes would differ among genes. An ideal reference gene would show a stable equal expression in all samples.

The model-based Normfinder approach provides a direct estimation of variance in so-called stability values, with lower numbers equating a more stable expression. The program does not sequentially eliminate unsuitable genes so the pre-exclusion of genes with large variances is necessary to achieve reliable results.

Normfinder analysis of the 10 candidate reference genes (Table 3) ranked *RPS3*, *RPLP0* and *EF1 $\alpha$*  as the three most stable genes considering immune challenge. The worst stability values (approximately 2-fold higher across all samples) were observed for *18S rRNA*, *actin* and *28S rRNA*. The overall ranking was not transferable to all specific tissues or to whole larvae because the stability of the candidates differed according to the sample type. Intragroup variation was generally low with only *28S rRNA*

showing variation (Table 10 in Sup B.2). Intergroup variation was generally much higher, with the highest scores generated by *18S rRNA*, *28S rRNA* and *actin* (Table 11 in Sup B.2).

Table 3: Normfinder ranking of the stability values of candidate reference genes.

Rank	Larvae	Midgut	Hindgut	Salivary glands	Crop	Fat body	Nerve ganglion	Overall
1	<i>RPLP0</i> (0.010)	<i>EF1α</i> (0.010)	<i>RPLP0</i> (0.006)	<i>PKA</i> (0.005)	<i>β-tubulin</i> (0.007)	<i>RPLP0</i> (0.006)	<i>PKA</i> (0.010)	<i>RPLP0</i> (0.027)
2	<i>actin</i> (0.017)	<i>actin</i> (0.010)	<i>EF1α</i> (0.012)	<i>RPS3</i> (0.005)	<i>actin</i> (0.011)	<i>18S rRNA</i> (0.007)	<i>GST1</i> (0.011)	<i>RPS3</i> (0.029)
3	<i>GAPDH</i> (0.020)	<i>GST1</i> (0.012)	<i>RPS3</i> (0.015)	<i>GAPDH</i> (0.014)	<i>PKA</i> (0.016)	<i>β-tubulin</i> (0.009)	<i>actin</i> (0.015)	<i>EF1α</i> (0.029)
4	<i>RPS3</i> (0.021)	<i>RPLP0</i> (0.014)	<i>GAPDH</i> (0.018)	<i>GST1</i> (0.016)	<i>RPS3</i> (0.019)	<i>RPS3</i> (0.013)	<i>18S rRNA</i> (0.017)	<i>PKA</i> (0.037)
5	<i>GST1</i> (0.022)	<i>PKA</i> (0.019)	<i>actin</i> (0.020)	<i>actin</i> (0.024)	<i>GAPDH</i> (0.026)	<i>PKA</i> (0.019)	<i>RPLP0</i> (0.022)	<i>GST1</i> (0.039)
6	<i>EF1α</i> (0.025)	<i>18S rRNA</i> (0.020)	<i>PKA</i> (0.022)	<i>β-tubulin</i> (0.027)	<i>GST1</i> (0.027)	<i>EF1α</i> (0.036)	<i>GAPDH</i> (0.029)	<i>GAPDH</i> (0.041)
7	<i>PKA</i> (0.026)	<i>β-tubulin</i> (0.020)	<i>β-tubulin</i> (0.028)	<i>EF1α</i> (0.039)	<i>18S rRNA</i> (0.030)	<i>GST1</i> (0.042)	<i>β-tubulin</i> (0.033)	<i>β-tubulin</i> (0.052)
8	<i>18S rRNA</i> (0.036)	<i>GAPDH</i> (0.021)	<i>18S rRNA</i> (0.033)	<i>RPLP0</i> (0.041)	<i>EF1α</i> (0.030)	<i>GAPDH</i> (0.044)	<i>RPS3</i> (0.034)	<i>18S rRNA</i> (0.061)
9	<i>β-tubulin</i> (0.037)	<i>RPS3</i> (0.031)	<i>GST1</i> (0.034)	<i>18S rRNA</i> (0.057)	<i>RPLP0</i> (0.030)	<i>actin</i> (0.056)	<i>EF1α</i> (0.037)	<i>actin</i> (0.068)
10	<i>28S rRNA</i> (0.051)	<i>28S rRNA</i> (0.074)	<i>28S rRNA</i> (0.056)	<i>28S rRNA</i> (0.073)	<i>28S rRNA</i> (0.036)	<i>28S rRNA</i> (0.131)	<i>28S rRNA</i> (0.078)	<i>28S rRNA</i> (0.072)

#### 4.1.6. Validation of candidate reference genes using GeNorm

Thus there is no ideal algorithm for reference genes assessment a second independent approach was applied. The GeNorm algorithm calculates the pairwise variation among all tested genes and assigns stability measures (M). In every cycle, the gene with the highest stability measure (i.e. the least stable) is excluded until only the two best genes remain. GeNorm analysis of the 10 candidate reference genes (Table 4) yielded similar results to Normfinder. GeNorm ranked *RPS3*, *RPLP0* and *EF1α* as the three best genes and *18S rRNA*, *actin* and *28S rRNA* as the three worst, with M values of 2 to 4-fold higher than the best candidates across all samples. As for the Normfinder data, the overall GeNorm ranking list was not transferable to all individual tissues or whole larvae.

To illustrate the differences in stability measures I also included *attacin-2*, which is strongly induced by immune-challenge and therefore expected to be unstable. As anticipated, the M value for *attacin-2* was ~20-fold higher than the most stable candidate genes in each sample (Table 4).

Table 4: GeNorm ranking of stability measures for candidate reference genes and *attacin-2*.

Rank	Larvae	Midgut	Hindgut	Salivary glands	Crop	Fat body	Nerve ganglion	Overall
1	<i>RPLP0</i>	<i>β-tubulin</i>	<i>actin</i>	<i>PKA</i>	<i>β-tubulin</i>	<i>RPLP0</i>	<i>EF1α</i>	<i>EF1α</i>
	(0.341)	(0.270)	(0.128)	(0.209)	(0.252)	(0.357)	(0.241)	(0.557)
1	<i>actin</i>	<i>EF1α</i>	<i>RPS3</i>	<i>RPS3</i>	<i>RPS3</i>	<i>RPS3</i>	<i>RPLP0</i>	<i>RPLP0</i>
	(0.341)	(0.270)	(0.128)	(0.209)	(0.252)	(0.357)	(0.241)	(0.557)
3	<i>EF1α</i>	<i>PKA</i>	<i>PKA</i>	<i>GAPDH</i>	<i>actin</i>	<i>β-tubulin</i>	<i>GAPDH</i>	<i>RPS3</i>
	(0.403)	(0.313)	(0.366)	(0.514)	(0.308)	(0.489)	(0.418)	(0.841)
4	<i>GAPDH</i>	<i>RPS3</i>	<i>RPLP0</i>	<i>β-tubulin</i>	<i>GSTI</i>	<i>18S rRNA</i>	<i>actin</i>	<i>GSTI</i>
	(0.512)	(0.356)	(0.424)	(0.522)	(0.384)	(0.636)	(0.452)	(1.164)
5	<i>GSTI</i>	<i>GAPDH</i>	<i>EF1α</i>	<i>actin</i>	<i>GAPDH</i>	<i>PKA</i>	<i>PKA</i>	<i>GAPDH</i>
	(0.586)	(0.427)	(0.408)	(0.536)	(0.410)	(0.778)	(0.672)	(1.154)
6	<i>18S rRNA</i>	<i>actin</i>	<i>GSTI</i>	<i>GSTI</i>	<i>PKA</i>	<i>GAPDH</i>	<i>GSTI</i>	<i>PKA</i>
	(0.588)	(0.557)	(0.522)	(0.620)	(0.540)	(0.947)	(0.646)	(1.219)
7	<i>RPS3</i>	<i>RPLP0</i>	<i>β-tubulin</i>	<i>EF1α</i>	<i>18S rRNA</i>	<i>EF1α</i>	<i>18S rRNA</i>	<i>β-tubulin</i>
	(0.712)	(0.550)	(0.608)	(0.685)	(0.729)	(0.983)	(0.656)	(1.266)
8	<i>PKA</i>	<i>GSTI</i>	<i>GAPDH</i>	<i>RPLP0</i>	<i>EF1α</i>	<i>GSTI</i>	<i>β-tubulin</i>	<i>18S rRNA</i>
	(0.694)	(0.547)	(0.691)	(0.730)	(0.825)	(1.015)	(0.698)	(1.637)
9	<i>β-tubulin</i>	<i>18S rRNA</i>	<i>18S rRNA</i>	<i>18S rRNA</i>	<i>RPLP0</i>	<i>actin</i>	<i>RPS3</i>	<i>actin</i>
	(0.817)	(0.660)	(0.838)	(1.339)	(0.859)	(1.207)	(0.820)	(1.836)
10	<i>28S rRNA</i>							
	(1.092)	(1.490)	(1.229)	(1.528)	(0.888)	(2.645)	(1.658)	(2.095)
<i>atta2</i>	<i>atta2</i>	<i>atta2</i>	<i>atta2</i>	<i>atta2</i>	<i>atta2</i>	<i>atta2</i>	<i>atta2</i>	<i>atta2</i>
	(6.201)	(5.662)	(5.874)	(3.501)	(5.550)	(8.538)	(4.569)	(5.888)

Because neither algorithm selected a single reference gene suitable for all samples, I used GeNorm pairwise variation comparison and select the most appropriate number of reference genes for normalization, which is an appropriate strategy when single reference genes are unsuitable (Vandesompele et al. 2002). This comparison ( $V_{n/n+1}$ ) examines the normalization factors  $NF_n$  and  $NF_{n+1}$  in each analysis cycle. If the calculated value falls below a set threshold of 0.15 (Vandesompele et al. 2002), the addition of further reference genes does not improve the quality of normalization. As shown in Figure 15, I found that most tissues reached the recommended threshold of 0.15 with just two reference genes, whereas three reference genes were required for the normalization of expression levels in the salivary glands ( $V_{2/3} = 0.17$ ). When comparing overall variation, the 0.15 threshold is reached at  $V_{6/7}$

which means that six reference genes would be necessary for appropriate simultaneous normalization within all tested samples.

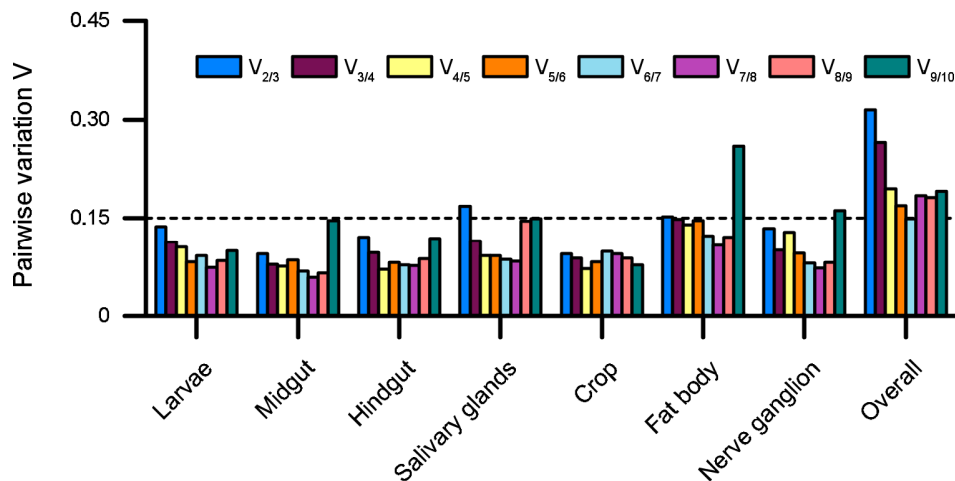


Figure 15: Determination of the optimal number of control genes for normalization. Pairwise variation ( $V_{n/n+1}$ ) analysis between the normalization factors  $NF_n$  and  $NF_{n+1}$  to determine the number of reference genes required for accurate normalization in every individual sample group. The dashed line at 0.15 represents the set threshold below which the number of reference genes is optimal.

#### 4.1.7. Gene expression analysis after *P. aeruginosa* immune challenge

To find the best set of reference genes I tried different combinations and amounts to analyze immune gene expression change upon *P. aeruginosa* challenge. The Cq values for *lucimycin*, *defensin-1* and *attacin-2* mRNA were therefore normalized using three combinations of candidate reference genes: (a) the two best candidate reference genes for every sample defined by GeNorm analysis; (b) the overall best three reference genes defined by both algorithms (*RPS3*, *RPLP0* and *EF1 $\alpha$* ); and (c) the overall best six reference genes defined by GeNorm pairwise variation comparison. My results show that the antifungal peptide *lucimycin* is not differentially expressed (Figure 16A), whereas *defensin-1*, which is specifically targeting Gram-positive bacteria, shows different upregulation in salivary glands, crop, nerve ganglion and fat body, ranging from a 8-fold induction in the nerve ganglion to a 290-fold induction in the fat body (Figure 16B). The strongest upregulation was monitored for *attacin-2* that targets primarily Gram-negative bacteria. *Attacin-2* was strongly induced by immune challenge in all tested tissues, ranging from a 37-fold induction in the salivary glands to a 51,463-fold induction in the fat body (Figure 16C). As shown in Figure 16, all three reference gene combinations lead to similar expression results with slight variations in relative values.

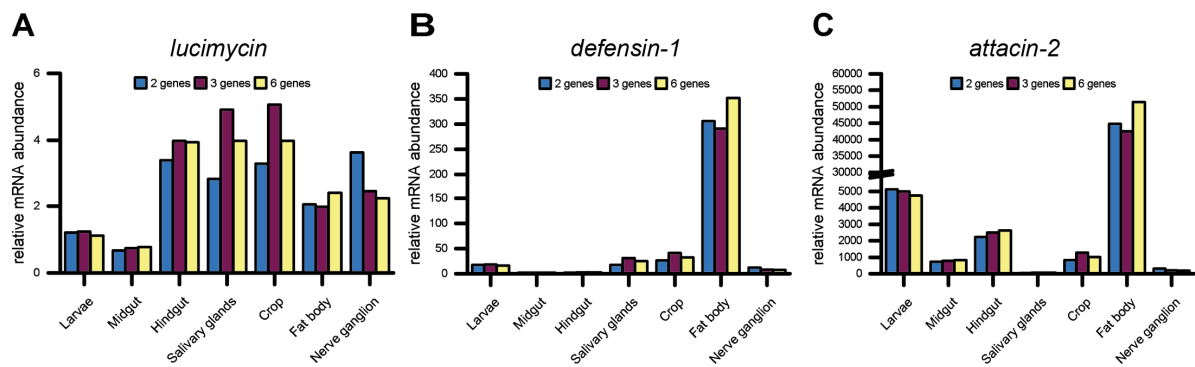


Figure 16: Quantitative RT-PCR analysis of *lucimycin*, *defensin-1* and *attacin-2* upon immune challenge. The mRNA expression of *lucimycin* (A), *defensin-1* (B) and *attacin-2* (C) was determined in different *L. sericata* tissues. Relative mRNA expression levels of individual immune genes were compared between immune-challenged and naïve samples and normalized with two, three or six reference genes.

## 4.2. Characterization of *L. sericata* Urate Oxidase

Results presented in this section were submitted to Insect Biochemistry and Molecular Biology as Baumann et al. (2016).

### 4.2.1. *UO* is expressed by Malpighian tube cells

To identify tissue expression profile of the two purine catabolism genes *UO* and *Allantoinase*, the 3 overall best reference genes (*RPS3*, *RPLPO* and *EF1 $\alpha$* ) determined previously (see 4.1.7) were used for normalization. *UO* is predominantly expressed (>5000 x) in Malpighian tubes (Figure 17A). Furthermore, it is noticeable in midgut and hindgut (160 x) compared to the tissue with the lowest expressed (nerve ganglion). *Alla* shows a uniform expression profile with highest expression in crop and lowest in fat body (Figure 17B). Although the relative qRT-PCR quantification cannot be used to compare the expression of two different genes in between each other, I observed much lower signal strength for *Alla*, which had to be compensated by using 25 x more cDNA than for all other genes. This data indicate no correlated expression between both genes and I focused exclusively on the allantoin producing enzyme *UO*.

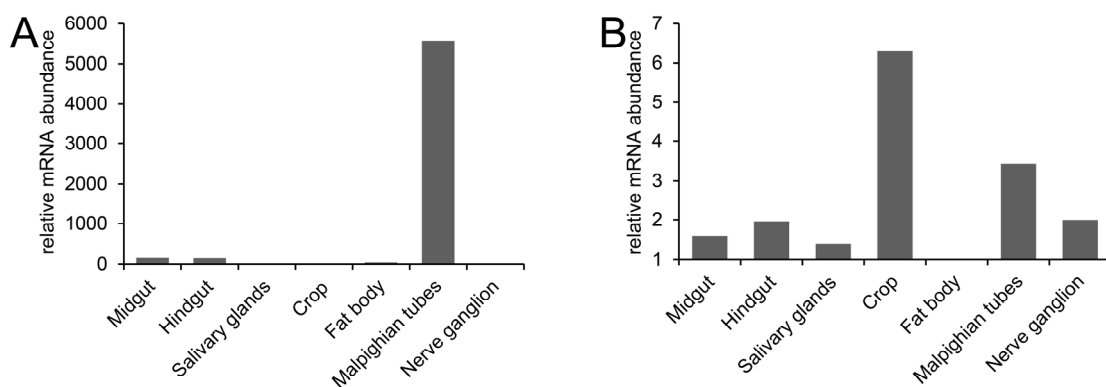


Figure 17: Quantitative RT-PCR analysis of *UO* and *Alla* expression in *L. sericata* tissues. The mRNA abundance relative to the lowest expressed tissue for *UO* (nerve ganglion) and *Alla* (fat body) was determined using three reference genes (*RPS3*, *RPLPO* and *EF1 $\alpha$* ).

Based on qRT-PCR gene expression analysis ISH was applied to visualize *UO* expression in Malpighian tubes and extended to the gut to illustrate its spatial organization. A strong *UO* expression was detected alongside most of the tube, except for the area from the gut intersection to the tube split (1) (Figure 18A). I observed a strict cytosolic expression leaving the nuclei unstained (Figure 18AB). No signal was observed inside the cells of negative control.

I did not detect any specific signal in the gut tissue. The only signal detected there was unspecific staining of the gut lumen (Figure 18; 2), which can also be observed in negative controls with only hybridization solution (Figure 18C). Moreover, once the gut was open (Figure 18; 3) no specific signal was detected in gut cells thus confirming its unspecificity.

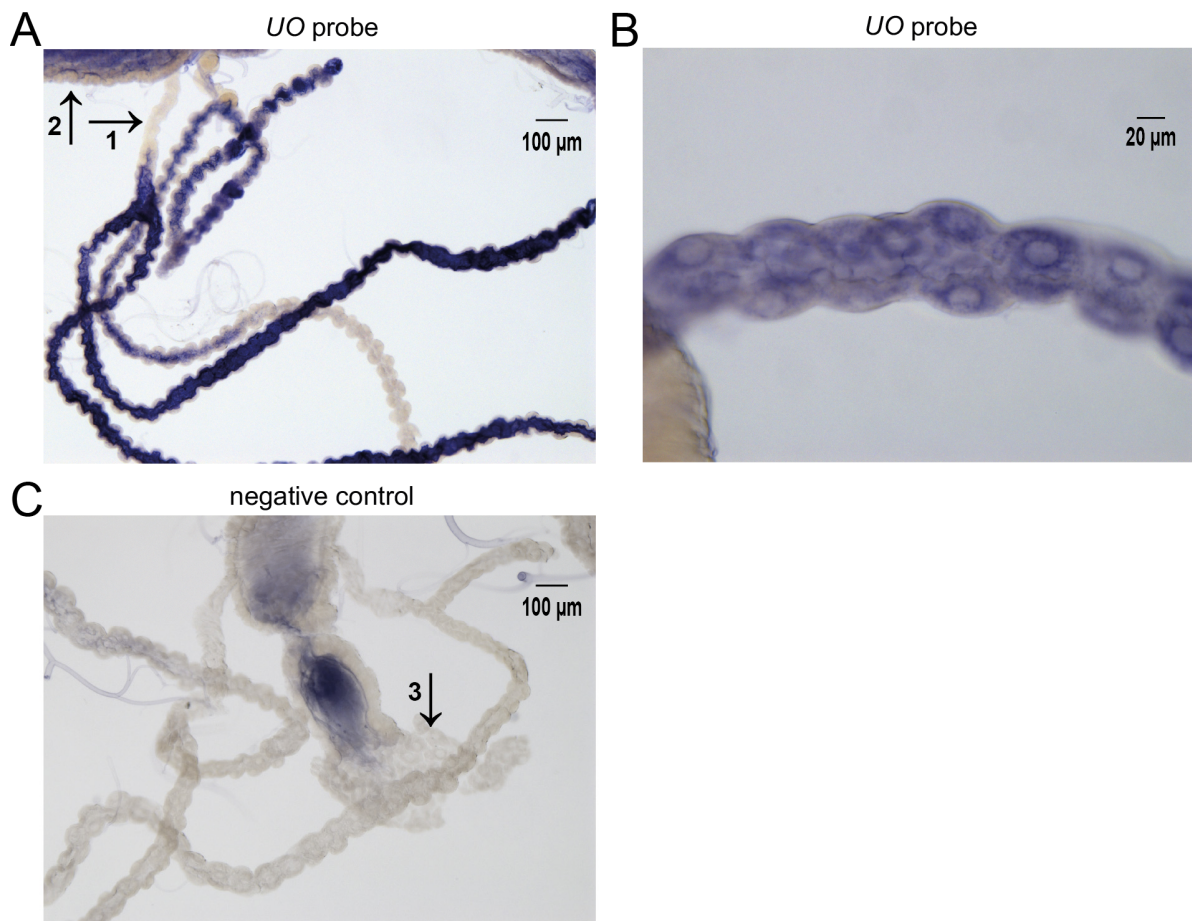


Figure 18: ISH of *L. sericata* gut and Malpighian tubes. A: Isolated *L. sericata* Malpighian tubes connected to the gut were stained with *UO* probe (A+B) or negative control (C). Strong *UO* expression was observed inside the Malpighian tubes (A, B). No signal was detected in the end part of Malpighian tube connecting to the gut (1) as well as in the gut wall (2). The unspecific binding of the hybridization solution to the gut lumen (C) was not detected once the gut tissue was opened (3).

#### 4.2.2. Recombinant production and refolding of *L. sericata* UO

*L. sericata* UO is a 340 amino acid enzyme with a theoretical pI of 7.73 and a molecular mass of 38.8 kDa that shows no precursor or export sequence. Recombinant Urate Oxidase (UO<sub>r</sub>) was produced in *E. coli* with N-terminal His<sub>6</sub>-Tag (Figure 10). Expression (Figure 19A) induction by anhydrotetracycline (1) lead to a clear band between 35 and 55 kDa that increased over the 3 h expression time (2-4). The inclusion bodies fraction was solubilized by guanidinium hydrochloride and purified via a cobalt based IMAC under denaturing conditions (Figure 19B) yielding 20 mg/L of enzyme. Purified enzyme was renatured by dialysis resulting in a single band matching the expected 40.5 kDa (\*) of active enzyme (Figure 19C, 13). Overall yield of active UO<sub>r</sub> was about 3 mg/L.

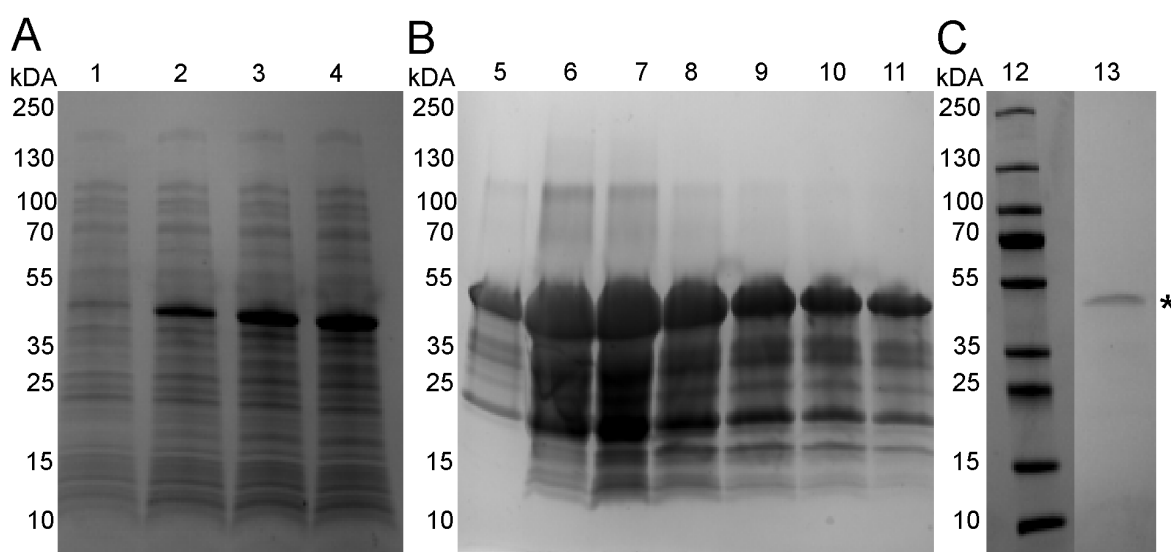


Figure 19: UO<sub>r</sub> expression, purification and refolding. A: Expression was induced by anhydrotetracycline (1) and samples were taken after 1 (2), 2 (3) and 3 h (4). B: UO<sub>r</sub> was purified by IMAC under denaturing conditions using cobalt resin. Enzyme was eluted by 200 mM imidazole and individual fractions collected manually (5-11). C: Purified enzyme was diluted to 100 µg/ml, reduced with β-mercaptoethanol and refolded two times by dialysis against Tris-buffer. Refolded enzyme was analyzed via denaturing SDS-PAGE (12; protein size standard) resulting in a single band (\*) matching the expected 40.5 kDa enzyme (13).

#### 4.2.3. $UO_r$ pH and temperature optimum

To determine crucial assay parameters  $UO_r$  activity was first tested at 25 °C in the pH range of 4-10. The enzyme showed uniformly high activity (80-100 %) in the alkaline area with strong activity decrease between the pH 7 to 6.5. No activity was detected at acidic pH of 6 and below (Figure 20A). To assure stable color development of formed Resorufin a pH of 7.5 was chosen for all subsequent analysis. Temperature optimum was tested between 20-60 °C and showed highest activity at 20 and 25 °C with a steady activity decline towards higher temperature range and in the end no activity at 60 °C (Figure 20B).

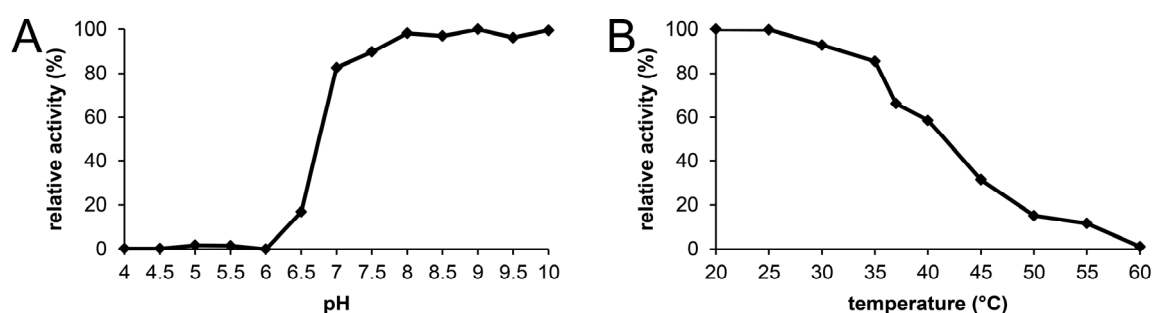


Figure 20:  $UO_r$  pH and temperature dependent activity. A:  $UO_r$  pH dependency was determined at 25 °C by a two step assay using 20 mM buffer (sodium citrate pH 4-5.5, sodium phosphate pH 6-8 or sodium borate 8.5-10) in the reaction step. In the quantification step the absorption at 515 nm was measured at pH 6 after 10 min and the highest activity was set to 100 % (n = 6). B:  $UO_r$  temperature dependence was determined at pH 7.5 in the range of 20-60 °C using continuous assay. The absorption at 560 nm was measured after 30 min and highest activity was set to 100 % (n = 6).

#### 4.2.4. $UO_r$ competitive inhibition, metal ion dependence and stability

With pH 7.5 and 25 °C as steady parameters further tests were performed. Inhibition by the known competitive inhibitor 8-azaxanthine showed half maximal inhibition at a 2:1 ratio of inhibitor to substrate (Figure 21A). Typical alkaline earth and transition metals showed no beneficial effect on enzyme activity as well as the chelator EDTA that would bind available metal ions (Figure 21B). Both results confirm that *L. sericata*  $UO$  is cofactor independent as known for other  $UO$  (Fetzner and Steiner 2010). Stability of  $UO_r$  under assay conditions (pH 7.5 and 25 °C) was monitored for a week and revealed high loss of activity within the first 24 h (about 50 %). Additionally  $UO_r$  lost another 10 % of activity in next 6 days making  $UO_r$  not suitable for prolonged application without further modification (Figure 21C).

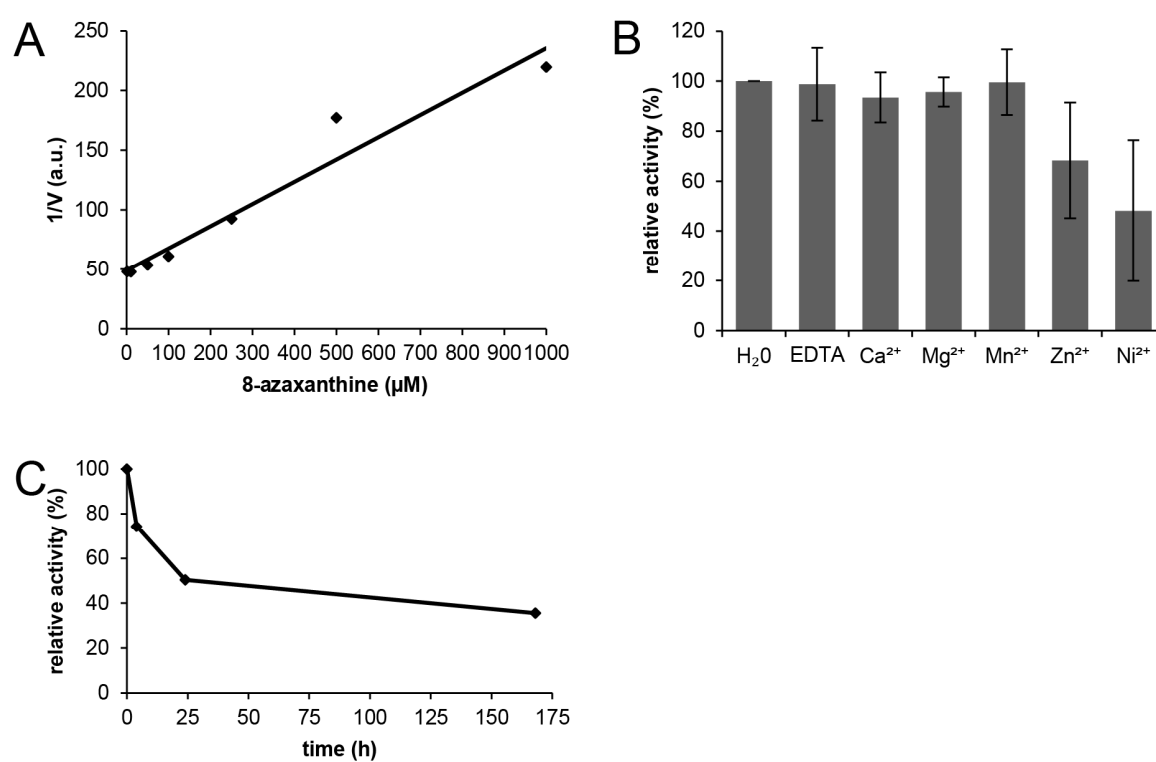


Figure 21:  $UO_r$  competitive inhibition, metal ion dependence and stability over time. A: The competitive inhibitor 8-azaxanthine was used in a range of 1-1000  $\mu$ M against 100  $\mu$ M uric acid. Inhibitor concentration was plotted against reciprocal activity ( $n = 9$ ). B: Metal ion dependence was determined with 10 mM individual metal ions or 50 mM EDTA for 30 min at 25 °C and H<sub>2</sub>O control activity was set to 100% ( $n = 9$ ). C: Stability of  $UO_r$  was tested for 0, 4, 24 and 168 h in 100 mM sodium chloride, 45 mM Tris-HCl, pH 7.5 at 25 °C and activity was measured after 30 min. Activity at 0 h was set to 100% ( $n = 6$ ).

#### 4.2.5. Native UO is exclusively present in Malpighian tubes

The detection of UO on protein level was facilitated by western blot analysis. Same larval tissues as for qRT-PCR (midgut, hindgut, salivary glands, crop, fat body, Malpighian tubes and nerve ganglion) supplemented by maggot secretory and excretory products (E/S) were tested. All samples were resolved by reducing SDS-PAGE and stained by coomassie (Figure 22A). Specific UO antibody (see 3.4.1) was apply to detect the native enzyme in individual tissues. As shown in Figure 22B I detected strong signal around 40.5 kDa in Malpighian tubes, while no signal was detected in any other tissue. The size of the detected band corresponds to the theoretical molecular weight of UO (38.8 kDa).

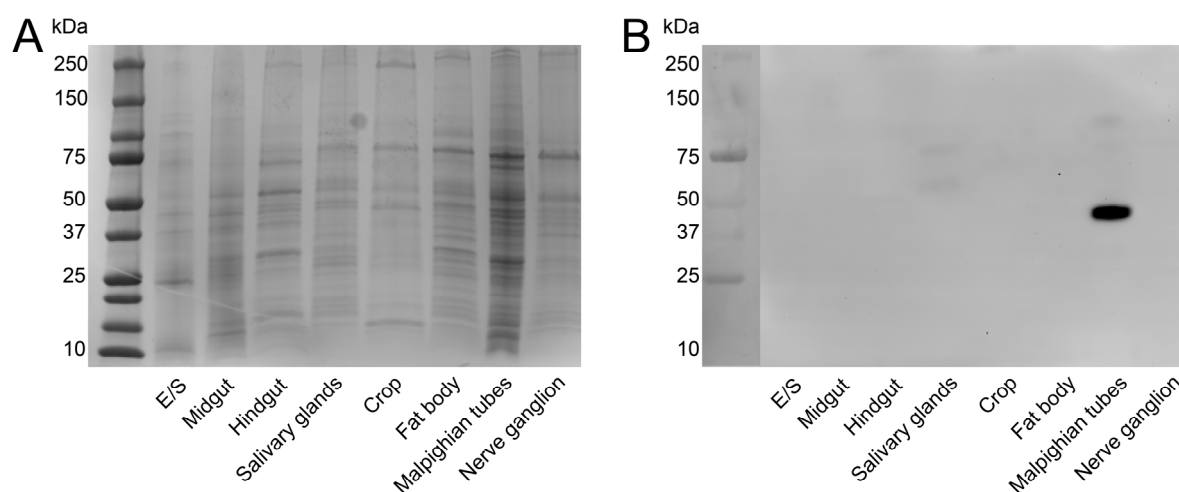


Figure 22: Coomassie staining and UO detection by western blot in *L. sericata* tissues and E/S. A: Coomassie staining after denaturing SDS-PAGE of *L. sericata* tissues and E/S samples. Sample amount of 5-15  $\mu$ l was estimated to yield clear band patterns. B: Equal sample amounts to A were used for western blot with anti-UO antibodies and visualized by HRP conjugated secondary antibody via chemiluminescence. Ladder was post stained with coomassie on polyvinylidene difluoride (PVDF) membrane.

Immunolocalization of native UO in Malpighian tubes using specific UO antibody and whole mount staining, clearly demonstrate the presence of native UO inside the Malpighian tube cells. A strong UO signal was observed in various cells along the whole tube with no signal at the intersection to the gut (1) and very weak or no signal in the gut tissue itself (Figure 23A). On single cell resolution I detected strict cytosolic localization of UO showing no sign of accumulation in vacuole like structures (Figure 23B). Pre-immune serum was used as a negative control (Figure 23C).

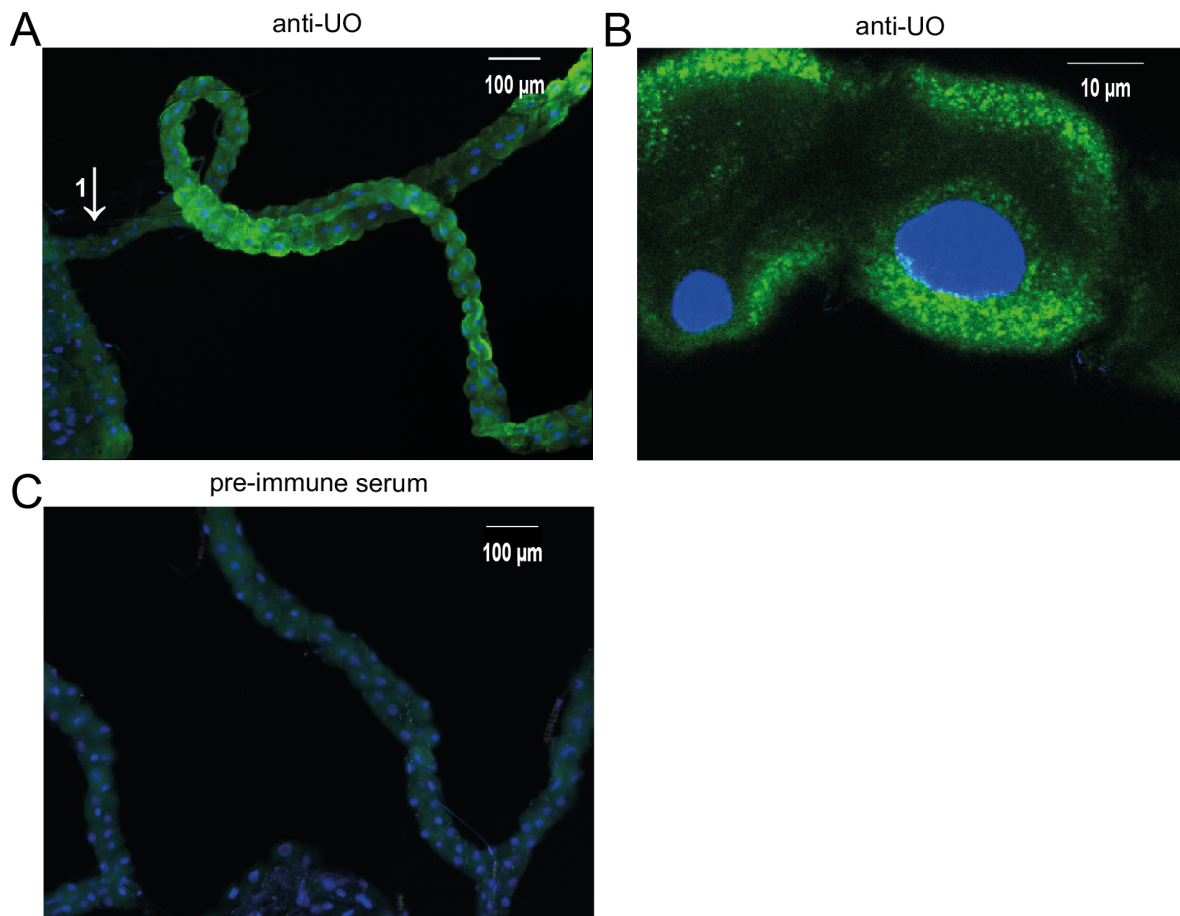


Figure 23: Whole mount staining of *L. sericata* gut and Malpighian tubes. Isolated *L. sericata* Malpighian tubes connected to the gut (1) were stained with anti-UO antiserum (A+B) or pre-immune serum (C) and visualized with an Alexa488 conjugated secondary antibody (green). Nuclei were counterstained with 4',6-diamidino-2-phenylindole (DAPI) (blue).

## 5. Discussion

*L. sericata* larvae applied during MDT have various beneficial effect on wound healing and their E/S represents a potential rich source of novel therapeutic compounds. To validate and narrow down candidate genes from transcriptome datasets qRT-PCR is a fast, precise and cheap approach, but relies highly on appropriate reference genes for the normalization of gene expression data. Those qRT-PCR results, enabled by appropriate reference genes, are the first step to gain better understanding of MDT from a basis research perspective as discussed in 5.1 and 5.2. Another challenge in insect enzyme research is the isolation of sufficient amount of highly pure enzymes for detailed analysis. This can be overcome by heterologous production of recombinant enzymes. Production of *L. sericata* recombinant enzymes seems to be an ideal approach, from an applied perspective as discussed in 5.3, to evaluate the medical and biotechnological potential of *L. sericata* candidate enzymes.

### 5.1. *L. sericata* reference gene assessment

Results of this thesis, published under Baumann et al. (2015), investigated the tissue specific expression stability of 10 candidate reference genes and 3 immune genes (*lucimycin*, *defensin-1* and *attacin-2*), which target various pathogen classes. I monitored the expression of these immune genes in different *L. sericata* tissues before and after the immune challenge with the Gram-negative bacterium *P. aeruginosa*, which was introduced into third-instar *L. sericata* larvae by pricking its dorsal part with a contaminated needle. Such an artificial infection far exceeds the intensity of the bacterial challenge that maggots encounter in human wounds. I am aware of the fact that this method leads to a higher variation in bacterial concentration compared to e.g. microinjection, but due to the high maggot motility a gentle restraining with modelling clay or more efficient one with tape were almost impossible. In both cases I faced a high number of escaping animals or high mortality due to drying out and/or ripping. Consequently hand pricking also introduces an increased variation in injection location targeting not only the hemolymph, but possibly also some tissues. Such an approach is not most suitable for an experimental setup that demands high reproducibility to get reliable results, but in this case the goal was to assess reference gene stability under harsh conditions thus this increase in variation is beneficial to robustly test the stability of the candidate reference genes.

The strongest expression after such an immune challenge was observed for *attacin-2* (targeting Gram-negative bacteria (Imler and Bulet 2005)). *Attacin-2* was monitored in all larval tissues reaching its maximum in fat body (over 50,000-fold). No differential expression was observed for the antifungal peptide *lucimycin*, which is known to have no effect against Gram-negative bacteria (Pöppel et al. 2014). Interestingly, *defensin-1* as a representative targeting Gram-positive bacteria (Imler and Bulet 2005), was

differentially upregulated in salivary glands, crop, nerve ganglion and fat body (Figure 16B). This unexpected result can be easily explained by the wounding procedure itself, which has been shown to induce insect immune response previously (Han et al. 1999). My results demonstrate that even under such harsh conditions, which heavily perturbed the system and led to the strong induction of *attacin-2*, the expression of most of the candidate reference genes remained stable. This success rate reflects the smart choice of reference gene candidates that have been already applied as references in other insects, allowing for a knowledge-based pre-selection of candidates that are likely to be suitable as reference genes in *L. sericata* (Bagnall and Kotze 2010; Ponton et al. 2011; Scharlaken et al. 2008; Sun et al. 2015; Toutges et al. 2010; Yuan et al. 2014).

The Normfinder and GeNorm algorithms (Table 3 and 4) were unable to identify a single optimal reference gene or an ideal combination of two to three reference genes that worked consistently across all tested tissues. *RPLP0*, *EF1 $\alpha$*  and *RPS3* were identified as the most stable reference genes across all samples even though each of them ranked low for stability in at least one of these samples. All three genes are involved in protein expression (Meriin et al. 2012; Polakiewicz et al. 1995; Rich and Steitz 1987) and a co-regulation cannot be completely ruled out as an explanation for their high ranking. However, comparison with the other candidate genes does not indicate generally co-regulated expression. Although it may be necessary to use specific gene candidates for particular tissues to achieve the most accurate data normalization, the use of these three overall best reference genes should be more than adequate for most experimental scenarios, as illustrated by my expression analysis of three immune genes (Figure 16).

Among the remaining candidates, genes some (e.g. *GST1* and *GAPDH*) occupy mid-ranking positions in many tissues and have poor scores in others but never rank as the most suitable reference gene, whereas others (e.g. *PKA* and  *$\beta$ -tubulin*) also occupy mid-ranking position in many tissues but are the most stable reference genes in others, i.e. the salivary glands and the nerve ganglion (*PKA*) or the crop ( *$\beta$ -tubulin*). Their overall mid-to-low ranking reflects their tendency to show good scores in a few tissues but poor scores in most others (Table 3 and 4).

Remarkably, *actin* has a low overall score but good scores in several tissues (second most stable reference in three tissues and third in another). However, the standard deviation of 2.1 Cq is the highest among all the tested candidate genes (Figure 13), reflecting high intergroup variation (Table 11 in Sub B.2) rather than changes in expression induced by the immune challenge, which would lead to higher intragroup variations (Table 10 in Sub B.2). It is not surprising that a fundamental structural protein like *actin* would be expressed at different levels in diverse tissues such as the gut and the fat body. Therefore, despite its

low overall ranking, *actin* would be useful as a reference gene in most individual tissues but not in more diverse collections of samples.

Compared to the other candidates, the genes for *18S* and *28S rRNA* were the least stable and therefore the least suitable for normalization, which contrasts with the findings in other arthropods (Bagnall and Kotze 2010; Majerowicz et al. 2011). This may be a species-dependent phenomenon, but may also reflect the technical approach, e.g. the method used for RNA isolation and cDNA synthesis. For example, I used oligo(dT)<sub>18</sub> primers which only partly reverse transcribe the rRNA genes due to the lack of a canonical polyadenylate tail.

While dissecting the fat body from immune-challenged larvae I observed the remodeling and/or degradation of this tissue. The physical appearance of the fat body changed from clusters of round cells to loosely-associated amorphous cells which yielded lower amounts of total RNA with poorer quality compared to the other tissues. After immune challenge, fat body total RNA from all biological replicates had to be precipitated and concentrated to meet the required criteria for cDNA synthesis. The insect fat body is responsible for AMP production (Hetru et al. 2003) and two defense pathways have been described in *Drosophila melanogaster*, i.e. the Toll pathway against Gram-positive species and the immune deficiency (IMD) pathway against Gram-negative species (Hoffmann and Reichhart 2002). Constitutive triggering of the IMD pathway has been shown to induce apoptosis (Georgel et al. 2001). My results show that although *attacin-2* is expressed ubiquitously and globally upregulated by immune challenge, the strongest induction (over 50,000-fold) occurs in the fat body (Figure 16C). I used *P. aeruginosa*, which as a Gram-negative species is targeted by *attacins* (Imler and Bulet 2005) and hypothesize that the IMD pathway plays a major role in this immune response. The induction of *attacin-2* may therefore be part of this IMD pathway response, ultimately resulting in apoptosis which may explain the physical changes in the fat body I observed.

Analysis of qRT-PCR expression data without normalization is impossible, because of variations in extraction yield, reverse-transcription yield, efficiency of amplification and other systemic variations like e.g. variation in pipetting that are inherent to all biological experiments (Bustin et al. 2009; Nolan et al. 2006). For such a precise method that can even detect low copy number targets the use of only a single reference gene is widely accepted as being insufficient (Gutierrez et al. 2008; Nolan et al. 2006). The demand for accurate normalization of gene expression data by validated reference genes for relative comparison of gene expression data led to several statistical algorithms (Andersen et al. 2004; Pfaffl et al. 2002; Vandesompele et al. 2002).

There is probably no universally ideal reference gene in any experimental system so it is important to distinguish between the best gene and combination of genes suitable for different experimental settings. Despite the diverse expression profiles of the 10 candidate reference genes in the dissected tissue samples, several combinations of these genes gave identical results when used for the normalization of immune genes expression during an immune challenge, suggesting that the analysis of six reference genes per sample or different reference genes in each tissue is unnecessary. From my own experience, the reliable normalization of *L. sericata* expression data among all dissected tissues (Figure 16) is also achieved using the three best reference genes based on the overall rankings (*RPLP0*, *EF1 $\alpha$*  and *RPS3*), which balances accuracy with convenience and the cost of additional experiments. The primer pairs and reference gene candidates evaluated in this thesis provided a valuable tool for the normalization of gene expression data in medical maggots, which will facilitate the identification and functional analysis of genes which are responsible for the beneficial effects of MDT. Furthermore reliable *L. sericata* reference genes are in demand in Forensic entomology. Nowadays genetic analysis to determine the exact species of found larvae and pupae are already established and save valuable time, because insect do not need to be grown in the lab until adult stage to determine the species by visual analysis (Amend 2004). Transcriptional analysis will boost accuracy in PMI determination even further especially for post feeding 3<sup>rd</sup> instar larvae and pupae. Developmental genes allowing this are under investigation and depend an accurate normalization of results by reliable reference genes (Boehme et al. 2013; Tarone and Foran 2011; Tarone et al. 2011).

## 5.2. UO and purine catabolism

Results submitted under Baumann et al. (2016) (Insect Biochemistry and Molecular Biology) I investigated *L. sericata* UO and its relations in purine catabolism. The *L. sericata* transcriptome (Franta et al. 2016) was used to identify enzymes involved in purine catabolism and thus nitrogen waste management. Further on the detailed expression analysis in individual larval tissues was performed via qRT-PCR using previously evaluated *L. sericata* reference genes. A gene encoding for Urate Oxidase, an unique enzyme responsible for allantoin production, was produced recombinantly and its native form, as well as RNA signal was detected in larval tissues using specific UO antibodies or ISH respectively. These data broaden our knowledge about the molecules involved in MDT and indicate that also secretion products play a beneficial roles in MDT.

Insects are the biggest and most diverse group of animals and their species diversity is also reflected in the variety of nitrogenous waste products. Spanning the whole scale from the house cricket *Acheta domestica* excreting mainly uric acid (Nation and Patton 1961), through all related purine metabolites (Bursell 1967) down to the American cockroach *Periplaneta Americana*, which is excreting mainly

ammonia (Mullins and Cochran 1972). Exploring *L. sericata* transcriptome identified only one gene encoding for both *UO* and *Allantoinase*, but no genes encoding for *Allantoicase* and/or *Urease*, respectively. Using qRT-PCR and ISH I show that *UO* is predominantly expressed in Malpighian tubes (Figure 17A). This result is in accordance with studies in mosquito *Aedes aegypti* and fruit fly *Drosophila melanogaster* where *UO* is also mainly expressed in Malpighian tubes (Scaraffia et al. 2008; Wallrath et al. 1990). *Allantoinase*, on the other hand, shows equal expression in various tissue (Figure 17B), thus excluding its necessary co-localization with *UO*. However qRT-PCR only enables relative comparisons of one gene and not among different genes, my observation that 25 times more cDNA is needed for *Allantoinase* compared to *UO* to get a similar signals for both genes is a clear hint for much lower abundance of *L. sericata Allantoinase*.

*UO* activity has been previously detected in various insect species, while *Allantoinase* activity could only be estimated for a few insect species due to the presence of allantoic acid (Bursell 1967). In *L. sericata* no allantoic acid was detected (Brown 1938) and this finding together with my results indicates no direct degradation of allantoin down to urea by *L. sericata*. Urea present in chronic wounds could be a result of subsequent degradation of allantoin by gut associated microbiota. This phenomenon is well known for other insects (Jurkevitch 2011; Lauzon et al. 2000), and is also indicated by the transcriptome search. Another explanation of urea presence in the wound could be due to its production by Arginase an enzyme that creates urea by hydrolysing the arginine side chain (von Dungern and Briegel 2001).

The antibody based detection of *L. sericata* *UO* on protein level shows the same trend as monitored for the *UO* gene expression (Figure 22 and 23). I detect native *UO* exclusively inside Malpighian tube cells and not in any other tissue nor in E/S as assumed previously (Brown 1938). Moreover, my results show that *L. sericata* *UO* enzyme is not present in any vacuole but rather freely available in the cell cytoplasm (Figure 23B). This finding groups insect *UOs* with bacterial and fungal counterparts (e.g. *Bacillus fastidiosus* or *Fusarium oxysporum*) that are soluble and in contrast to the mammalian and other vertebrate *UOs* not cluster with other purine catabolism enzyme in peroxisomes (Vogels and Van der Drift 1976; Volkl et al. 1988). My findings indicate that allantoin is excreted as a primal waste product of nitrogen disposal of *L. sericata*. Presence of allantoin and other substances such as ammonium bicarbonate or urea are believed to maintain the wound pH in the alkaline (Fleischmann et al. 2004), which is crucial for activity of *L. sericata* digestive proteases during debridement (Chambers et al. 2003). As the wound proceed towards the healing process, the wound pH shifts from alkaline to neutral until it reaches the acidic pH of healthy skin (Gethin 2007). During the healing and remodeling phase allantoin was shown to be involved in the hastened healing (Araujo et al. 2010; DiSalvo 2002).

My localization of *L. sericata* UO on mRNA as well as protein level in different *L. sericata* tissues show its exclusive localization inside the Malpighian tube cells (Figure 17, 18, 22 and 23). Allantoin is produced by UO to remove uric acid from the insect hemolymph, which is finally excreted via the hindgut as nitrogenous waste product. My findings show that not only actively secreted molecules, but also excretion products contribute to the beneficial effects of MDT.

### 5.3. UO<sub>r</sub> and application potential

Submitted under Baumann et al. (2016) (Insect Biochemistry and Molecular Biology) I utilize the *L. sericata* UO sequence data as well to produce the enzyme recombinantly. I am the first to produce and characterize an insect UO, an enzyme that creates allantoin, which contributes to the wound healing process (Araujo et al. 2010; DiSalvo 2002). I produced UO<sub>r</sub> in *E. coli*, purify it via IMAC and test for its pH optimum, temperature optimum, competitive inhibition, cofactors and stability (Figure 20 and 21).

UO<sub>r</sub> is cofactor independent which is a typical feature for this class of enzymes (Fetzner and Steiner 2010). As well as the inhibition by the known competitive inhibitor 8-azaxanthine (2:1 ratio) (Colloc'h et al. 1997). It has a temperature optimum around 20-25 °C, this suits to an enzyme localized inside the larvae, which have a standard rearing temperature of 28 °C (Shiravi et al. 2011). It would also be active in the wound bed, which shows a temperature of 33 °C (like the skin) or above (Dini et al. 2015) and even in an internal application at 37 °C the enzyme would still show an activity of 70%. The pH optimum in the alkaline is also in agreement with the internal pH in insect Malpighian tubes and cells that is slightly above 7 (Petzel et al. 1999). Below pH 7 UO<sub>r</sub> activity steeply declines and shows no activity at pH 6 and below. From an application point of view the pH profile is unfavorable. The enzyme would be active in the alkaline early wound stages, but not in the final healing phase where the pH is shifted back to the acidic (Gethin 2007) and in that phase the produced allantoin would be beneficial to hasten the healing process.

Allantoin is in use for cosmetics and topical pharmaceuticals for over 70 years. It is FDA classified as Category I (safe and effective) as an active ingredient for skin protection. Its keratolytic (softens skin) properties without any adverse effects (e.g. no skin irritation) made it a part of many cosmetics (AKEMA fine chemicals; [www.akema.it](http://www.akema.it)). Remarkable for a substance with assumed healing properties that is in wide use for so long there are no studies that quantify the beneficial effects or investigate the specific mechanism. The first study proving the healing properties of allantoin was published in 2010 (Araujo et al. 2010). One explanation for the lack of studies is originated in the production of allantoin. It can be chemically synthesized by uric acid oxidation with permanganate. A method that was invented by Liebig

and Wöhler (1837) and an important source for allantoin in the 1930s. Nowadays a major source are extracts of the comfrey plant (*Symphytum officinale*), their roots and herbs contain 0.6-1 % allantoin (Staiger 2012). Most studies and cosmetic use those plant extract and thus observed effects do not solely originate from allantoin and can not be attributed to a single component (Araujo et al. 2012).

Due to the dysfunctional human UO there are several health complications related to high level of uric acid in humans. Tumor lysis syndrome (TLS) is such an example, where high amounts of uric acid flush the human body due to cell lysis during chemotherapy. Rasburicase a recombinant UO originating from fungus *Aspergillus flavus* was approved by FDA for TLS application in 2009 (Ueng 2005). *A. flavus* UO was at first homolog expressed and marketed as Uricozyme, but due to severe allergic reactions discontinued. Rasburicase is nowadays expressed in *Saccharomyces cerevisiae* (Garay et al. 2012) and *E. coli* expression in soluble active form was also proven possible (Legoux et al. 1992). Recombinant Rasburicase lowers plasma uric acid levels prior to chemotherapy thus preventing acute renal failure and ultimately death of patients, but its application still results in high prevalence (15-24 % patients) of allergic reaction or antibodies development (Goldman et al. 2001).

For long term reduction of plasma uric acid levels to prevent uric acid precipitations (tophi) or reduce the effects of chronic gout allopurinol is the current standard treatment. This competitive inhibitor of Xanthine Oxidase reduces the synthesis of uric acid. It is oral bioavailable, but requires longer time than UO treatment to show effects and several years to dissolve tophi (Perez-Ruiz and Liote 2007). Several recombinant UOs have been tested for long term applications like treatment failure gout failure. The standard treatment (allopurinol) shows no more effect in long term treatment or causes an immunogenic reaction, but without positive outcome. Krystexxa (Pegloticase) is a PEGylated chimeric Pig-Baboon UO. The polyethylene glycol (PEG) conjugation masks the enzyme surface, thus reducing antigenicity and prolonging enzyme half-life (Jevsevar et al. 2010). This first recombinant mammalian UO combines the highly active porcine UO with the C-terminal baboon UO sequence to further reduce immunogenicity (Ganson et al. 2006). The urgent need for any alternative in treatment failure gout led to FDA approval (2010) of Krystexxa (Sundy et al. 2011; Sundy and Hershfield 2007), even if it resulted in serious adverse effects in 18 % of patients.

Over the last 40 years many improvements in UO production, activity and stability were made, but the adverse side effects of all tested recombinant UOs creates a demand for new, active UOs with low immunogenicity, which could be successfully applied in long term treatments. One interesting approach to overcome immunoreactivity is to reactivate human UO by ancestral sequence reconstruction (Kratzer et al. 2014). Another possible solution could be offered by insect UOs.

## 5.4. Outlook

The qRT-PCR approach established during this thesis allows the tissue specific expression analysis of candidate genes in immune challenge experiments and provides reliable *L. sericata* reference genes for normalization of those data. It was already applied in the identification and validation of genes encoding for various proteases from maggots (Franta et al. 2016; Pöppel et al. 2016), thus improving our understanding of MDT and contributing to the transformation from classic maggot therapy to modern biosurgery. Furthermore the reference genes could contribute in forensic entomology to boost accuracy in PMI determination. Transcriptional analysis especially for post feeding 3rd instar larvae and pupae would not only save time by making rearing unnecessary, but could also be more precise and especially for this reference genes are needed to obtain accurate results.

The *L. sericata* Urate Oxidase produced and characterized during this thesis is the first insect UO expressed heterologously and analysed in detailed manner. From a basic research point of view those findings improve our understanding of MDT. From an application point of view UO<sub>r</sub> would need to undergo severe further modifications to improve its overall stability, catalytic activity and solubility. Catalytic activity could be improved by a different expression strategy that has a higher chance of yielding soluble enzyme. By this the enzyme might differ in folding and could be more active. One option would be the cry-tag (Hayakawa et al. 2010) the other a host like yeast or insect cells (Spohner et al. 2016; Zitzmann et al. 2017). Another option could be to improve catalytic activity systematically by a directed evolution strategy followed by rational site directed mutagenesis of promising amino acids positions determined before (Packer and Liu 2015). To increase enzyme stability the introduction of an additional Cysteine recently identified in zebra fish UO would also be an option (Marchetti et al. 2016). This Cysteine residue was shown to promote inter monomer linkage and thus increased the stability of the active homotetramer. Additionally PEGylation could improve in vivo stability of the enzyme. A promising approach that would overcome the solubility issues and increase stability while also reducing immunogenicity would be the immobilization of UO on nanoparticles like fumed silica (Cruz et al. 2011). If the immunogenicity of those nanoparticles itself is low the restricted access inside the particles could mask the enzyme from the immune system and be a promising approach for long term applications.

Insects, especially their secretions, venoms but also other products (e.g. honey) are finding its way into modern western medicine (Cherniack 2010) with *L. sericata* maggots and honey bees as the vanguard of this field. Several clinical trials prove the beneficial effects and healing potential of insect compounds, but their majority is strictly limited in both amount of active substance as well as strict topical application (McIntosh and Thomson 2006; Steenvoorde et al. 2007). Recombinant production of insect derived

enzymes could overcome this problem by providing sufficient amount of pure enzymes, which can be applied either single or in combination with other substances in both modern biomedicine and biotechnology.

## 6. References

- Altincicek, B and Vilcinskas, A (2009) Septic injury-inducible genes in medicinal maggots of the green blow fly *Lucilia sericata*. *Insect Mol Biol* **18**: 119-25.
- Altman, RD, Schultz, DR, Collins-Yudiskas, B, Aldrich, J, Arnold, PI and Brown, HE (1984) The effects of a partially purified fraction of an ant venom in rheumatoid arthritis. *Arthritis Rheum* **27**: 277-84.
- Alvarez-Lario, B and Macarron-Vicente, J (2010) Uric acid and evolution. *Rheumatology (Oxford)* **49**: 2010-5.
- Alvarez-Lario, B and Macarron-Vicente, J (2011) Is there anything good in uric acid? *QJM* **104**: 1015-24.
- Amendt, J, Krettek, R and Zehner, R (2004) Forensic entomology. *Naturwissenschaften* **91**: 51-65.
- Andersen, CL, Jensen, JL and Orntoft, TF (2004) Normalization of real-time quantitative reverse transcription-PCR data: a model-based variance estimation approach to identify genes suited for normalization, applied to bladder and colon cancer data sets. *Cancer research* **64**: 5245-50.
- Araujo, LU, Grabe-Guimaraes, A, Mosqueira, VC, Carneiro, CM and Silva-Barcellos, NM (2010) Profile of wound healing process induced by allantoin. *Acta cirurgica brasileira / Sociedade Brasileira para Desenvolvimento Pesquisa em Cirurgia* **25**: 460-6.
- Araujo, LU, Reis, PG, Barbosa, LC, Saude-Guimaraes, DA, Grabe-Guimaraes, A, Mosqueira, VC, Carneiro, CM and Silva-Barcellos, NM (2012) In vivo wound healing effects of *Symphytum officinale* L. leaves extract in different topical formulations. *Pharmazie* **67**: 355-60.
- Attinger, C and Wolcott, R (2012) Clinically Addressing Biofilm in Chronic Wounds. *Adv Wound Care (New Rochelle)* **1**: 127-132.
- Bagnall, NH and Kotze, AC (2010) Evaluation of reference genes for real-time PCR quantification of gene expression in the Australian sheep blowfly, *Lucilia cuprina*. *Medical and veterinary entomology* **24**: 176-81.
- Barnes, KM, Dixon, RA and Gennard, DE (2010) The antibacterial potency of the medicinal maggot, *Lucilia sericata* (Meigen): variation in laboratory evaluation. *Journal of microbiological methods* **82**: 234-7.
- Baumann, A, Lehmann, R, Beckert, A, Vilcinskas, A and Franta, Z (2015) Selection and Evaluation of Tissue Specific Reference Genes in *Lucilia sericata* during an Immune Challenge. *PLoS One* **10**: e0135093.
- Baumann, A, Skaljic, M, Lehmann, R, Vilcinskas, A and Franta, Z (2016) Urate Oxidase produced by *Lucilia sericata* medicinal maggots promotes wound healing indirectly via the synthesis of allantoin. *submitted to Insect Biochemistry and Molecular Biology*.
- Beckert, A, Wiesner, J, Baumann, A, Pöppel, AK, Vogel, H and Vilcinskas, A (2015) Two c-type lysozymes boost the innate immune system of the invasive ladybird *Harmonia axyridis*. *Developmental and comparative immunology* **49**: 303-12.
- Beckert, A, Wiesner, J, Schmidtberg, H, Lehmann, R, Baumann, A, Vogel, H and Vilcinskas, A (2016) Expression and characterization of a recombinant i-type lysozyme from the harlequin ladybird beetle *Harmonia axyridis*. *Insect Mol Biol* **25**: 202-15.
- Bexfield, A, Bond, AE, Morgan, C, Wagstaff, J, Newton, RP, Ratcliffe, NA, Dudley, E and Nigam, Y (2010) Amino acid derivatives from *Lucilia sericata* excretions/secretions may contribute to the beneficial effects of maggot therapy via increased angiogenesis. *Br J Dermatol* **162**: 554-62.
- Bexfield, A, Bond, AE, Roberts, EC, Dudley, E, Nigam, Y, Thomas, S, Newton, RP and Ratcliffe, NA (2008) The antibacterial activity against MRSA strains and other bacteria of a <500Da

- fraction from maggot excretions/secretions of *Lucilia sericata* (Diptera: Calliphoridae). *Microbes and infection / Institut Pasteur* **10**: 325-33.
- Boehme, P, Spahn, P, Amendt, J and Zehner, R (2013) Differential gene expression during metamorphosis: a promising approach for age estimation of forensically important *Calliphora vicina* pupae (Diptera: Calliphoridae). *International Journal of Legal Medicine* **127**: 243-249.
- Bomalaski, JS, Holtsberg, FW, Ensor, CM and Clark, MA (2002) Uricase formulated with polyethylene glycol (uricase-PEG 20): biochemical rationale and preclinical studies. *J Rheumatol* **29**: 1942-9.
- Bonfield, JK and Whitwham, A (2010) Gap5--editing the billion fragment sequence assembly. *Bioinformatics* **26**: 1699-703.
- Bowling, FL, Salgami, EV and Boulton, AJ (2007) Larval therapy: a novel treatment in eliminating methicillin-resistant *Staphylococcus aureus* from diabetic foot ulcers. *Diabetes Care* **30**: 370-1.
- Broughton, G, 2nd, Janis, JE and Attinger, CE (2006) The basic science of wound healing. *Plast Reconstr Surg* **117**: 12S-34S.
- Brown, A, Horobin, A, Blount, DG, Hill, PJ, English, J, Rich, A, Williams, PM and Pritchard, DI (2012) Blow fly *Lucilia sericata* nuclease digests DNA associated with wound slough/eschar and with *Pseudomonas aeruginosa* biofilm. *Medical and Veterinary Entomology* **26**: 432-439.
- Brown, AW (1938) The nitrogen metabolism of an insect (*Lucilia sericata* Mg.): Uric acid, allantoin and uricase. *Biochem J* **32**: 895-902.
- Burns, CM and Wortmann, RL (2011) Gout therapeutics: new drugs for an old disease. *Lancet* **377**: 165-77.
- Bursell, E (1967) The Excretion of Nitrogen in Insects. *Advances in Insect Physiology* **Volume 4**: 33-67.
- Bustin, SA (2002) Quantification of mRNA using real-time reverse transcription PCR (RT-PCR): trends and problems. *Journal of molecular endocrinology* **29**: 23-39.
- Bustin, SA, Benes, V, Garson, JA, Hellemsans, J, Huggett, J, Kubista, M, Mueller, R, Nolan, T, Pfaffl, MW, Shipley, GL, Vandesompele, J and Wittwer, CT (2009) The MIQE guidelines: minimum information for publication of quantitative real-time PCR experiments. *Clin Chem* **55**: 611-22.
- Cazander, G, Pritchard, DI, Nigam, Y, Jung, W and Nibbering, PH (2013) Multiple actions of *Lucilia sericata* larvae in hard-to-heal wounds: larval secretions contain molecules that accelerate wound healing, reduce chronic inflammation and inhibit bacterial infection. *Bioessays* **35**: 1083-92.
- Cazander, G, van Veen, KE, Bernards, AT and Jukema, GN (2009a) Do maggots have an influence on bacterial growth? A study on the susceptibility of strains of six different bacterial species to maggots of *Lucilia sericata* and their excretions/secretions. *Journal of tissue viability* **18**: 80-7.
- Cazander, G, van Veen, KE, Bouwman, LH, Bernards, AT and Jukema, GN (2009b) The influence of maggot excretions on PAO1 biofilm formation on different biomaterials. *Clin Orthop Relat Res* **467**: 536-45.
- Cerovsky, V and Bem, R (2014) Lucifensins, the Insect Defensins of Biomedical Importance: The Story behind Maggot Therapy. *Pharmaceuticals (Basel)* **7**: 251-64.
- Chambers, L, Woodrow, S, Brown, AP, Harris, PD, Phillips, D, Hall, M, Church, JCT and Pritchard, DI (2003) Degradation of extracellular matrix components by defined proteinases from the greenbottle larva *Lucilia sericata* used for the clinical debridement of non-healing wounds. *British Journal of Dermatology* **148**: 14-23.

- Chapman, AD (2009) *Numbers of Living Species in Australia and the World 2nd edition*, 2nd edition edn. Australian Government, Department of the Environment, Water, Heritage and the Arts.
- Cherniack, EP (2010) Bugs as drugs, Part 1: Insects: the "new" alternative medicine for the 21st century? *Altern Med Rev* **15**: 124-35.
- Chernin, E (1986) Surgical maggots. *South Med J* **79**: 1143-5.
- Church, JC (1996) The traditional use of maggots in wound healing, and the development of larva therapy (biosurgery) in modern medicine. *J Altern Complement Med* **2**: 525-7.
- Colloc'h, N, el Hajji, M, Bachet, B, L'Hermite, G, Schiltz, M, Prange, T, Castro, B and Mornon, JP (1997) Crystal structure of the protein drug urate oxidase-inhibitor complex at 2.05 Å resolution. *Nat Struct Biol* **4**: 947-52.
- Cruz, JC, Wurges, K, Kramer, M, Pfromm, PH, Rezac, ME and Czermak, P (2011) Immobilization of enzymes on fumed silica nanoparticles for applications in nonaqueous media. *Methods Mol Biol* **743**: 147-60.
- Davidson, MB, Thakkar, S, Hix, JK, Bhandarkar, ND, Wong, A and Schreiber, MJ (2004) Pathophysiology, clinical consequences, and treatment of tumor lysis syndrome. *Am J Med* **116**: 546-54.
- Davies, CE, Hill, KE, Wilson, MJ, Stephens, P, Hill, CM, Harding, KG and Thomas, DW (2004) Use of 16S ribosomal DNA PCR and denaturing gradient gel electrophoresis for analysis of the microfloras of healing and nonhealing chronic venous leg ulcers. *Journal of clinical microbiology* **42**: 3549-57.
- Davydov, L (2011) Maggot therapy in wound management in modern era and a review of published literature. *Journal of pharmacy practice* **24**: 89-93.
- Del Toro, G, Morris, E and Cairo, MS (2005) Tumor lysis syndrome: pathophysiology, definition, and alternative treatment approaches. *Clin Adv Hematol Oncol* **3**: 54-61.
- Dini, V, Salvo, P, Janowska, A, Di Francesco, F, Barbini, A and Romanelli, M (2015) Correlation Between Wound Temperature Obtained With an Infrared Camera and Clinical Wound Bed Score in Venous Leg Ulcers. *Wounds* **27**: 274-8.
- DiSalvo, RM (2002) Allantoin. In: *Chemistry and Manufacture of Cosmetics, Vol 3*, . pp. 29-43.
- Dow, G, Browne, A and Sibbald, RG (1999) Infection in chronic wounds: controversies in diagnosis and treatment. *Ostomy Wound Manage* **45**: 23-7, 29-40; quiz 41-2.
- Dunbar, GK (1944) Notes on the Ngemba tribe of the Central Darling River of Western New South Wales. *Mankind* **3**:177-80
- Edwards, NL (2008) Treatment-failure gout: a moving target. *Arthritis Rheum* **58**: 2587-90.
- Eggert, A-K, Müller, J, Wimmer, E and Zissler, D (2010) Fortpflanzung und Entwicklung. In: *Lehrbuch der Entomologie* (Dettner, K and Peters, W, eds.). pp. 357-463. Spektrum Akademischer Verlag (Heidelberg).
- Eming, SA, Krieg, T and Davidson, JM (2007) Inflammation in wound repair: molecular and cellular mechanisms. *J Invest Dermatol* **127**: 514-25.
- Fazli, M, Bjarnsholt, T, Kirketerp-Moller, K, Jorgensen, B, Andersen, AS, Krogfelt, KA, Givskov, M and Tolker-Nielsen, T (2009) Nonrandom distribution of *Pseudomonas aeruginosa* and *Staphylococcus aureus* in chronic wounds. *Journal of clinical microbiology* **47**: 4084-9.
- Fetzner, S and Steiner, RA (2010) Cofactor-independent oxidases and oxygenases. *Appl Microbiol Biotechnol* **86**: 791-804.
- Fleischmann, W, Grassberger, M and Sherman, R (2004) *Maggot Therapy: A Handbook of Maggot-Assisted Wound Healing*. Thieme Verlag Stuttgart.
- Fraisse, L, Bonnet, MC, de Farcy, JP, Agut, C, Dersigny, D and Bayol, A (2002) A colorimetric 96-well microtiter plate assay for the determination of urate oxidase activity and its kinetic parameters. *Analytical Biochemistry* **309**: 173-179.

- Franta, Z, Vogel, H, Lehmann, R, Rupp, O, Goesmann, A and Vilcinskas, A (2016) Next Generation Sequencing Identifies Five Major Classes of Potentially Therapeutic Enzymes Secreted by *Lucilia sericata* Medical Maggots. *Biomed Res Int* **2016**: 8285428.
- Freeman, WH and Bracegirdle, B (1971) *An atlas of invertebrate structure*. Heinemann Educational Books London, ISBN 0-435-60315-9.
- Fujiwara, S and Noguchi, T (1995) Degradation of purines: only ureidoglycollate lyase out of four allantoin-degrading enzymes is present in mammals. *Biochem J* **312 ( Pt 1)**: 315-8.
- Gabison, L, Chiadmi, M, Colloc'h, N, Castro, B, El Hajji, M and Prange, T (2006) Recapture of [S]-allantoin, the product of the two-step degradation of uric acid, by urate oxidase. *FEBS Lett* **580**: 2087-91.
- Ganson, NJ, Kelly, SJ, Scarlett, E, Sundy, JS and Hershfield, MS (2006) Control of hyperuricemia in subjects with refractory gout, and induction of antibody against poly(ethylene glycol) (PEG), in a phase I trial of subcutaneous PEGylated urate oxidase. *Arthritis Res Ther* **8**: R12.
- Garay, RP, El-Gewely, MR, Labaune, JP and Richette, P (2012) Therapeutic perspectives on uricases for gout. *Joint Bone Spine* **79**: 237-42.
- Georgel, P, Naitza, S, Kappler, C, Ferrandon, D, Zachary, D, Swimmer, C, Kopczynski, C, Duyk, G, Reichhart, JM and Hoffmann, JA (2001) *Drosophila* immune deficiency (IMD) is a death domain protein that activates antibacterial defense and can promote apoptosis. *Developmental cell* **1**: 503-14.
- Gethin, G (2007) The significance of surface pH in chronic wounds. *Wounds UK* **3**: 52.
- Goldman, SC, Holcenberg, JS, Finklestein, JZ, Hutchinson, R, Kreissman, S, Johnson, FL, Tou, C, Harvey, E, Morris, E and Cairo, MS (2001) A randomized comparison between rasburicase and allopurinol in children with lymphoma or leukemia at high risk for tumor lysis. *Blood* **97**: 2998-3003.
- Goldstein, H ( 1931) Maggots in the treatment of wound and bone infections. *J. Bone Jt. Surg.* **13**:476-78.
- Gottrup, F and Jorgensen, B (2011) Maggot debridement: an alternative method for debridement. *Eplasty* **11**: e33.
- Grabherr, MG, Haas, BJ, Yassour, M, Levin, JZ, Thompson, DA, Amit, I, Adiconis, X, Fan, L, Raychowdhury, R, Zeng, Q, Chen, Z, Mauceli, E, Hacohen, N, Gnirke, A, Rhind, N, di Palma, F, Birren, BW, Nusbaum, C, Lindblad-Toh, K, Friedman, N and Regev, A (2011) Full-length transcriptome assembly from RNA-Seq data without a reference genome. *Nature biotechnology* **29**: 644-52.
- Grassberger, M, Sherman, RA, Gileve, O, Kim, C and Mumcuoglu, KY (2013) *Biotherapy - History, Principles and Practice*. Springer.
- Green, MR and MacCallum, P (2012) *Molecular Cloning: A Laboratory Manual* Fourth Edition edn. Cold Spring Harbor Laboratory Press.
- Groombridge, B and Jenkins, MD (2002) *World Atlas of Biodiversity*. University of California press.
- Gutierrez, L, Mauriat, M, Guenin, S, Pelloux, J, Lefebvre, JF, Louvet, R, Rusterucci, C, Moritz, T, Guerineau, F, Bellini, C and Van Wuytswinkel, O (2008) The lack of a systematic validation of reference genes: a serious pitfall undervalued in reverse transcription-polymerase chain reaction (RT-PCR) analysis in plants. *Plant biotechnology journal* **6**: 609-18.
- Han, YS, Chun, J, Schwartz, A, Nelson, S and Paskewitz, SM (1999) Induction of mosquito hemolymph proteins in response to immune challenge and wounding. *Developmental and comparative immunology* **23**: 553-62.
- Harris, LG, Nigam, Y, Sawyer, J, Mack, D and Pritchard, DI (2013) *Lucilia sericata* Chymotrypsin Disrupts Protein Adhesin-Mediated Staphylococcal Biofilm Formation. *Applied and Environmental Microbiology* **79**: 1393-1395.

- Hayakawa, T, Sato, S, Iwamoto, S, Sudo, S, Sakamoto, Y, Yamashita, T, Uchida, M, Matsushima, K, Kashino, Y and Sakai, H (2010) Novel strategy for protein production using a peptide tag derived from *Bacillus thuringiensis* Cry4Aa. *FEBS J* **277**: 2883-91.
- Hayashi, S, Fujiwara, S and Noguchi, T (2000) Evolution of urate-degrading enzymes in animal peroxisomes. *Cell Biochem Biophys* **32 Spring**: 123-9.
- Hernandez, R (2006) The use of systemic antibiotics in the treatment of chronic wounds. *Dermatol Ther* **19**: 326-37.
- Hetru, C, Troxler, L and Hoffmann, JA (2003) *Drosophila melanogaster* antimicrobial defense. *The Journal of infectious diseases* **187 Suppl 2**: S327-34.
- Hoffmann, JA and Reichhart, JM (2002) *Drosophila* innate immunity: an evolutionary perspective. *Nature immunology* **3**: 121-6.
- Honomichl, K (2010) Systematik. In: *Lehrbuch der Entomologie* (Dettner, K and Peters, W, eds.). pp. 735-751. Spektrum Akademischer Verlag, Heidelberg.
- Horobin, AJ, Shakesheff, KM and Pritchard, DI (2005) Maggots and wound healing: an investigation of the effects of secretions from *Lucilia sericata* larvae upon the migration of human dermal fibroblasts over a fibronectin-coated surface. *Wound Repair and Regeneration* **13**: 422-433.
- Horobin, AJ, Shakesheff, KM and Pritchard, DI (2006) Promotion of human dermal fibroblast migration, matrix remodelling and modification of fibroblast morphology within a novel 3D model by *Lucilia sericata* larval secretions. *J Invest Dermatol* **126**: 1410-8.
- Howell-Jones, RS, Wilson, MJ, Hill, KE, Howard, AJ, Price, PE and Thomas, DW (2005) A review of the microbiology, antibiotic usage and resistance in chronic skin wounds. *J Antimicrob Chemother* **55**: 143-9.
- Huberman, L, Gollop, N, Mumcuoglu, KY, Block, C and Galun, R (2007a) Antibacterial properties of whole body extracts and haemolymph of *Lucilia sericata* maggots. *J Wound Care* **16**: 123-7.
- Huberman, L, Gollop, N, Mumcuoglu, KY, Breuer, E, Bhusare, SR and Shai, Y (2007b) Antibacterial substances of low molecular weight isolated from the blowfly, *Lucilia sericata*. *Medical and Veterinary Entomology* **21**: 127-131.
- Imler, JL and Bulet, P (2005) Antimicrobial peptides in *Drosophila*: structures, activities and gene regulation. *Chemical immunology and allergy* **86**: 1-21.
- Jacobs and Renner (2007) *Biologie und Ökologie der Insekten*, 4th edition edn. Spektrum Akademischer Verlag.
- Jansohn, M and Rothhämel, S (2012) *Gentechnische Methoden*. Spektrum Verlag.
- Jeffcoate, WJ and Harding, KG (2003) Diabetic foot ulcers. *Lancet* **361**: 1545-51.
- Jevsevar, S, Kunstelj, M and Porekar, VG (2010) PEGylation of therapeutic proteins. *Biotechnol J* **5**: 113-28.
- Juan, EC, Hoque, MM, Shimizu, S, Hossain, MT, Yamamoto, T, Imamura, S, Suzuki, K, Tsunoda, M, Amano, H, Sekiguchi, T and Takenaka, A (2008) Structures of *Arthrobacter globiformis* urate oxidase-ligand complexes. *Acta Crystallogr D Biol Crystallogr* **D64**: 815-22.
- Jurkevitch, E (2011) Riding the Trojan horse: combating pest insects with their own symbionts. *Microb Biotechnol* **4**: 620-7.
- Kahl, M, Gokcen, A, Fischer, S, Baumer, M, Wiesner, J, Lochnit, G, Wygrecka, M, Vilcinskas, A and Preissner, KT (2015) Maggot excretion products from the blowfly *Lucilia sericata* contain contact phase/intrinsic pathway-like proteases with procoagulant functions. *Thrombosis and Haemostasis* **114**: 277-288.

- Kawabata, T, Mitsui, H, Yokota, K, Ishino, K, Oguma, K and Sano, S (2010) Induction of antibacterial activity in larvae of the blowfly *Lucilia sericata* by an infected environment. *Medical and veterinary entomology* **24**: 375-81.
- Keebaugh, AC and Thomas, JW (2010) The evolutionary fate of the genes encoding the purine catabolic enzymes in hominoids, birds, and reptiles. *Mol Biol Evol* **27**: 1359-69.
- Kim, MJ, Hopfer, H and Mayr, M (2016) [Uric acid, kidney disease and nephrolithiasis]. *Ther Umsch* **73**: 159-65.
- Kratzer, JT, Lanaspá, MA, Murphy, MN, Cicerchi, C, Graves, CL, Tipton, PA, Ortlund, EA, Johnson, RJ and Gaucher, EA (2014) Evolutionary history and metabolic insights of ancient mammalian uricases. *Proc Natl Acad Sci U S A* **111**: 3763-8.
- Kuzhivelil, BT and Mohamed, UV (1998) Allantoin and allantoinic acid titre in the faeces and tissues of the developing larva of the moth, *Orthaga exvinacea* Hampson. *Insect Biochem Mol Biol* **28**: 979-86.
- Langmead, B, Trapnell, C, Pop, M and Salzberg, SL (2009) Ultrafast and memory-efficient alignment of short DNA sequences to the human genome. *Genome biology* **10**: R25.
- Larrey, DJ (1829) Observations on wounds and their complications by erysipelas, gangrene and tetanus. *Paris: Clin. Chir. Transl. EF Rivinus, 1932. p. 34. Philadelphia: Key, Mielke & Biddle.* pp. 51– 52.
- Lauzon, CR, Sjogren, RE and Prokopy, RJ (2000) Enzymatic Capabilities of Bacteria Associated with Apple Maggot Flies: A Postulated Role in Attraction. *Journal of Chemical Ecology* **26**: 953-967.
- Lee, RE, Elnitsky, MA, Rinehart, JP, Hayward, SAL, Sandro, LH and Denlinger, DL (2006) Rapid cold-hardening increases the freezing tolerance of the Antarctic midge *Belgica antarctica*. *Journal of Experimental Biology* **209**: 399-406.
- Legoux, R, Delpuch, B, Dumont, X, Guillemot, JC, Ramond, P, Shire, D, Caput, D, Ferrara, P and Loison, G (1992) Cloning and expression in *Escherichia coli* of the gene encoding *Aspergillus flavus* urate oxidase. *J Biol Chem* **267**: 8565-70.
- Liebig and Wöhler (1837) Ueber die Natur der Harnsäure. *Annalen der Physik* **117**: 561-662.
- Majerowicz, D, Alves-Bezerra, M, Logullo, R, Fonseca-de-Souza, AL, Meyer-Fernandes, JR, Braz, GR and Gondim, KC (2011) Looking for reference genes for real-time quantitative PCR experiments in *Rhodnius prolixus* (Hemiptera: Reduviidae). *Insect molecular biology* **20**: 713-22.
- Marchetti, M, Liuzzi, A, Fermi, B, Corsini, R, Folli, C, Speranzini, V, Gandolfi, F, Bettati, S, Ronda, L, Cendron, L, Berni, R, Zanotti, G and Percudani, R (2016) Catalysis and Structure of Zebrafish Urate Oxidase Provide Insights into the Origin of Hyperuricemia in Hominoids. *Sci Rep* **6**: 38302.
- Mayne, N, Keady, S and Thacker, M (2008) Rasburicase in the prevention and treatment of tumour lysis syndrome. *Intensive Crit Care Nurs* **24**: 59-62.
- McCallon, SK, Weir, D and Lantis, JC, 2nd (2014) Optimizing Wound Bed Preparation With Collagenase Enzymatic Debridement. *J Am Coll Clin Wound Spec* **6**: 14-23.
- McCarthy, H, Rudkin, JK, Black, NS, Gallagher, L, O'Neill, E and O'Gara, JP (2015) Methicillin resistance and the biofilm phenotype in. *Frontiers in cellular and infection microbiology* **5**: 1.
- McIntosh, CD and Thomson, CE (2006) Honey dressing versus paraffin tulle gras following toenail surgery. *J Wound Care* **15**: 133-6.
- Meriin, AB, Zaarur, N and Sherman, MY (2012) Association of translation factor eEF1A with defective ribosomal products generates a signal for aggresome formation. *Journal of cell science* **125**: 2665-74.

- Mihai, MM, Holban, AM, Giurcaneanu, C, Popa, LG, Buzea, M, Filipov, M, Lazar, V, Chifriuc, MC and Popa, MI (2014) Identification and phenotypic characterization of the most frequent bacterial etiologies in chronic skin ulcers. *Romanian journal of morphology and embryology = Revue roumaine de morphologie et embryologie* **55**: 1401-8.
- Milde, J (2010) Nervensystem. In: *Lehrbuch der Entomologie* (Dettner, K and Peters, W, eds.). pp. 205-227. Spektrum Akademischer Verlag, Heidelberg.
- Monner, DA, Jonsson, S and Boman, HG (1971) Ampicillin-resistant mutants of Escherichia coli K-12 with lipopolysaccharide alterations affecting mating ability and susceptibility to sex-specific bacteriophages. *Journal of bacteriology* **107**: 420-32.
- Mulcahy, LR, Isabella, VM and Lewis, K (2014) Pseudomonas aeruginosa biofilms in disease. *Microbial ecology* **68**: 1-12.
- Mullins, DE and Cochran, DG (1972) Nitrogen excretion in cockroaches: uric Acid is not a major product. *Science* **177**: 699-701.
- Mumcuoglu, KY, Davidson, E, Avidan, A and Gilead, L (2012) Pain related to maggot debridement therapy. *J Wound Care* **21**: 400, 402, 404-5.
- Mumcuoglu, KY, Miller, J, Mumcuoglu, M, Friger, M and Tarshis, M (2001) Destruction of bacteria in the digestive tract of the maggot of Lucilia sericata (Diptera : Calliphoridae). *Journal of Medical Entomology* **38**: 161-166.
- Nation, JL and Patton, RL (1961) A Study of Nitrogen Excretion in Insects. *Journal of Insect Physiology* **6**: 299-308.
- Nijhof, AM, Balk, JA, Postigo, M and Jongejan, F (2009) Selection of reference genes for quantitative RT-PCR studies in Rhipicephalus (Boophilus) microplus and Rhipicephalus appendiculatus ticks and determination of the expression profile of Bm86. *BMC molecular biology* **10**: 112.
- Nolan, T, Hands, RE and Bustin, SA (2006) Quantification of mRNA using real-time RT-PCR. *Nat Protoc* **1**: 1559-82.
- Packer, MS and Liu, DR (2015) Methods for the directed evolution of proteins. *Nat Rev Genet* **16**: 379-94.
- Perez-Ruiz, F and Liote, F (2007) Lowering serum uric acid levels: what is the optimal target for improving clinical outcomes in gout? *Arthritis Rheum* **57**: 1324-8.
- Peters, W (2010) Ernährung und Verdauung. In: *Lehrbuch der Entomologie* (Dettner, K and Peters, W, eds.). pp. 91-126. Spektrum Akademischer Verlag, Heidelberg.
- Petzel, DH, Pirotte, PT and Van Kerkhove, E (1999) Intracellular and luminal pH measurements of Malpighian tubules of the mosquito Aedes aegypti: the effects of cAMP. *Journal of Insect Physiology* **45**: 973-982.
- Pfaffl, MW (2001) A new mathematical model for relative quantification in real-time RT-PCR. *Nucleic acids research* **29**: e45.
- Pfaffl, MW, Horgan, GW and Dempfle, L (2002) Relative expression software tool (REST) for group-wise comparison and statistical analysis of relative expression results in real-time PCR. *Nucleic acids research* **30**: e36.
- Polakiewicz, RD, Munroe, DJ, Sait, SN, Tycowski, KT, Nowak, NJ, Shows, TB, Housman, DE and Page, DC (1995) Mapping of ribosomal protein S3 and internally nested snoRNA U15A gene to human chromosome 11q13.3-q13.5. *Genomics* **25**: 577-80.
- Ponton, F, Chapuis, MP, Pernice, M, Sword, GA and Simpson, SJ (2011) Evaluation of potential reference genes for reverse transcription-qPCR studies of physiological responses in Drosophila melanogaster. *Journal of insect physiology* **57**: 840-50.
- Pöppel, AK, Kahl, M, Baumann, A, Wiesner, J, Gokcen, A, Beckert, A, Preissner, KT, Vilcinskis, A and Franta, Z (2016) A Jonah-like chymotrypsin from the therapeutic maggot Lucilia

- sericata plays a role in wound debridement and coagulation. *Insect Biochemistry and Molecular Biology* **70**: 138-147.
- Pöppel, AK, Koch, A, Kogel, KH, Vogel, H, Kollwe, C, Wiesner, J and Vilcinskas, A (2014) Lucimycin, an antifungal peptide from the therapeutic maggot of the common green bottle fly *Lucilia sericata*. *Biological chemistry* **395**: 649-56.
- Pöppel, AK, Vogel, H, Wiesner, J and Vilcinskas, A (2015) Antimicrobial peptides expressed in medicinal maggots of the blow fly *Lucilia sericata* show combinatorial activity against bacteria. *Antimicrobial agents and chemotherapy*.
- Posnett, J, Gottrup, F, Lundgren, H and Saal, G (2009) The resource impact of wounds on health-care providers in Europe. *J Wound Care* **18**: 154-161.
- Raven, PH and Yeates, DK (2007) Australian biodiversity: threats for the present, opportunities for the future.
- Rich, BE and Steitz, JA (1987) Human acidic ribosomal phosphoproteins P0, P1, and P2: analysis of cDNA clones, in vitro synthesis, and assembly. *Molecular and cellular biology* **7**: 4065-74.
- Robinson, W (1935) Allantoin, a Constituent of Maggot Excretions, Stimulates Healing of Chronic Discharging Wounds. *The Journal of parasitology* **21**: 354-358.
- Scaraffia, PY, Tan, G, Isoe, J, Wysocki, VH, Wells, MA and Miesfeld, RL (2008) Discovery of an alternate metabolic pathway for urea synthesis in adult *Aedes aegypti* mosquitoes. *Proc Natl Acad Sci U S A* **105**: 518-23.
- Scharlaken, B, de Graaf, DC, Goossens, K, Brunain, M, Peelman, LJ and Jacobs, FJ (2008) Reference Gene Selection for Insect Expression Studies Using Quantitative Real-Time PCR: The Head of the Honeybee, *Apis mellifera*, After a Bacterial Challenge. *Journal of insect science* **8**: 1-10.
- Sen, CK, Gordillo, GM, Roy, S, Kirsner, R, Lambert, L, Hunt, TK, Gottrup, F, Gurtner, GC and Longaker, MT (2009) Human skin wounds: a major and snowballing threat to public health and the economy. *Wound Repair Regen* **17**: 763-71.
- Sherman, RA (2002) Maggot versus conservative debridement therapy for the treatment of pressure ulcers. *Wound Repair and Regeneration* **10**: 208-214.
- Sherman, RA (2003) Maggot therapy for treating diabetic foot ulcers unresponsive to conventional therapy. *Diabetes Care* **26**: 446-51.
- Sherman, RA (2009) Maggot therapy takes us back to the future of wound care: new and improved maggot therapy for the 21st century. *J Diabetes Sci Technol* **3**: 336-44.
- Sherman, RA (2014) Mechanisms of maggot-induced wound healing: what do we know, and where do we go from here? *Evid Based Complement Alternat Med* **2014**: 592419.
- Sherman, RA, Hall, MJ and Thomas, S (2000) Medicinal maggots: an ancient remedy for some contemporary afflictions. *Annu Rev Entomol* **45**: 55-81.
- Sherman, RA, Sherman, J, Gilead, L, Lipo, M and Mumcuoglu, KY (2001) Maggot debridement therapy in outpatients. *Arch Phys Med Rehabil* **82**: 1226-9.
- Sherman, RA, Wyle, F and Vulpe, M (1995) Maggot therapy for treating pressure ulcers in spinal cord injury patients. *J Spinal Cord Med* **18**: 71-4.
- Sherwood, V (1996) Chapter 21: Most Heat Tolerant. In: *Book of Insect Records*. pp. Department of Entomology & Nematology, University of Florida, Gainesville.
- Shiravi, A, Mostafavi, R, Akbarzadeh, K and Oshaghi, M (2011) Temperature Requirements of Some Common Forensically Important Blow and Flesh Flies (Diptera) under Laboratory Conditions. *Iran J Arthropod Borne Dis* **5**: 54-62.
- Spohner, SC, Schaum, V, Quitmann, H and Czermak, P (2016) *Kluyveromyces lactis*: An emerging tool in biotechnology. *J Biotechnol* **222**: 104-16.
- Staiger, C (2012) Comfrey: a clinical overview. *Phytother Res* **26**: 1441-8.

- Steenvoorde, P, Jacobi, CE, Van Doorn, L and Oskam, J (2007) Maggot debridement therapy of infected ulcers: patient and wound factors influencing outcome - a study on 101 patients with 117 wounds. *Ann R Coll Surg Engl* **89**: 596-602.
- Stevens, J and Wall, R (1996) Species, sub-species and hybrid populations of the blowflies *Lucilia cuprina* and *Lucilia sericata* (Diptera:Calliphoridae). *Proc Biol Sci* **263**: 1335-41.
- Subrahmanyam, M (1991) Topical application of honey in treatment of burns. *Br J Surg* **78**: 497-8.
- Sun, M, Lu, MX, Tang, XT and Du, YZ (2015) Exploring valid reference genes for quantitative real-time PCR analysis in *Sesamia inferens* (Lepidoptera: Noctuidae). *PLoS one* **10**: e0115979.
- Sundy, JS, Baraf, HS, Yood, RA, Edwards, NL, Gutierrez-Urena, SR, Treadwell, EL, Vazquez-Mellado, J, White, WB, Lipsky, PE, Horowitz, Z, Huang, W, Maroli, AN, Waltrip, RW, 2nd, Hamburger, SA and Becker, MA (2011) Efficacy and tolerability of pegloticase for the treatment of chronic gout in patients refractory to conventional treatment: two randomized controlled trials. *JAMA* **306**: 711-20.
- Sundy, JS and Hershfield, MS (2007) Uricase and other novel agents for the management of patients with treatment-failure gout. *Curr Rheumatol Rep* **9**: 258-64.
- Tarone, AM and Foran, DR (2011) Gene expression during blow fly development: improving the precision of age estimates in forensic entomology. *J Forensic Sci* **56 Suppl 1**: S112-22.
- Tarone, AM, Picard, CJ, Spiegelman, C and Foran, DR (2011) Population and Temperature Effects on *Lucilia sericata* (Diptera: Calliphoridae) Body Size and Minimum Development Time. *Journal of Medical Entomology* **48**: 1062-1068.
- Telford, G, Brown, AP, Seabra, RA, Horobin, AJ, Rich, A, English, JS and Pritchard, DI (2010) Degradation of eschar from venous leg ulcers using a recombinant chymotrypsin from *Lucilia sericata*. *Br J Dermatol* **163**: 523-31.
- Thomas, S (2006) Cost of managing chronic wounds in the U.K., with particular emphasis on maggot debridement therapy. *J Wound Care* **15**: 465-9.
- Thomas, S, Wynn, K, Fowler, T and Jones, M (2002) The effect of containment on the properties of sterile maggots. *Br J Nurs* **11**: S21-2, S24, S26 passim.
- Tolker-Nielsen, T (2014) *Pseudomonas aeruginosa* biofilm infections: from molecular biofilm biology to new treatment possibilities. *APMIS. Supplementum*: 1-51.
- Toutges, MJ, Hartzler, K, Lord, J and Oppert, B (2010) Evaluation of reference genes for quantitative polymerase chain reaction across life cycle stages and tissue types of *Tribolium castaneum*. *Journal of agricultural and food chemistry* **58**: 8948-51.
- Ueng, S (2005) Rasburicase (Elitek): a novel agent for tumor lysis syndrome. *Proc (Bayl Univ Med Cent)* **18**: 275-9.
- Valachova, I, Majtan, T, Takac, P and Majtan, J (2014) Identification and characterisation of different proteases in *Lucilia sericata* medicinal maggots involved in maggot debridement therapy. *Journal of Applied Biomedicine* **12**: 171-177.
- van der Plas, MJ, van der Does, AM, Baldry, M, Dogterom-Ballering, HC, van Gulpen, C, van Dissel, JT, Nibbering, PH and Jukema, GN (2007) Maggot excretions/secretions inhibit multiple neutrophil pro-inflammatory responses. *Microbes Infect* **9**: 507-14.
- van der Plas, MJ, van Dissel, JT and Nibbering, PH (2009) Maggot secretions skew monocyte-macrophage differentiation away from a pro-inflammatory to a pro-angiogenic type. *PLoS One* **4**: e8071.
- van der Plas, MJA, Jukema, GN, Wai, SW, Dogterom-Ballering, HCM, Legendijk, EL, van Gulpen, C, van Dissel, JT, Bloemberg, GV and Nibbering, PH (2008) Maggot excretions/secretions are differentially effective against biofilms of *Staphylococcus aureus* and *Pseudomonas aeruginosa*. *Journal of Antimicrobial Chemotherapy* **61**: 117-122.

- Vanderwee, K, Clark, M, Dealey, C, Gunningberg, L and Defloor, T (2007) Pressure ulcer prevalence in Europe: a pilot study. *J Eval Clin Pract* **13**: 227-35.
- Vandesompele, J, De Preter, K, Pattyn, F, Poppe, B, Van Roy, N, De Paepe, A and Speleman, F (2002) Accurate normalization of real-time quantitative RT-PCR data by geometric averaging of multiple internal control genes. *Genome biology* **3**: RESEARCH0034.
- Vogels, GD and Van der Drift, C (1976) Degradation of purines and pyrimidines by microorganisms. *Bacteriol Rev* **40**: 403-68.
- Volkl, A, Baumgart, E and Fahimi, HD (1988) Localization of urate oxidase in the crystalline cores of rat liver peroxisomes by immunocytochemistry and immunoblotting. *J Histochem Cytochem* **36**: 329-36.
- von Dungern, P and Briegel, H (2001) Protein catabolism in mosquitoes: ureotely and uricotely in larval and imaginal *Aedes aegypti*. *J Insect Physiol* **47**: 131-141.
- Walker, SE and Lorsch, J (2013) RNA purification--precipitation methods. *Methods in enzymology* **530**: 337-43.
- Wallrath, LL, Burnett, JB and Friedman, TB (1990) Molecular characterization of the *Drosophila melanogaster* urate oxidase gene, an ecdysone-repressible gene expressed only in the malpighian tubules. *Mol Cell Biol* **10**: 5114-27.
- Wasserthal, LT (2010) Atemsystem. In: *Lehrbuch der Entomologie* (Dettner, K and Peters, W, eds.). pp. 165-183. Spektrum Akademischer Verlag, Heidelberg.
- Weil, GC, Simon, RJ and Sweadner, WR (1933) A biological, bacteriological and clinical study of larval or maggot therapy in the treatment of acute and chronic pyogenic infections. *Am. J. Surg.* **19**:36-48.
- Wendler, G (2010) Fortbewegung und sensomotorische Integration. In: *Lehrbuch der Entomologie* (Dettner, K and Peters, W, eds.). pp. 229-272. Spektrum Akademischer Verlag, Heidelberg.
- Whitaker, IS, Twine, C, Whitaker, MJ, Welck, M, Brown, CS and Shandall, A (2007) Larval therapy from antiquity to the present day: mechanisms of action, clinical applications and future potential. *Postgrad Med J* **83**: 409-13.
- Willemstein, SC (1987) An Evolutionary Basis for Pollination Ecology. In: *Book An Evolutionary Basis for Pollination Ecology* (Editor, ed.^eds.). Vol., pp. Leiden Botanical Series, City.
- Williams, KA and Villet, MH (2014) Morphological identification of *Lucilia sericata*, *Lucilia cuprina* and their hybrids (Diptera, Calliphoridae). *Zookeys*: 69-85.
- Wright, PA (1995) Nitrogen excretion: three end products, many physiological roles. *J Exp Biol* **198**: 273-81.
- Yao, K, Bae, L and Yew, WP (2013) Post-operative wound management. *Aust Fam Physician* **42**: 867-70.
- Yuan, M, Lu, Y, Zhu, X, Wan, H, Shakeel, M, Zhan, S, Jin, BR and Li, J (2014) Selection and evaluation of potential reference genes for gene expression analysis in the brown planthopper, *Nilaparvata lugens* (Hemiptera: Delphacidae) using reverse-transcription quantitative PCR. *PLoS one* **9**: e86503.
- Zimmerman, SG, Peters, NC, Altaras, AE and Berg, CA (2013) Optimized RNA ISH, RNA FISH and protein-RNA double labeling (IF/FISH) in *Drosophila* ovaries. *Nat Protoc* **8**: 2158-79.
- Zitzmann, J, Weidner, T and Czermak, P (2017) Optimized expression of the antimicrobial protein Gloverin from *Galleria mellonella* using stably transformed *Drosophila melanogaster* S2 cells. *Cytotechnology*.

## Abbreviations

°C	Degree Celsius
4-AAP	4-amino-antipyrine
bp	Base pair
BSA	Bovine serum albumin
cDNA	Complementary deoxyribonucleic acid
Cq	quantification cycle
DAPI	4, 6-Diamidino-2-phenylindole
ddH <sub>2</sub> O	Double-distilled water
DCHBS	3,5-dichloro-2-hydroxybenzene sulfonic acid
DEPC	Diethylpyrocarbonate
DNA	Deoxyribonucleic acid
DSM	German Collection of Microorganisms and Cell Cultures
dT	Deoxy-thymidine nucleotides
E/S	secretions and excretions
<i>E. coli</i>	<i>Escherichia coli</i>
EDTA	Ethylenediamine tetraacetic acid
Fc	Final concentration
Fwd	Forward
g	Relative centrifugal force
h	hour
His6-Tag	Hexa-Histidine-Tag
HRP	horseradish peroxidase
i.a.	Inter alia
IMAC	Immobilized Metal Affinity Chromatography
LB	Lennox Broth
M	Mol/l
min	minute
<i>P. aeruginosa</i>	<i>Pseudomonas aeruginosa</i>
p.a.	Analytical grade
PEG	polyethylene glycol

---

PBS	Phosphate buffered saline
PVDF	Polyvinylidene difluoride
qRT-PCR	Quantitative reverse transcription polymerase chain reaction
Rev	Reverse
RNA	Ribonucleic acid
RT	Room temperature
TB	Terrific Broth
TBS	Tris buffer saline
Tm	Melting temperature
V	Volt ( $\text{kg}\cdot\text{m}^2\cdot\text{s}^{-3}\cdot\text{A}^{-1}$ )

## List of figures

Figure 1: Animal species infographics according to Chapman (2009).....	2
Figure 2: <i>Lucilia sericata</i> .....	4
Figure 3: The life-cycle of <i>L. sericata</i> .....	5
Figure 4: Maggot anatomy. ....	6
Figure 5: History of maggot therapy. ....	9
Figure 6: Overview of proven and postulated mechanisms by which medical maggots promote wound healing .....	10
Figure 7: MDT treatment of chronic wounds.....	13
Figure 8: UO reaction mechanism.....	15
Figure 9: General purine catabolism pathway overview.....	16
Figure 10: DNA and protein sequence of codon optimized <i>L. sericata</i> Urate Oxidase. ....	26
Figure 11: Two-step colorimetric UO assay.....	28
Figure 12: <i>L. sericata</i> RNA .....	32
Figure 13: Distribution of quantification cycle (Cq) values for <i>L. sericata</i> candidate genes obtained by qRT-PCR.....	33
Figure 14: Validation of <i>P. aeruginosa</i> immune challenge.....	34
Figure 15: Determination of the optimal number of control genes for normalization. ....	37
Figure 16: Quantitative RT-PCR analysis of lucimycin, defensin-1 and attacin-2 upon immune challenge. ....	38
Figure 17: Quantitative RT-PCR analysis of <i>UO</i> and <i>Alla</i> expression in <i>L. sericata</i> tissues. ....	39
Figure 18: ISH of <i>L. sericata</i> gut and Malpighian tubes.....	40
Figure 19: <i>UO<sub>r</sub></i> expression, purification and refolding.....	41
Figure 20: <i>UO<sub>r</sub></i> pH and temperature dependent activity.....	42
Figure 21: <i>UO<sub>r</sub></i> competitive inhibition, metal ion dependence and stability over time.....	43
Figure 22: Coomassie staining and UO detection by western blot in <i>L. sericata</i> tissues and E/S. ....	44
Figure 23: Whole mount staining of <i>L. sericata</i> gut and Malpighian tubes. ....	45
Figure 24: Melt curves of all applied qRT-PCR primer pairs. ....	78

---

## List of tables

<b>Table 1: Genes and qRT-PCR primers evaluated in this thesis.....</b>	<b>21</b>
<b>Table 2: ISH primer used in this thesis. ....</b>	<b>25</b>
<b>Table 3: Normfinder ranking of the stability values of candidate reference genes.....</b>	<b>35</b>
<b>Table 4: GeNorm ranking of stability measures for candidate reference genes and <i>attacin-2</i>. ....</b>	<b>36</b>
<b>Table 5: Chemicals and reagents .....</b>	<b>69</b>
<b>Table 6: Consumables.....</b>	<b>72</b>
<b>Table 7: Devices.....</b>	<b>73</b>
<b>Table 8: Standards and kits.....</b>	<b>73</b>
<b>Table 9: Buffers and solutions.....</b>	<b>74</b>
<b>Table 10: Normfinder intragroup variation for all candidate reference genes. ....</b>	<b>79</b>
<b>Table 11: Normfinder intergroup variation for all candidate reference genes. ....</b>	<b>79</b>

## Supplement A: Materials

### A.1 Chemicals and reagents

Table 5: Chemicals and reagents

Substance	Vendor	Catalog number
$\beta$ -mercaptoethanol	Bio-Rad, Hercules, US	161-0710
3,5-dichloro-2-hydroxybenzene sulfonic acid	Sigma-Aldrich, Munich, Germany	D4645-5G
4,6-Diamidino-2-phenylindole (DAPI)	Sigma-Aldrich, Munich, Germany	32670
4-amino-antipyrine	Carl Roth, Karlsruhe, Germany	2671.1
8-azaxanthine	Sigma-Aldrich, Munich, Germany	11460-1G
Acetic acid	Carl Roth, Karlsruhe, Germany	3738.4
Agar-Agar, bacteriological	Carl Roth, Karlsruhe, Germany	2266.2
Ampicillin sodium salt	Carl Roth, Karlsruhe, Germany	K029.2
Anhydrotetracycline	Sigma-Aldrich, Munich, Germany	94664
Aqua-Poly/Mount	Polysciences, Hirschberg an der Bergstrasse, Germany	18606-20
BL21(DE3) Competent <i>E. coli</i>	New England Biolabs, Ipswich, US	C2527H
Boric acid	Carl Roth, Karlsruhe, Germany	P010.1
Bromphenol blue	Carl Roth, Karlsruhe, Germany	A512.1
Bovine Serum Albumin	Sigma-Aldrich, Munich, Germany	A9418
Calcium chloride	Carl Roth, Karlsruhe, Germany	T885.2
Citric acid	Carl Roth, Karlsruhe, Germany	X863.2
Columbia Agar with Sheep Blood PLUS	Thermo Scientific Oxoid, Schwerte, Germany	10516583
Diethylpyrocarbonate	Carl Roth, Karlsruhe, Germany	K028.1
Di-Sodium hydrogen phosphate	Carl Roth, Karlsruhe, Germany	4984.2
Ethanol 100 % (p.a.)	Carl Roth, Karlsruhe, Germany	9065.2
Ethylenediamine tetraacetic acid (EDTA)	Carl Roth, Karlsruhe, Germany	CN06.1
Formamide	Sigma-Aldrich, Munich, Germany	F-9037
Glycerol	Carl Roth, Karlsruhe, Germany	3783.2

Glycin	Carl Roth, Karlsruhe, Germany	3908.3
goat anti guinea pig F(ab') <sub>2</sub> fragment Alexa488 conjugate antibody	Dianova, Hamburg, Germany	106-546-003
goat anti guinea pig F(ab') <sub>2</sub> fragment HRP conjugate antibody	Dianova, Hamburg, Germany	106-036-003
Guanidine hydrochloride	Carl Roth, Karlsruhe, Germany	0037.1
Heparin	Sigma-Aldrich, Munich, Germany	H-3393
Horseradish peroxidase	Sigma-Aldrich, Munich, Germany	P8375-5KU
Imidazole	Sigma-Aldrich, Munich, Germany	3899.3
<i>L. sericata</i> larvae	BioMonde GmbH, Barsbüttel, Germany	4701521
LB Broth (Lennox)	Carl Roth, Karlsruhe, Germany	X964.3
Magnesium chloride	Carl Roth, Karlsruhe, Germany	2189.2
Mini-PROTEAN TGX Gel 4-15 %	Bio-Rad, Hercules, US	#456-1084
Manganese(II) chloride	Sigma-Aldrich, Munich, Germany	244589
Sodium hydroxide	Carl Roth, Karlsruhe, Germany	6771.1
Nickel(II) sulfate	Sigma-Aldrich, Munich, Germany	31483
Nitroblue tetrazolium and bromo-chloro-indolyl-phosphate solution	Roche, Mannheim, Germany	11681451001
Paraformaldehyde (16%)	Polysciences, Hirschberg an der Bergstrasse, Germany	18814
pASK IBA37plus	IBA, Göttingen, Germany	2-1437-000
Proteinase K	Sigma-Aldrich, Munich, Germany	P2308
Qiagen Blocking Reagent	Qiagen, Hilden, Germany	34460
RNase free H <sub>2</sub> O	Macherey-Nagel, Weilmünster, Germany	740955.50
Roti-Blue quick	Carl Roth, Karlsruhe, Germany	4829.2
Roti-ImmunoBlock	Carl Roth, Karlsruhe, Germany	T144.1
Saline-sodium citrate (5 x)	Sigma-Aldrich, Munich, Germany	S-6639

Salmon testes DNA	Sigma-Aldrich, Munich, Germany	D-7656
Sheep anti-digoxigenin antibody alkaline phosphatase (AP)-labelled	Roche, Mannheim, Germany	11093274910
Sodium acetate (RNase free)	Fisher Scientific, Schwerte, Germany	#R1181
Sodium chloride	Carl Roth, Karlsruhe, Germany	9265.2
Sodium dihydrogen phosphate	Carl Roth, Karlsruhe, Germany	T879.2
Sodiumdodecylsulfate ultra pure (SDS)	Carl Roth, Karlsruhe, Germany	2326.1
SYBR Green PCR Master Mix	Applied Biosystems, Foster City, US	4367659
SYBR Safe	Thermo Scientific, Schwerte, Germany	S33102
TALON resin	Clontech, Mountain View, US	635504
Terrific broth medium	Carl Roth, Karlsruhe, Germany	X972.3
Tris-Base	Carl Roth, Karlsruhe, Germany	AE15.3
Tris-HCl	Carl Roth, Karlsruhe, Germany	9090.3
Trisodium citrate	Carl Roth, Karlsruhe, Germany	4088.3
Triton X-100	Carl Roth, Karlsruhe, Germany	3051.3
Tween 20	Carl Roth, Karlsruhe, Germany	9127.1
Urea	Carl Roth, Karlsruhe, Germany	3941.2
Uric acid	Carl Roth, Karlsruhe, Germany	4999.1
Xylene cyanole	Carl Roth, Karlsruhe, Germany	A513.1
Zinc chloride	Sigma-Aldrich, Munich, Germany	7646-85-7

## A.2 Consumables

Table 6: Consumables

<b>Consumables</b>	<b>Vendor</b>	<b>Catalog number</b>
96-well plate (qRT-PCR).	Applied Biosystems, Foster City, US	4346906
96-well plate (spectrophotometer)	Greiner Bio-One, Frickenhausen, Germany	655185
Bioreactor 50	TubeSpin, Trasadingen, Switzerland	87050
Eppendorf tube 1,5 ml	Eppendorf, Hamburg, Germany	0030 120-086
Falcon tube 50 ml	Greiner Bio-One, Frickenhausen, Germany	227261
Fine tip tweezers (Type 5, Dumont)	Carl Roth, Karlsruhe, Germany Roth	TE73.1
Forceps made of spring steel	Carl Roth, Karlsruhe, Germany Roth	AL99.1
Metal pestle	Carl Roth, Karlsruhe, Germany Roth	YE14.1
Microscope slide (diagnostic 3 cambers)	Carl Roth, Karlsruhe, Germany Roth	L196.1
Needle 0.5 x 16 mm	B.Braun, Melsung, Germany	4658302
Petri dishes (94 x 16 mm)	Greiner Bio-One, Frickenhausen, Germany	633180
PVDF membrane	Merck Millipore, Billerica, US	P2938
96-well plate (spectrophotometer)	Greiner Bio-One, Frickenhausen, Germany	655185

### A.3 Devices

Table 7: Devices

Device	Vendor
Binocular microscope, No813522	Will, Wetzlar, Germany
Centrifuge, Mikro 220R	Hettich Tuttlingen, Germany
Centrifuge, Rotina 420R	Hettich Tuttlingen, Germany
Eon microplate spectrophotometer	BioTek, Bad Friedrichshall, Germany
Hybridization oven, Memmert UNB 500	Memmert, Schwabach, Germany
Incubator, Heraeus Oven Typ T6	Thermo Scientific, Schwerte, Germany
Leica Mz16 F microscope	Leica Microsystems, Wetzlar, Germany
Leica TCS SP8 confocal microscope	Leica Microsystems, Wetzlar, Germany
Mini-PROTEAN Tetra System	Bio-Rad, Hercules, US
MP110PS high pressure microfluidiser	Microfluidics, Newton, US
Photometer, Specord 210	Analytik Jena, Jena, Germany
Purified water system, TKA-GenPure	Thermo Scientific, Schwerte, Germany
SE-04 FPLC system	ECOM, Prague, Czech Republic
Shake incubator, Multitron II	INFORS HAT, Bottmingen, Switzerland
StepOnePlus Real-Time PCR System	Applied Biosystems, Foster City, US
Take3 plate microdrop reader	BioTek, Bad Friedrichshall, Germany
TransBlot Turbo Transfer System	Bio-Rad, Hercules, US
Versadoc Imaging System	Bio-Rad, Hercules, US
Water bath, Microprocessor control MPC	Huber, Offenburg, Germany

### A.4 Standards and kits

Table 8: Standards and kits

Kit	Vendor	Catalog number
Amplex Red Uricase Assay Kit	Fisher Scientific, Schwerte, Germany	A22181
BCA Protein Assay Kit	Thermo Scientific Pierce, Schwerte, Germany	23227
First Strand cDNA Synthesis Kit	Thermo Fisher Scientific, Schwerte, Germany	K1682

Lumi-Light <sup>PLUS</sup> Western Blotting Substrate	Roche, Mannheim, Germany	12015196001
NucleoSpin RNA Kit	Macherey-Nagel, Weilmünster, Germany	740955.50
PageRule Plus Prestained Protein Ladder	Thermo Scientific Fermentas, Schwerte, Germany	26619
PCR DIG Probe synthesis kit	Roche, Mannheim, Germany	11636090910
Penta-His HRP Conjugate Kit	Qiagen, Hilden, Germany	34460

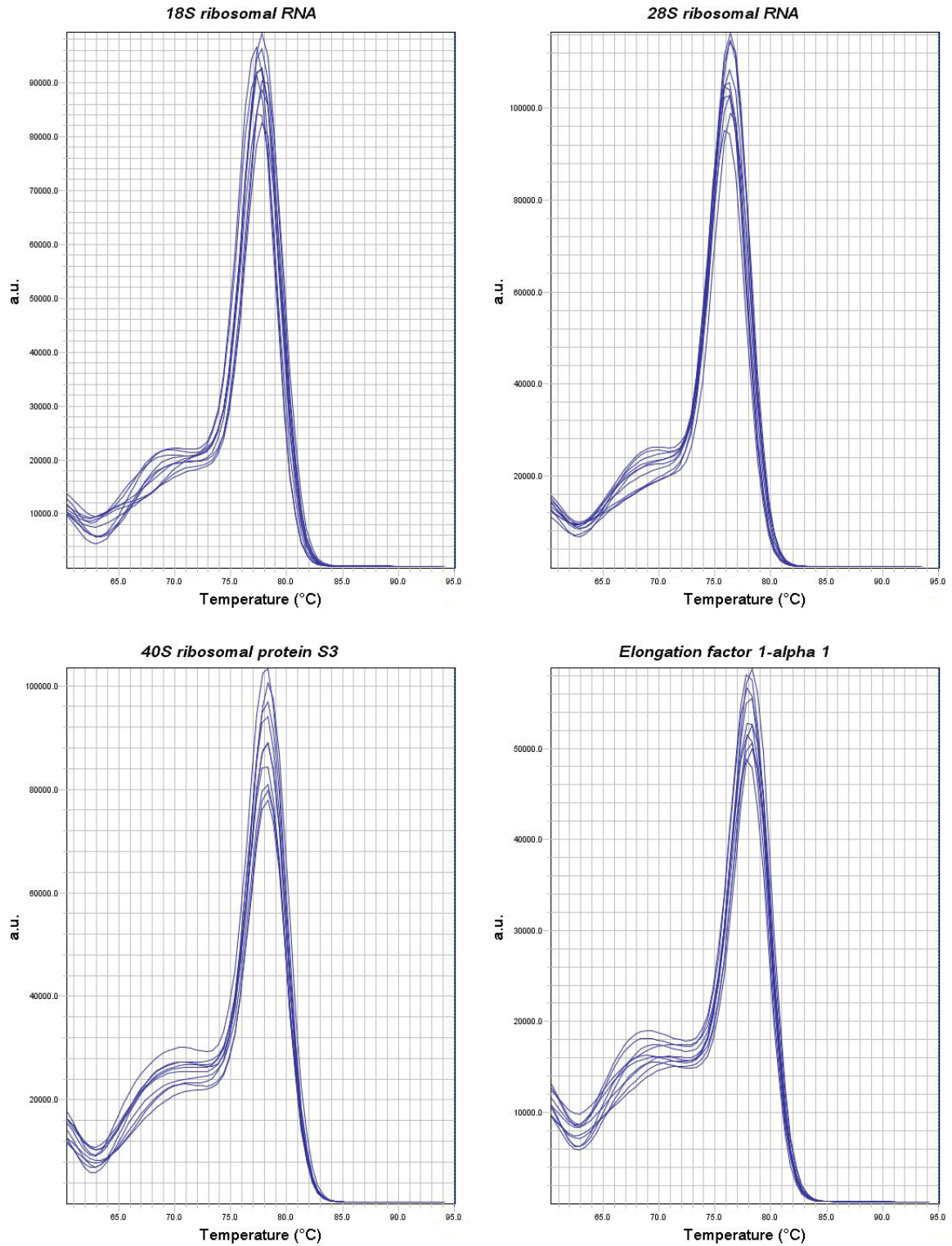
## A.5 Buffer and solutions

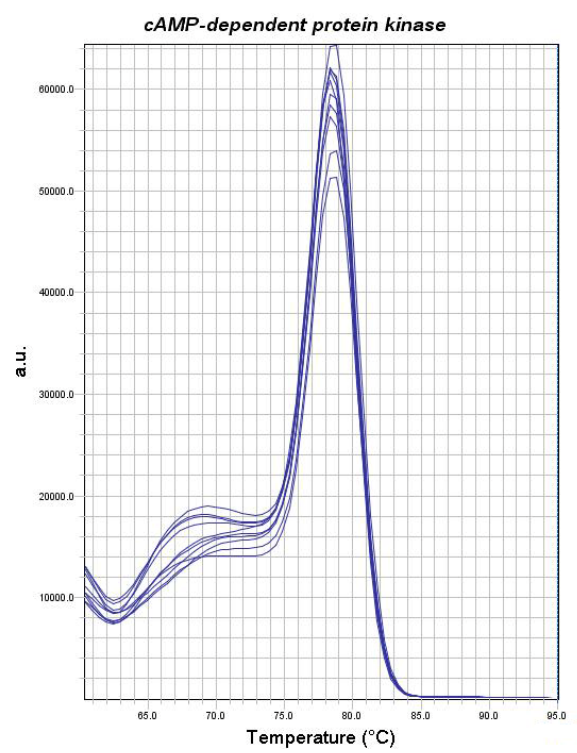
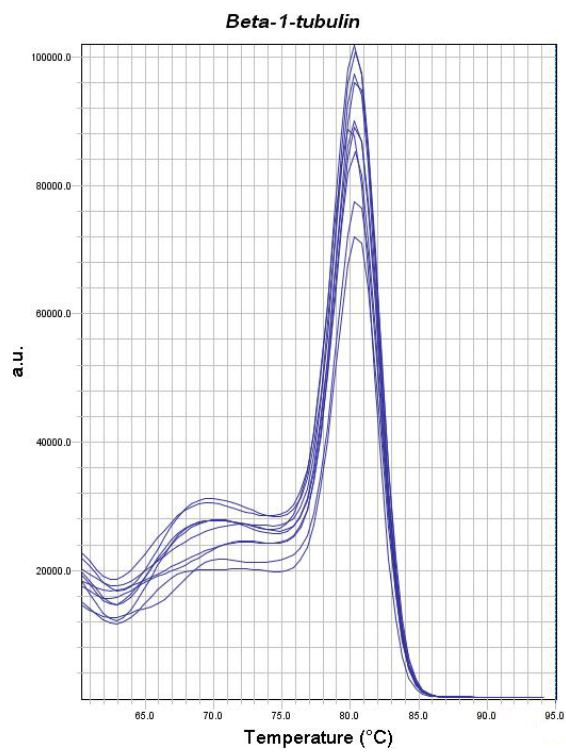
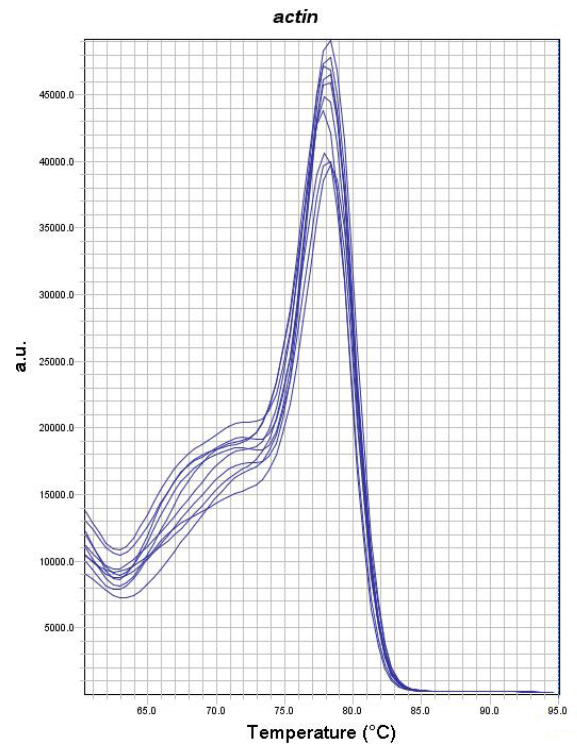
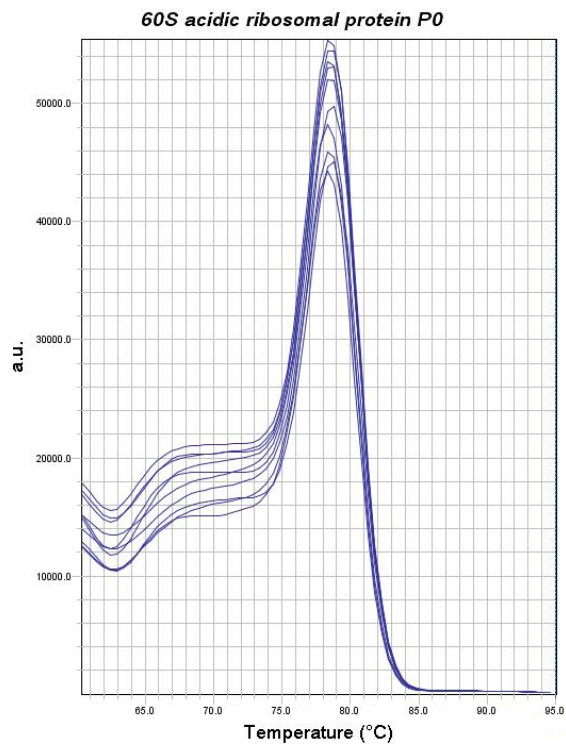
Table 9: Buffers and solutions

Name	Composition
AP buffer	100 mM Tris-Base, 100 mM NaCl, 50 mM MgCl <sub>2</sub> , 0.1 % Tween 20, pH 9.5
Chaotropic buffer	8 M guanidine hydrochloride, 30 mM Tris, pH 7.5
Dialysis buffer (1 x)	20 mM Tris-Base, 150 mM NaCl, pH 7.5
IMAC buffer A	6 M urea, 30 mM Tris-Base, 100 mM NaCl, pH 7.5
IMAC buffer B	6 M urea, 30 mM Tris-Base, 100 mM NaCl, 200 mM imidazole, pH 7.5
Laemmli-buffer (1 x)	62.5 mM Tris-HCl, 2 % SDS, 10 % Glycerol, 2 % $\beta$ -mercaptoethanol, 0.005 % Bromophenol blue, pH 6.8
Lysis buffer	30 mM Tris-Base, 100 mM NaCl, pH 7.5
Phosphate buffer saline (PBS)	0.01 M phosphate buffer, 0.0027 M potassium chloride, 0.137 M sodium chloride, pH 7.4 (Sigma-Aldrich P44170)
RA1 buffer	Component of NucleoSpin RNA Kit (Macherey-Nagel 740955) consisting of chaotropic salt.
RNA loading buffer (5 x)	8 M urea, 0.5 mM EDTA, 0.1 % Bromphenol blue, 0.1 % Xylene cyanol
TAE buffer (1 x)	40 mM Tris-Base, 20 mM acetic acid, 1 mM EDTA, pH 8.3
TBST-buffer (1 x)	50 mM Tris-Base, 150 mM NaCl, 0.1 % Tween 20, pH 7.4
Tris-buffer saline (TBS) (1 x)	50 mM Tris-Base, 150 mM NaCl, pH 7.4

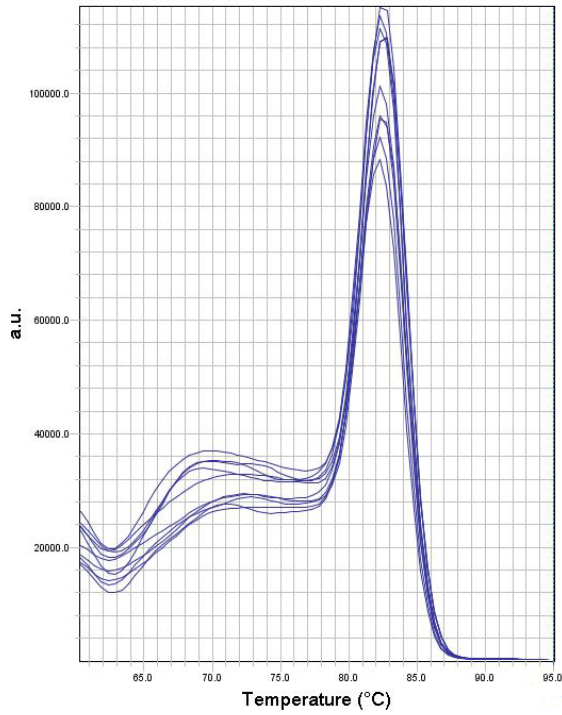
## Supplement B: Support information

### B.1 Melt curves of all applied qRT-PCR primer pairs.

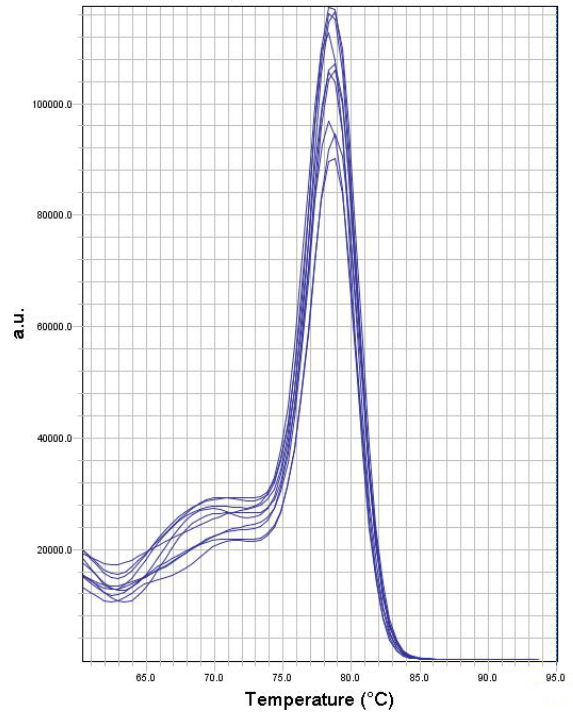




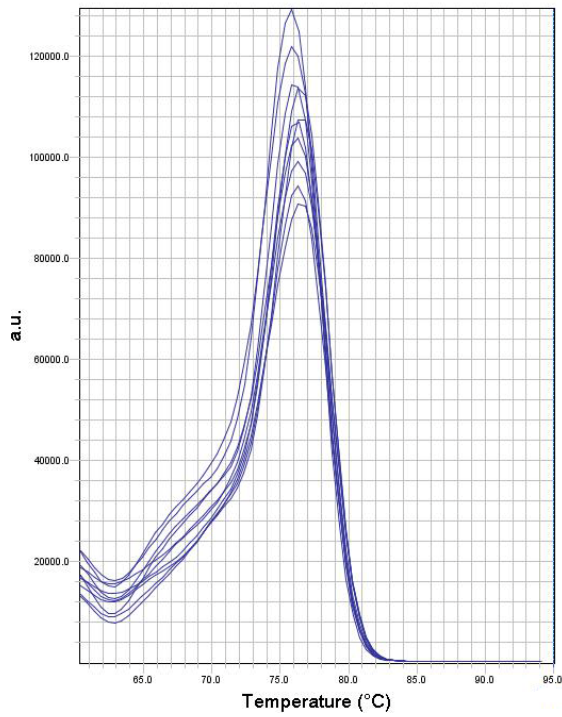
*Glyceraldehyde-3-phosphate dehydrogenase 1*



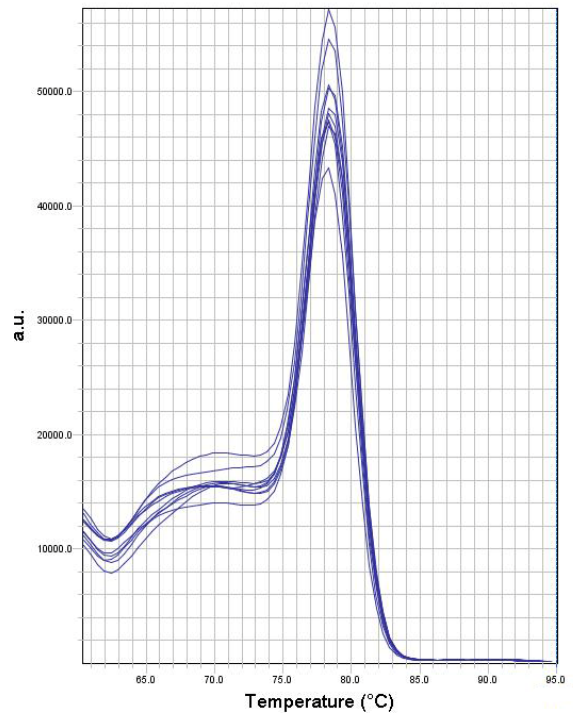
*Glutathione S-transferases 1-1*



*attacin-2*



*defensin-1*



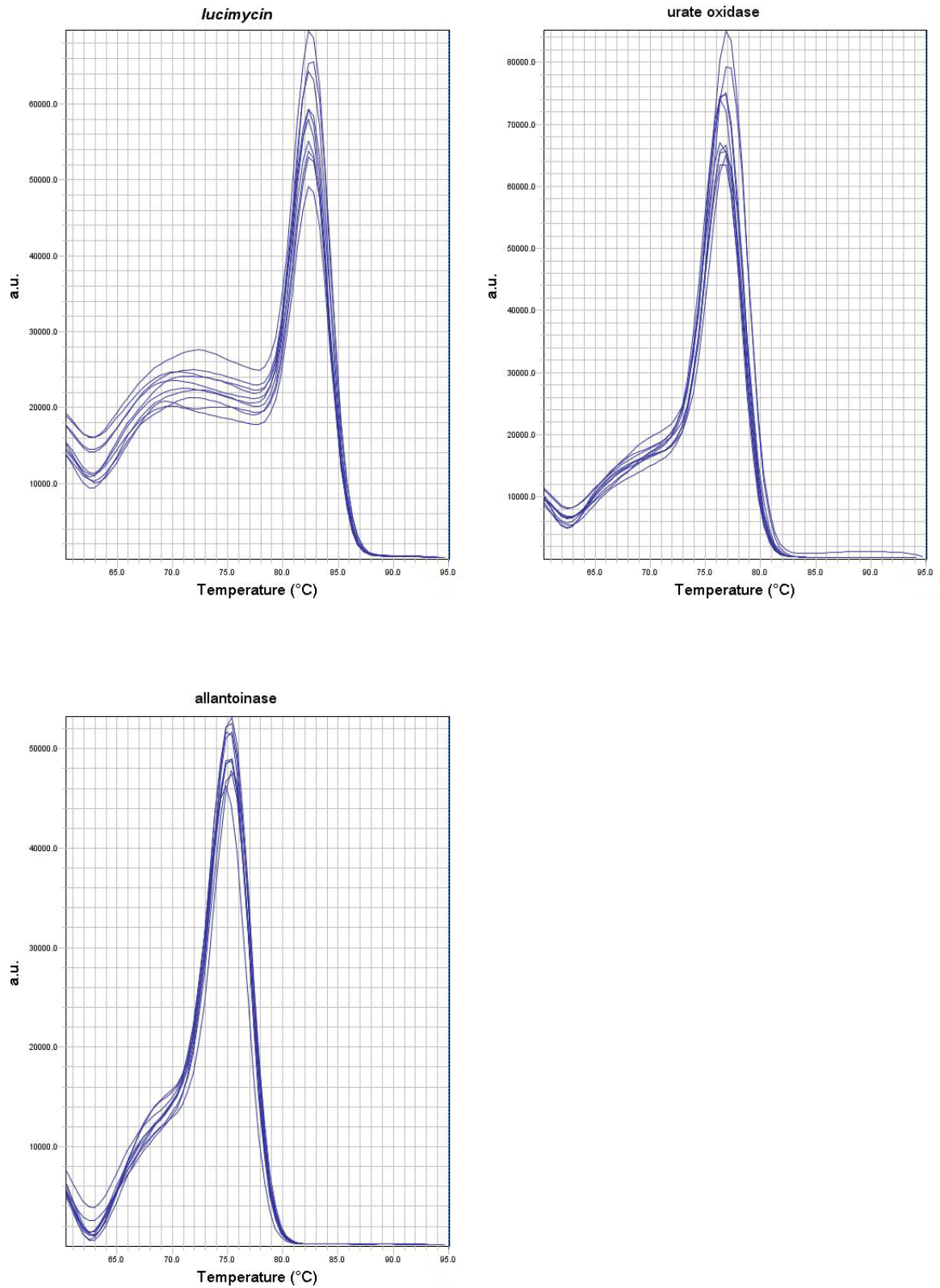


Figure 24: Melt curves of all applied qRT-PCR primer pairs.

## B.2 Normfinder intra and intergroup variations

Table 10: Normfinder intragroup variation for all candidate reference genes.

Gene	Larvae	Midgut	Hindgut	Salivary glands	Crop	Fat body	Nerve ganglion
<i>18S rRNA</i>	0.001	0.000	0.001	0.003	0.001	0.000	0.000
<i>28S rRNA</i>	0.003	0.005	0.003	0.005	0.001	0.017	0.006
<i>RPS3</i>	0.000	0.001	0.000	0.000	0.000	0.000	0.001
<i>EF1<math>\alpha</math></i>	0.001	0.000	0.000	0.002	0.001	0.001	0.001
<i>RPLP0</i>	0.000	0.000	0.000	0.002	0.001	0.000	0.000
<i>actin</i>	0.000	0.000	0.000	0.001	0.000	0.003	0.000
<i><math>\beta</math>-tubulin</i>	0.001	0.000	0.001	0.001	0.000	0.000	0.001
<i>PKA</i>	0.001	0.000	0.000	0.000	0.000	0.000	0.000
<i>GAPDH</i>	0.000	0.000	0.000	0.000	0.001	0.002	0.001
<i>GST1</i>	0.000	0.000	0.001	0.000	0.001	0.002	0.000

Table 11: Normfinder intergroup variation for all candidate reference genes.

Gene	Larvae	Midgut	Hindgut	Salivary glands	Crop	Fat body	Nerve ganglion
<i>18S rRNA</i>	0.032	0.018	0.066	-0.053	-0.016	-0.100	0.053
<i>28S rRNA</i>	-0.011	-0.027	0.064	-0.047	0.062	-0.089	0.048
<i>RPS3</i>	0.028	0.015	0.008	-0.023	0.012	-0.012	-0.028
<i>EF1<math>\alpha</math></i>	-0.001	-0.001	0.002	-0.028	0.022	-0.024	0.030
<i>RPLP0</i>	-0.028	-0.009	-0.004	-0.010	0.019	-0.010	0.042
<i>actin</i>	-0.103	0.016	-0.006	0.084	-0.099	0.094	0.012
<i><math>\beta</math>-tubulin</i>	0.055	0.008	-0.069	-0.003	-0.045	0.078	-0.024
<i>PKA</i>	-0.007	0.003	-0.023	-0.028	0.042	0.052	-0.038
<i>GAPDH</i>	-0.004	-0.018	0.011	0.056	0.025	0.006	-0.075
<i>GST1</i>	0.039	-0.005	-0.047	0.052	-0.023	0.005	-0.021

## Licenses and copyright

Figures 1 “Animal species infographic” (according to Chapman (2009)), 7 “MDT treatment of chronic wounds”, 8 “UO reaction mechanism”, 11 “Two-step colorimetric UO assay “ (according to Fraisse et al (2002)), 19 “UO<sub>r</sub> expression, purification and refolding”, tables 2, 5, 6, 7, 8 and 9 were created by M. Sc. Andre Baumann for the purpose of this thesis.

Figure 2 “[Green\\_bottle\\_fly3.jpg](#) “[Calibas](#) is licensed under [CC-BY-SA 4.0](#) and thus free to use with this attribution.

Figure 3 “The life-cycle of *L. sericata*” was designed (according to Grassberger et al. (2013)) and kindly provided by Dr. Henrike Schmidtberg.

Figure 4 “Maggot anatomy” was designed (according to Fleischmann et al. (2004)) and kindly provided by Dr. Henrike Schmidtberg.

Figure 5 “History of maggot therapy” was designed (according to Fleischmann et al. (2004)) and kindly provided by Dr. Anne Pöppel.

Figure 6 “[Overview of proven and postulated mechanisms by which medical maggots promote wound healing](#)” from Sherman (2014) published in the Hindawi journal Evidence-Based Complementary and Alternative Medicine is licensed under [CC BY 4.0](#) and thus free to use with this attribution.

All the content used from the Insect Biochemistry and Molecular Biology submission Baumann et al. (2016) was created by M. Sc. Andre Baumann. The Elsevier’s “prior publication” policy applies for this material, which can thus be published within the journal criteria (<https://www.elsevier.com/authors/journal-authors/policies-and-ethics>). This policy applies to figures 9, 10, 17, 18, 20, 21, 22, 23 and all text passages including those used in methods, results and discussion.

All the content used from the PLOS ONE article [Baumann et al. \(2015\)](#) is licensed under [CC BY 4.0](#) and free to use with this attribution. All the material published within this article was created by M. Sc. Andre Baumann. This applies to figures 12, 13, 14, 15, 16, 24, tables 1, 3, 4 10 11 as well as all text passages including those used in Methods, Results and Discussion.

## Zusammenfassung

Die Maden-Débridement-Therapie (MDT) ist eine durch die *U.S. Food and Drug Administration* (FDA) und *European Medicines Agency* (EMA) zugelassene Behandlung für verschiedene chronische und hartnäckige Wunden. MDT wurde in zahlreichen Fallstudien erfolgreich angewendet (Sherman 2002; Sherman 2003), welche die fördernden Eigenschaften in Débridement, Desinfektion sowie beschleunigter Wundheilung zeigten (Sherman 2014). Maden Sekretions- und Exkretionsprodukte (E/S) sind eine komplexe Mischung aus Enzymen, AMPs und niedermolekularen Verbindungen und als solches eine reiche Quelle für neue Therapeutika (Sherman 2014). Die Komplexität dieser Mischung macht es sehr schwer, die exakte Rolle und die positiven Effekte einzelner Komponenten im Heilungsprozess zu bestimmen und macht detailliertere Analysen erforderlich (Davydov 2011).

Diese Arbeit besteht aus zwei Teilen. Der erste Teil, wie in Baumann et al. (2015) publiziert, hat den Schwerpunkt in der Etablierung eines *qRT-PCR* Ansatzes zur gewebespezifischen Untersuchung der Expressionsstabilität von 10 Referenzgen-Kandidaten in Immunisierungs-Experimenten. Quantitative *RT-PCR* ist der Goldstandard im Bereich der Genexpressionsanalyse (Bustin et al. 2009; Nolan et al. 2006) und seine Etablierung in *L. sericata* stellt ein wichtiges Werkzeug für die Identifizierung und Validierung von Genen, die an der Madentherapie beteiligt sind, dar. Meine Arbeit zeigt, dass die Kombination der drei Referenzgene *RPLP0*, *EF1 $\alpha$*  und *RPS3* eine verlässliche Normalisierung von *L. sericata* Expressionsdaten in allen getesteten Proben ermöglicht. Dies erlaubt zum ersten Mal die präzise Normalisierung der Genexpression in Madengewebe, welche eine Rolle in der Produktion von E/S spielen. Die Methoden zur Bearbeitung von Gewebeproben und zur Genexpressionsanalyse, die im Rahmen dieser Arbeit etabliert wurden, haben auch zu den Publikationen Beckert et al. (2015) und Beckert et al. (2016) beigetragen. Außerdem fanden die Referenzgene bereits Anwendung in Pöppel et al. (2016) und Franta et al. (2016).

Im zweiten Teil dieser Arbeit, eingereicht als Baumann et al. (2016) (*Insect Biochemistry and Molecular Biology*) wurde die Uratoxidase (UO) von *L. sericata* heterolog exprimiert und charakterisiert. Dieses Enzym erzeugt Allantoin, welches zum Wundheilungsprozess beiträgt (Araujo et al. 2010; DiSalvo 2002). Ich war der Erste, der eine Insekten UO exprimiert und charakterisiert hat. Das rekombinante Enzym wurde in *E. coli* exprimiert, mittels IMAC unter denaturierenden Bedingungen aufgereinigt, rückgefaltet und hinsichtlich pH-Optimum (im Basischen), Temperaturoptimum (20-25 °C), kompetitiver Inhibition (typisch für UOs), Kofaktoren (Kofaktor unabhängig) und Stabilität (kurze Halbwertszeit) untersucht. Des Weiteren wurde *L. sericata* UO sowohl auf mRNA- als auch auf Proteinebene in verschiedenen *L. sericata* Geweben lokalisiert. Ich konnte zeigen, dass sowohl die UO-mRNA als auch das native UO-Enzym vorwiegend in den Zellen der Malpighischen Gefäße und

dort in beiden Fällen strikt zytosolisch lokalisiert ist. Basierend auf diesen Ergebnissen kann angenommen werden, dass Allantoin durch UO produziert wird, um Harnsäure aus der Insektenhämolymphe über die Malpighischen Gefäße zu entfernen und über den Hinterdarm als Stickstoff-Abfallprodukt zu exkretieren. Diese Ergebnisse unterstützen die Hypothese, dass nicht nur aktiv sekretierte Moleküle, sondern auch Exkretionsprodukte zu den positiven Effekten der MDT beitragen.

## Danksagung

Mein Dank gilt allen Personen, die zur Entstehung dieser Arbeit beigetragen oder diese überhaupt ermöglicht haben. Besonders bedanken möchte ich mich bei Prof. Andreas Vilcinskas für die Überlassung des spannenden Themas und die Bereitstellung der ausgezeichneten Forschungsmöglichkeit. Die Möglichkeit einen Teil zur Insektenbiotechnologie beitragen zu dürfen sehe ich als exzellentes Sprungbrett auf meinem Karriereweg. Prof. Peter Czermak danke ich herzlich für die Übernahme der Betreuung als Zweitgutachter und dem damit verbundenen Aufwand.

Ein besonderer Dank gilt dem Fraunhofer IME und dem hessischen Ministerium für Wissenschaft und Kunst (Forschungsförderungsprogramms LOEWE) ohne die die Durchführung des Projektes in dieser Art nicht möglich gewesen wäre.

I would particular like to thank my group leader RNDr. Zdeněk Franta Ph.D. for his by far more than excellent supervision. For his constant support in all aspects not only with his scientific knowledge that lead to many stimulating talks and amazing feedback, but also his friendly support. He always pushed to make me more diplomatic. Without him neither this thesis nor the papers would be nearly as good as they got and I am deeply thankful for this.

Dr. Annika Boas danke ich dafür, dass sie mich permanent angetrieben hat, auch wenn ich nie ihren Ansprüchen gerecht werden konnte. Des Weiteren danke ich ihr für das hervorragendes Feedback beim Verfassen der Thesis sowie für ihr stets offenes Ohr in vielen nicht nur fachlichen Fragestellungen.

Meinen ehemaligen und aktuellen Kolleginnen und Kollegen danke ich für ihre freundschaftliche Zusammenarbeit, das angenehme und produktive Arbeitsklima und die wunderbare Zeit. Besonders hervorheben möchte ich Anne, Lea und Anke, die nicht nur im Laboralltag stets hilfsbereit waren sondern auch abseits der Arbeit die Zeit in Gießen mit ihrer Freundschaft zu etwas Besonderem gemacht haben. Die vielen anderen tollen Kollegen wie Philipp, Jens, Derya, Doris, Hendrich, Gundi, Thorben, Henni, Marisa, Pedja, Tanja, Sara, Tilo, Miriam, Thomas, Tobi, Max, Matze, Tina, Christoph, Rayko, Angela, Tanja, Marc, Irina, Sabine, Ying, Jonas, Christina, Caro und Christian will ich hier nicht unterschlagen auch euch danke ich zutiefst für eure freundliche Zusammenarbeit.

Henni danke ich außerdem für die unglaublichen Abbildungen bei denen sie, wie befürchtet viel zu viel Zeit investiert hat und weit übers Ziel hinausgeschossen ist.

## **Erklärung**

Ich erkläre:

Ich, Andre Baumann (geb. 12.04.1982 in Herne), habe die vorgelegte Dissertation selbständig und ohne unerlaubte fremde Hilfe und nur mit den Hilfen angefertigt, die ich in der Dissertation angegeben habe. Alle Textstellen, die wörtlich oder sinngemäß aus veröffentlichten Schriften entnommen sind, und alle Angaben, die auf mündlichen Auskünften beruhen, sind als solche kenntlich gemacht. Bei den von mir durchgeführten und in der Dissertation erwähnten Untersuchungen habe ich die Grundsätze guter wissenschaftlicher Praxis, wie sie in der „Satzung der Justus-Liebig-Universität Gießen zur Sicherung guter wissenschaftlicher Praxis“ niedergelegt sind, eingehalten.

---

Gießen, den 20. Februar 2017